



Article

A Novel Dialkylamino-Functionalized Chalcone, DML6, Inhibits Cervical Cancer Cell Proliferation, In Vitro, via Induction of Oxidative Stress, Intrinsic Apoptosis and Mitotic Catastrophe

Jenna M. Len ^{1,†}, Noor Hussein ^{1,†}, Saloni Malla ^{1,†}, Kyle Mcintosh ¹, Rahul Patidar ², Manivannan Elangovan ^{2,*}, Karthikeyan Chandrabose ³, N. S. Hari Narayana Moorthy ³, Manoj Pandey ⁴, Dayanidhi Raman ⁵ , Piyush Trivedi ⁶ and Amit K. Tiwari ^{1,2,*} 

¹ Department of Pharmacology and Experimental Therapeutics, College of Pharmacy & Pharmaceutical Sciences, University of Toledo, Toledo, OH 43614, USA; jenna.len@rockets.utoledo.edu (J.M.L.); noor.hussein@rockets.utoledo.edu (N.H.); saloni.malla@rockets.utoledo.edu (S.M.); kyle.mcintosh@rockets.utoledo.edu (K.M.)

² School of Pharmacy, Devi Ahilya Vishwavidyalaya, Indore 452001, India; r.patidar16@yahoo.in

³ Department of Pharmacy, Indira Gandhi National Tribal University, Amarkantak 484887, India; karthinobel@gmail.com (K.C.); nshnarayanamoorthy@gmail.com (N.S.H.N.M.)

⁴ Department of Biomedical Sciences, Cooper Medical School of Rowan University, Camden, NJ 08103, USA; pandey@rowan.edu

⁵ Department of Cancer Biology, College of Medicine and Life Sciences, University of Toledo, Toledo, OH 43614, USA; dayanidhi.raman@utoledo.edu

⁶ Center of Innovation and Translational Research, Poona College of Pharmacy, Bhartiya Vidyapeeth, Pune 411038, India; piyushtrivedi304@gmail.com

* Correspondence: drmanislab@gmail.com (M.E.); amit.tiwari@utoledo.edu (A.K.T.); Tel.: +91-831-925-2570 (M.E.); +1-419-383-1913 (A.K.T.); Fax: +1-419-383-1909 (A.K.T.)

† Equal Contributions.



Citation: Len, J.M.; Hussein, N.; Malla, S.; Mcintosh, K.; Patidar, R.; Elangovan, M.; Chandrabose, K.; Moorthy, N.S.H.N.; Pandey, M.; Raman, D.; et al. A Novel Dialkylamino-Functionalized Chalcone, DML6, Inhibits Cervical Cancer Cell Proliferation, In Vitro, via Induction of Oxidative Stress, Intrinsic Apoptosis and Mitotic Catastrophe. *Molecules* **2021**, *26*, 4214. <https://doi.org/10.3390/molecules26144214>

Academic Editor: Ines Bruno

Received: 9 May 2021

Accepted: 6 July 2021

Published: 11 July 2021

Publisher's Note: MDPI stays neutral with regard to jurisdictional claims in published maps and institutional affiliations.



Copyright: © 2021 by the authors. Licensee MDPI, Basel, Switzerland. This article is an open access article distributed under the terms and conditions of the Creative Commons Attribution (CC BY) license (<https://creativecommons.org/licenses/by/4.0/>).

Abstract: In this study, we designed, synthesized and evaluated, in vitro, novel chalcone analogs containing dialkylamino pharmacophores in the cervical cancer cell line, OV2008. The compound, **DML6** was selective and significantly decreased the proliferation of OV2008 and HeLa cells in sub-micromolar concentrations, compared to prostate, lung, colon, breast or human embryonic kidney cell line (HEK293). **DML6**, at 5 μ M, arrested the OV2008 cells in the G2 phase. Furthermore, **DML6**, at 5 μ M, increased the levels of reactive oxygen species and induced a collapse in the mitochondrial membrane potential, compared to OV2008 cells incubated with a vehicle. **DML6**, at 5 μ M, induced intrinsic apoptosis by significantly (1) increasing the levels of the pro-apoptotic proteins, Bak and Bax, and (2) decreasing the levels of the anti-apoptotic protein, Bcl-2, compared to cell incubated with a vehicle. Furthermore, **DML6**, at 5 and 20 μ M, induced the cleavage of caspase-9, followed by subsequent cleavage of the executioner caspases, caspase-3 and caspase-7, which produced OV2008 cell death. Overall, our data suggest that **DML6** is an apoptosis-inducing compound that should undergo further evaluation as a potential treatment for cervical cancer.

Keywords: cervical cancer; chalcone; dialkylamino; intrinsic apoptosis; mitotic catastrophe; drug discovery

1. Introduction

Cervical cancer is the fourth-leading cause of cancer-related deaths in women worldwide resulting in an estimated 600,000 new cervical cancer cases and 342,000 deaths, yearly [1]. About 85% of all cervical cancer cases are from underdeveloped or developing nations with 18-fold higher mortality rate compared to developed or high-income countries [2,3]. The majority of cervical cancer is caused primarily due to human papillomavirus

(HPV) [4,5]. Other causes of cervical cancer includes infections, smoking, higher number of childbirths and prolonged use of oral contraceptive devices [6,7]. Among all high-risk types, HPV-16 has the highest carcinogenic capacity accounting for 60% of all cervical cancer cases [8,9]. The standard treatment of cervical cancer ranges from cervical conization, hysterectomy and radiotherapy to chemotherapy, depending on the stage of cervical cancer [10]. However, adoption of adjuvant chemotherapy along with chemoradiotherapy to prevent recurrence of locally advanced and metastatic cervical cancers are associated with increased adverse events, morbidity rate and therapeutic failure [11]. Women with locally advanced cervical carcinoma have worse prognosis, poor survival and higher recurrence rate than patients with early-staged cervical cancer [12,13]. Different chemotherapeutic drugs and their combinations have been used to improve the clinical response (CR) and overall survival (OS) in patients with advanced cervical cancer [14]. Despite initial therapeutic response, the majority of patients either undergo relapse or succumb to the disease as a result of resistance to chemotherapy [15]. Chemoresistance is the most important factor that decreases or abrogates the efficacy of chemotherapy in many cancers including advanced cervical cancer, producing an increase in tumor progression, which results in high rates of cancer-related deaths [16,17]. Many factors contribute to chemoresistance, including but not limited to, alterations in DNA damage and repair capacity, and overexpression of ATP-binding cassette (ABC) transporters, notably the ABCB1 transporter [18,19]. Consequently, there is an urgent need for the discovery and development of novel chemotherapeutic drugs that can overcome the aforementioned limitations of therapies used to treat cervical cancer.

Chalcones are an essential structural motif that has been extensively used for many years to synthesize novel anticancer drugs [20–23]. The basic structure of chalcone, which consists of two phenyl rings attached to an α,β -unsaturated carbonyl skeleton at the 1,3 position, provides numerous opportunities for structural alterations to yield novel molecules that selectivity decreases the proliferation of cancer cells [21,23]. Currently, many chalcone derivatives have been synthesized and shown to be efficacious *in vitro* and *in vivo* in various cancer cells [20,23]. It has been reported that increasing the rigidity of chalcones produces heterocyclic analogues that have anti-cancer efficacy [24,25]. The 4,5-dihydro-1*H*-pyrazole derivatives synthesized from chalcones have been shown to have potential anticancer efficacy [26]. The addition of a dimethylamino group to chalcone derivatives could be important, as this would improve their solubility and anticancer efficacy [27,28]. Indeed, the dimethylamino function is a structural feature in certain anticancer drugs, such as topotecan [29], pyrvinium [30], and onapristone [31] (Figure 1). Therefore, in this study, we report the synthesis of novel chalcones and their 4,5-dihydro-1*H*-pyrazoles analogues containing the dialkylamine and their *in vitro* efficacy in various cancer cell lines. Furthermore, we conducted experiments to determine their mechanism of action.

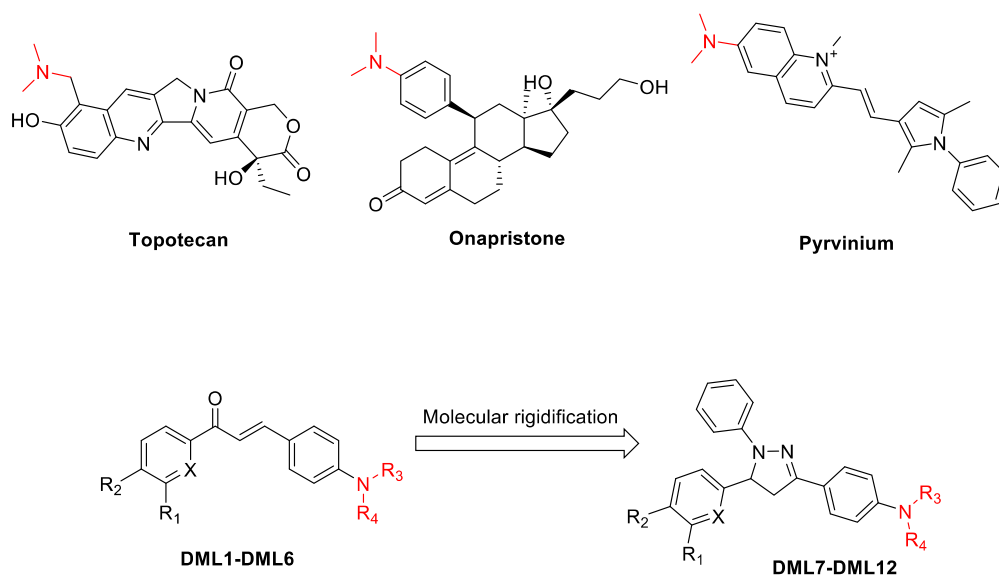
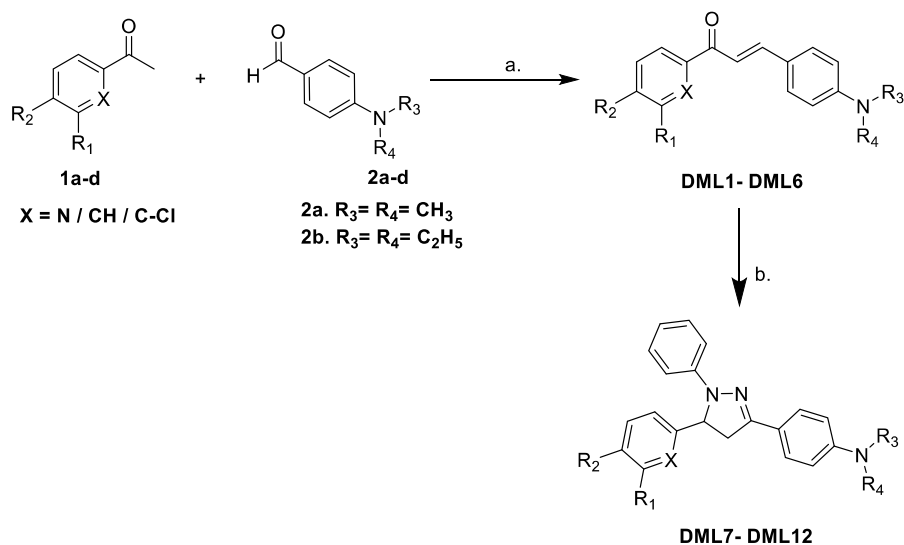


Figure 1. Representative structures of chalcone, dihydropyrazoles and dimethylamine functionalized-derived anticancer compounds.

2. Results and Discussion

2.1. Chemistry

Initially, the target compounds, **DML1–DML6**, were synthesized using a simple Claisen-Schmidt condensation reaction, with various substituted acetophenones and 4-dimethylamino- or 4-diethylamino-substituted benzaldehydes in the presence of 40% NaOH solution in EtOH, as described in Scheme 1. Further reaction of the dialkylamino chalcones **DML1–DML6** with phenylhydrazine in glacial acetic acid under reflux produced the respective 1,3,5-triphenyl-4,5-dihydro-1*H*-pyrazole **DML7–DML12** in good (74 to 86%) yields. The structures of the newly synthesized dialkylamino chalcones **DML1–DML6** and their heterocyclic derivatives, 1,3,5-triphenyl-4,5-dihydro-1*H*-pyrazoles **DML7–DML12**, were confirmed by microanalyses, FTIR, ¹H-NMR and mass spectral analysis. All of the synthesized compounds produced satisfactory analytical and spectroscopic, data, which were in full agreement with their proposed structures. The structures, properties and reaction yield of DML compounds are provided in Table 1.



Scheme 1. Reagents and conditions: (a) 40% aqueous NaOH, EtOH, RT, stirring; (b) C₆H₅NHNH₂, CH₃COOH, reflux, 6 h.

Table 1. Molecular structures, properties and reaction yields of compounds DML1–DML12.

Comp Code	Substitution					Molecular Formula	Molecular Weight	Yield %
	X	R ₁	R ₂	R ₃	R ₄			
DML1	N	H	H	CH ₃	CH ₃	C ₁₆ H ₁₆ N ₂ O	252.32	84
DML2	N	H	H	C ₂ H ₅	C ₂ H ₅	C ₁₈ H ₂₀ N ₂ O	280.37	82
DML3	CH	H	OCH ₃	CH ₃	CH ₃	C ₁₈ H ₁₉ NO ₂	281.36	86
DML4	CH	OCH ₃	OCH ₃	CH ₃	CH ₃	C ₁₉ H ₂₁ NO ₃	311.38	84
DML5	CH	H	OCH ₃	C ₂ H ₅	C ₂ H ₅	C ₂₀ H ₂₃ NO ₂	309.41	85
DML6	C-Cl	H	Cl	CH ₃	CH ₃	C ₁₇ H ₁₅ Cl ₂ NO	320.21	81
DML7	N	H	H	CH ₃	CH ₃	C ₂₂ H ₂₂ N ₄	342.45	79
DML8	N	H	H	C ₂ H ₅	C ₂ H ₅	C ₂₄ H ₂₆ N ₄	370.50	80
DML9	CH	H	OCH ₃	CH ₃	CH ₃	C ₂₄ H ₂₅ N ₃ O	371.48	74
DML10	CH	OCH ₃	OCH ₃	CH ₃	CH ₃	C ₂₅ H ₂₇ N ₃ O ₂	401.51	75
DML11	CH	H	OCH ₃	C ₂ H ₅	C ₂ H ₅	C ₂₆ H ₂₉ N ₃ O	399.54	78
DML12	C-Cl	H	Cl	CH ₃	CH ₃	C ₂₃ H ₂₁ Cl ₂ N ₃	410.34	76

2.2. Structure–Activity Relationships for the Dialkylamine Substituted Chalcones and Their Corresponding Dihydropyrazoles, Based on Data Obtained Using the 3-(4,5-Dimethylthiazol-2-yl)-2,5-diphenyltetrazolium Bromide (MTT) Cytotoxicity Assay

All of the synthesized compounds (DML1 to DML12) were evaluated to determine their *in vitro* antiproliferative efficacy in cervical (OV2008), breast (MDA-MB-231), lung (A549), colon (LOVO), prostate (DU145) and the normal cell lines, human embryonic kidney cells (HEK293), human colon fibroblast cells (CRL1459) and Chinese hamster ovary cells (CHO), using the MTT assay. The newly synthesized compounds were tested at concentrations from 0.1 to 100 μ M. The concentration of the tested compounds that produced a 50% inhibition of cell growth (IC₅₀) was determined. The calculated IC₅₀ values of compounds tested in cancer cell lines are shown in Table 2.

Table 2. The antiproliferative efficacy of the DML1–DML12 compounds on the proliferation of cancer cell lines (breast, colon, lung, prostate and cervical) and a normal, non-cancerous cell line, HEK293.

Comp Code	IC ₅₀ ± SD (μ M)					
	Kidney	Breast	Colon	Lung	Prostate	Cervical
	HEK293	MDA-MB-231	LOVO	A549	DU145	OV2008
DML1	>100	>100	>100	>100	>100	>100
DML2	>100	>100	>100	>100	>100	>100
DML3	>100	>100	>100	>100	>100	>100
DML4	68.5 ± 2.1	26.2 ± 23.9	45 ± 22.6	66.3 ± 4.6	22.5 ± 4.9	13.8 ± 7
DML5	>100	>100	94 ± 8.4	>100	>100	79.3 ± 29.2
DML6	70 ± 42.4	91.9 ± 11.5	65 ± 49.5	84.9 ± 21.4	96.9 ± 4.4	7.8 ± 0
DML7	>100	>100	>100	>100	>100	>100
DML8	>100	>100	>100	>100	>100	>100
DML9	>100	>100	>100	>100	>100	>100
DML10	>100	>100	>100	>100	>100	>100
DML11	>100	>100	>100	>100	>100	>100
DML12	>100	>100	>100	>100	>100	>100

Among the 12 compounds evaluated for antiproliferative efficacy, only three chalcone derivatives, DML4, DML5 and DML6, had moderate to good anti-proliferative efficacy in a wide range of cancer cell lines, compared to normal cells. Compound DML6, with a chloro-substitution at X and R₂ positions and a 4-dimethyl amine group, i.e., R₃ = R₄ = CH₃ in chalcone core structure, had significant *in vitro* antiproliferative efficacy in all of the cancer cell lines, with IC₅₀ values ranging from 7.8 to 91.9 μ M (Table 2). The most efficacious compound, DML6, had an IC₅₀ value of 7.8 ± 0, in the OV2008 cervical cancer

cells. Similarly, compounds **DML4** and **DML5** were efficacious in the OV2008 cancer cells, with IC_{50} values of $13.8 \pm 7 \mu\text{M}$ and $79.3 \pm 29.2 \mu\text{M}$, respectively. **DML4**, which had a smaller alkyl substitution at the R_3 and R_4 positions, had greater antiproliferative efficacy in the OV2008 cancer cells compared to **DML5**, which had larger alkyl groups at the same position. Based on the cytotoxicity results of DML-4 and DML-5, we found that changing the alkyl chain length of the dialkylamine substituents at the R_3 and R_4 positions from methyl to ethyl decreased the antiproliferative efficacy. For the chalcone derivatives, **DML1–DML6**, the chloro and methoxy substituents produced the highest efficacy in the R_1 and R_2 positions, whereas the 2-pyridyl substituent ($X = \text{N}$) in the chalcone structures decreased the antiproliferative efficacy in OV2008 cells. Similarly, the result of cytotoxicity assay performed in another cervical HeLa cells were similar to that of OV2008 cells (Table S1). **DML6** was the most potent agent with an IC_{50} value of $9.08 \pm 0.69 \mu\text{M}$, whereas the IC_{50} values of **DML1**, and **DML5** in HeLa cell line were greater than $70 \mu\text{M}$, and **DML5** was around $40 \mu\text{M}$, suggesting that **DML6** were most effective in cervical cancer.

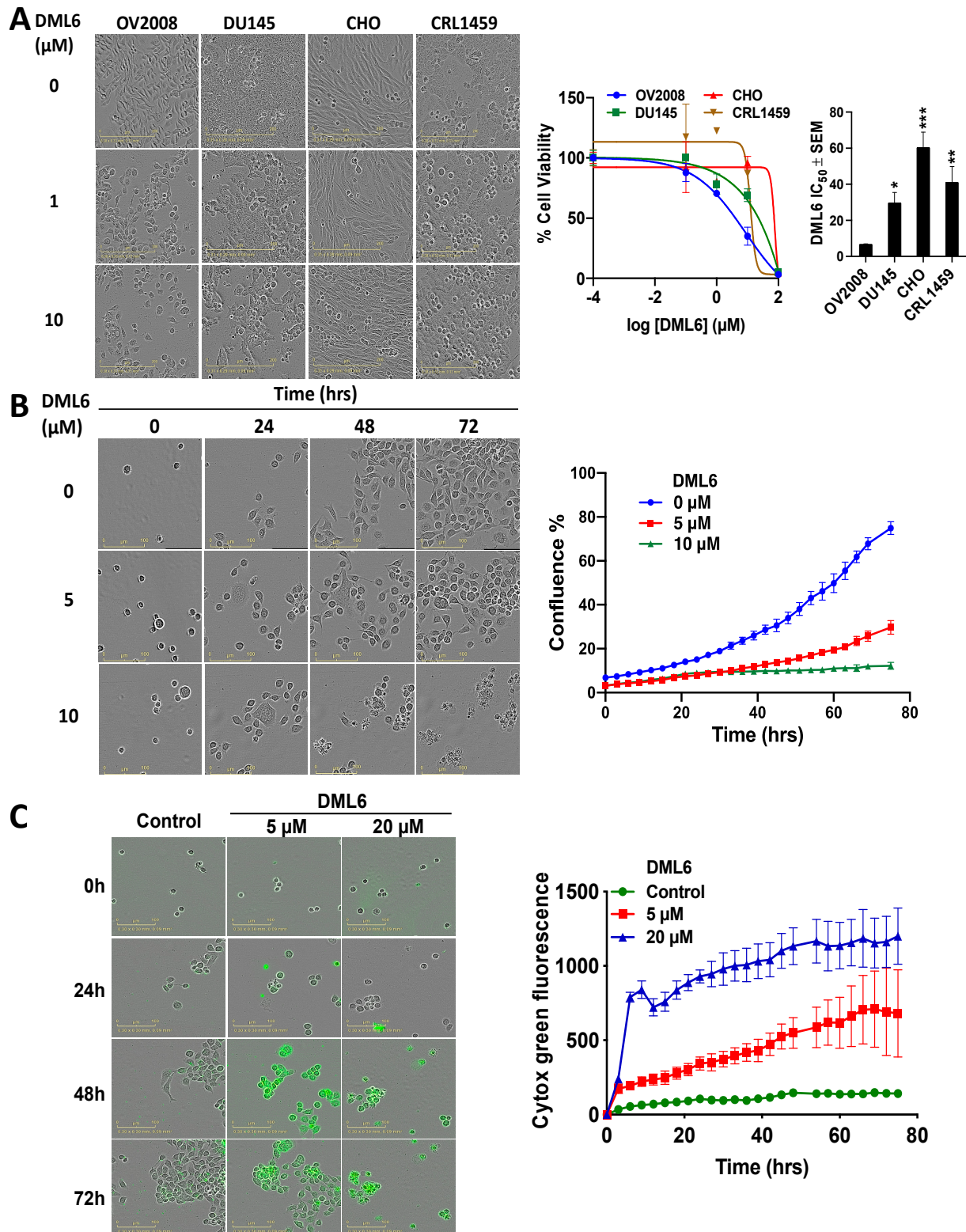
Among the compounds evaluated in DU145 prostate cancer cells, **DML4** had the highest efficacy, with an IC_{50} value of $22.5 \pm 4.9 \mu\text{M}$. However, **DML6**, which was the most efficacious compound in OV2008 and HeLa cells, had a low antiproliferative efficacy in DU145 prostate cancer cells, with an IC_{50} value of $96.9 \pm 4.4 \mu\text{M}$. **DML4**, which has two methoxy groups at the R_1 and R_2 position, had the highest efficacy in all five cancer cell lines, whereas **DML5**, with only one methoxy group at the R_2 positions, had a moderate inhibitory efficacy in the cervical and colon cancer cells. Furthermore, **DML4** significantly decreased the proliferation in breast (MDA-MB-231), lung (A549) and colon (LOVO) cancer cells, with IC_{50} values of 26.7 ± 23.9 , 45 ± 22.6 , and $66.3 \pm 4.6 \mu\text{M}$, respectively. None of the dialkylamine functionalized dihydropyrazole derivatives, **DML7–DML12**, had efficacy in the cancer cells, even at a maximum concentration of $100 \mu\text{M}$. Finally, it is important to note that two of the dimethylamino functionalized chalcone derivatives, **DML4** and **DML6**, inhibited the proliferation of HEK-293 cells at a concentration $> 65 \mu\text{M}$.

These above results indicate that the chalcone skeleton in compounds **DML1–DML6** played an important role in inhibiting the proliferation of the cancer cell lines used in this study. There was only one structural difference between compounds **DML1–DML6** and compounds **DML7–DML12**: the former six compounds had the chalcone skeleton. Based on the structure-activity relationship of these compounds, the α,β -unsaturated carbonyl system is a key structural characteristic present in the chalcone scaffold that modulates the antiproliferative efficacy. Furthermore, our study indicates that the dialkylamino substitution on the chalcone scaffold increased the antiproliferative efficacy. However, for the dihydropyrazole motif, the same substitution did not significantly increase efficacy.

2.3. **DML6** Antiproliferative Efficacy and Selectivity on Cervical Cancer Cell Lines

Overall, our MTT results indicate that compound **DML6** was the most optimal candidate for further mechanistic investigations, based on its efficacy in cervical cancer cell lines. In terms of selectivity, **DML6** was significantly less efficacious in decreasing the viability of Chinese hamster ovary cells (CHO) and normal CRL-1459 cells, compared to the cancer cell lines, as illustrated in Figure 2A. Thus, **DML6** significantly inhibited the growth of the cervical and prostate cancer cells. In contrast, **DML6** did not produce significant cytotoxicity in the normal cells, CRL1459 and CHO cells. Figure 2B shows representative pictures of the confluence of OV2008 following incubation with the vehicle, 5 or $20 \mu\text{M}$ of **DML6**, at 0, 24, 48, and 72 h. The control cells that were incubated with the vehicle grew over time, reaching their highest confluence after 72 hours of incubation ($\approx 70\%$, Figure 2B). However, the cells incubated with **DML6** grew significantly slower and only had a very low confluence ($\approx 40\%$ and $\approx 10\%$, respectively, at 5 and $20 \mu\text{M}$ of **DML6**, Figure 2B) at 72 hours. A detailed graph illustrating the results for **DML6** was evaluated at each time point to determine the cytotoxicity over time. Similarly, the results of the IncuCyte Cytotox green assay, as seen in Figure 2C indicates that the fluorescence signal emitted by the dead or non-viable cells incubated with vehicle was very low, suggesting that the cells were

viable. However, the fluorescent signal increased significantly in OV2008 cells incubated with DML6, indicating that DML6 increased the number of dead cells, i.e., it produced cytotoxicity over time, compared to cells incubated with a vehicle.



survival was determined using the MTT assay. The IC_{50} values are represented as the means \pm SD of three independent experiments performed in triplicate. * $p < 0.05$, ** $p < 0.01$, *** $p < 0.001$. (B) The changes in OV2008 cell morphology produced by vehicle (0 μ M), 5 or 10 μ M of **DML6** after 0, 24, 48 and 72 h of incubation and its confluence graph. (C) The real time IncuCyte cytotox green fluorescent reagent assay showing the number of dead OV2008 cancer cells present over time after incubation with vehicle (0 μ M), 5 or 10 μ M of **DML6**. The data are presented as images showing the fluorescence level at the 0 and 72 h time points. A representative time curve quantitatively summarizing the results at each time point. The data are presented as the means \pm SEM of three independent studies. All images were captured in each cell lines after incubation with the vehicle or **DML6** by the IncuCyte[®] S3 Live-Cell Analysis System at 20 \times magnification and a representative picture, along with its graph, are shown.

2.4. **DML6** Induces Oxidative Stress in OV2008 Cells

The total intracellular level of reactive oxygen species (ROS) was determined by staining the cells with 2,7-dichlorofluorescein diacetate (H2DCFDA). In this assay, cellular esterases cleave the nonfluorescent H2DCFDA molecule to yield H2DCF, by removing the lipophilic moiety (a diacetate group) [20]. Subsequently, H2DCF is oxidized by ROS to 2',7'-dichlorofluorescein (DCF), which is a highly fluorescent dye [32]. ROS levels were quantified based on the fluorescence level of DCF detected using EVOS microscope. The levels of DCF fluorescence were significantly higher in cells incubated with 5 or 20 μ M **DML6**, compared to cells incubated with the vehicle (Figure 3), indicating that **DML6** induced the formation of ROS.

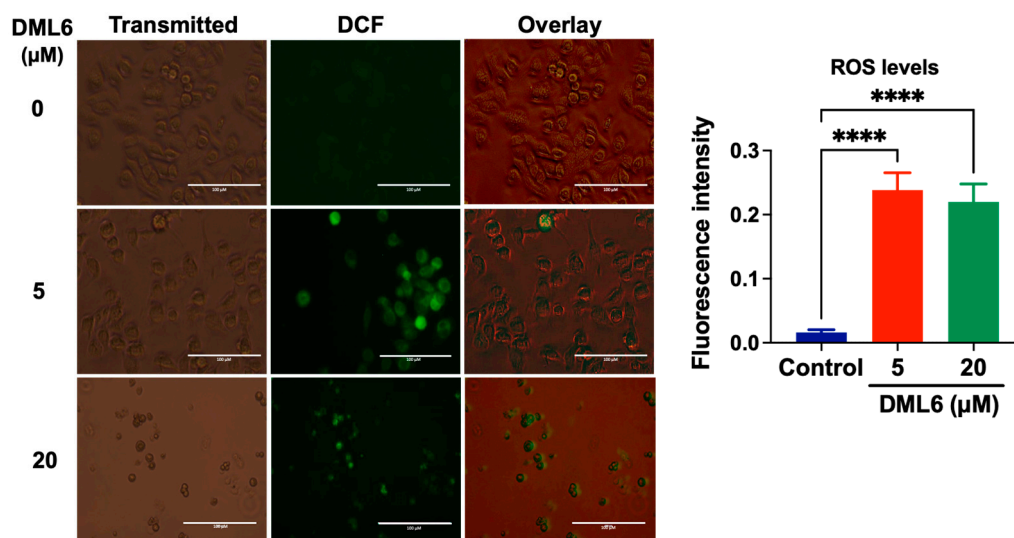


Figure 3. The detection of **DML6**-induced cellular oxidative stress by DCF in OV2008 cells. Representative images of fluorescent DCFDA levels following incubation with the vehicle (control) (0 μ M), 5 or 20 μ M of **DML6** for 24 h. The images were taken using an EVOS digital fluorescent microscope at 40 \times magnification. A histogram quantitatively summarizing the change in the % of fluorescence intensity of DCFDA in cells incubated with 5 and 20 μ M of **DML6** as compared to cells incubated with the vehicle, is also shown. **** $p < 0.0001$. The experiment was repeated in triplicate for each cell line. Scale bar: 100 μ M.

2.5. **DML6** Arrests the Cell Cycle of OV2008 at G2 Phase

To further determine the mechanisms by which **DML6** inhibits cervical cancer cell proliferation, a cell cycle analysis was conducted using flow cytometry cell cycle analysis with propidium iodide (PI). **DML6** produced a significant concentration-dependent increase in the percentage of cells in the G2 phase in OV2008 cells. The percentage of cells in the G2 phase increased from 4.18% in cells incubated with the vehicle to 42.56% and 59.96% with 5 or 20 μ M of **DML6**, respectively ($p < 0.01$, $p < 0.001$, respectively; Figure 4). Furthermore, **DML6** significantly ($p < 0.0001$) decreased the percentage of cells in the G1

phase from 85.99% in the cells incubated with the vehicle, to 16.01% and 27.84% after incubation with 5 or 20 μM , respectively, of **DML6** (Figure 4). **DML6**, at 5 μM , significantly ($* p < 0.05$) increased the percentage of cells in the S phase. However, 20 μM of **DML6** did not significantly increase the percentage of cells in the S phase. Finally, neither 5 or 10 μM of **DML6** significantly altered the percentage of cells in the sub G1 phase.

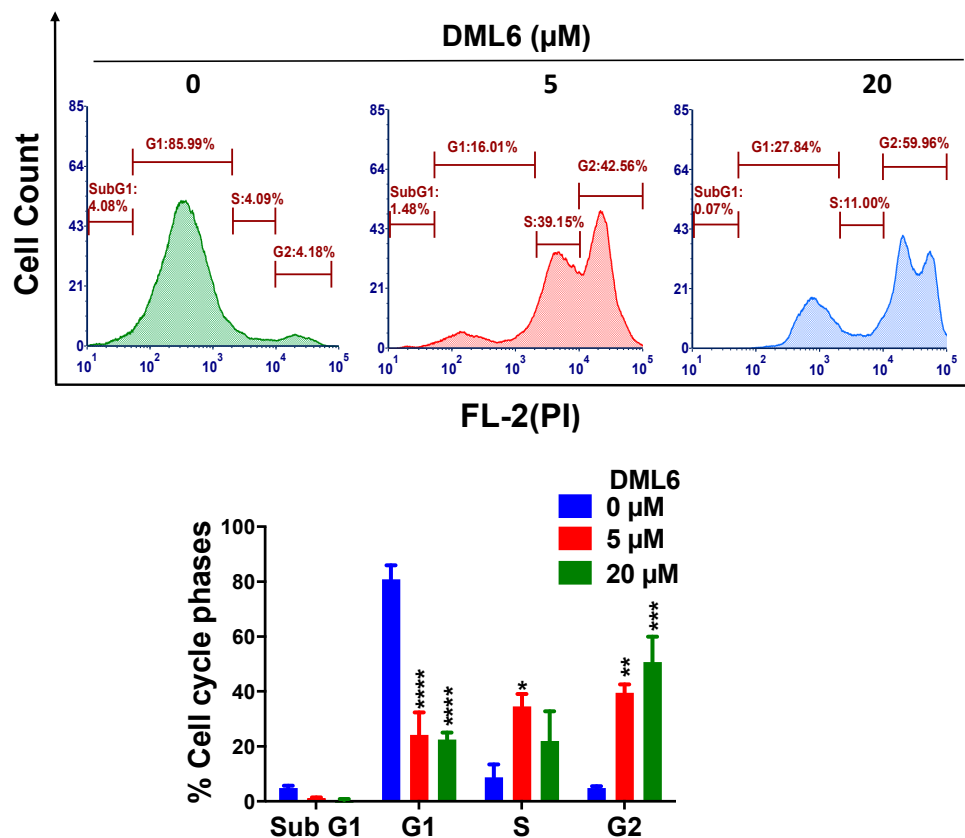


Figure 4. The effect of **DML6** on the cell cycle. A representative figure illustrating the effect of **DML6** on the distribution of the OV2008 cell populations in the cell cycle phases. OV2008 cells were incubated with the vehicle, 5 or 20 μM of **DML6** for 24 h and were subjected to cell cycle analysis using flow cytometry with propidium iodide (PI) (X-axis)/cell counts(Y-axis); A histogram quantitatively summarizing the change in the % of cells in each phase of the cell cycle due to **DML6**, is also shown. $* p < 0.05$, $** p < 0.01$, $*** p < 0.001$, $**** p < 0.0001$. The data represent the means \pm SEM of three independent experiments performed in triplicate.

2.6. **DML6** Induces Mitotic Catastrophe and Apoptosis in OV2008 Cells

In vitro, **DML6** produced morphological features indicative of apoptosis in the OV2008 cells, including cell shrinkage, cellular membrane blebbing and the formation of apoptotic bodies, as well as arrest of the cell cycle at the G2 phase. Therefore, we also determined the effect of **DML6** on the nuclear morphology of OV2008 cells, using the Hoechst 33342 dye. The nuclear changes in OV2008 cells after incubation with the vehicle, 5 or 20 μM of **DML6** for 24 h were visualized and recorded (Figure 5). As shown in Figure 5, the cells incubated with the vehicle had a normal nuclear shape, consisting of an oval, non-condensed shape, with a low level of bright-blue staining (indicative of viable cells). However, the incubation of cells with 5 μM of **DML6** for 24 h increased the number of cells with condensed, fragmented nuclei, indicating apoptosis. The incubation of OV2008 cells with 20 μM of **DML6** resulted in decondensed, multiple micronuclei and some single, highly condensed nuclei (Figure 5A), indicative of mitotic catastrophe and apoptosis, respectively. The percentage of apoptotic nuclei produced as a result of **DML6** incubation is significantly higher than control incubated with the vehicle. The prominent morphological

hallmarks of apoptosis are the presence of apoptotic bodies, i.e., nuclear fragmentation and chromatin condensation [33]. In contrast, mitotic catastrophe (MC) is characterized by the presence of nuclei consisting of two or more lobes or micronuclei in a single cell [34]. Cells incubated with various chemotherapeutic drugs die in the interphase or become arrested at G1 and/or G2 phase [35,36]. The inability of these cells to repair the DNA damage is due to an impairment in checkpoint functions, which causes cells to enter into early mitosis [34]. Their fate is dependent on various conditions, which produces MC, where the cells become viable for a short period of time without replicative capacity (known as permanent growth arrest) or apoptosis and eventually, cell death [34,37–39]. Interestingly, apoptosis and MC have similar biochemical features, such as mitochondrial outer membrane permeabilization (MOMP) and the activation of certain caspases [40]. The loss of the MOMP is detrimental as several proteins involved in apoptosis, such as the apoptotic protease-activating factor (APAF-1) and cytochrome c are present in the space between the outer and inner membrane of mitochondria [41]. This results in the loss of mitochondria membrane potential and the disruption of mitochondria function, producing cell death [42,43]. Therefore, the apoptogenic potential of a compound can be determined by its efficacy to induce a loss of the mitochondrial membrane potential. Therefore, we evaluated the induction of apoptosis using MitoTracker™ Red & Annexin V Alexa Fluor® 488 in OV2008 cells. During apoptosis, phosphatidylserine (PS) is translocated to the extracellular side from its regular intracellular mitochondrial localization, leading to phosphatidylserine being present on the extracellular surface [44,45]. The exposed PS binds with high affinity to the fluorophore-labeled human vascular anticoagulant protein, annexin V [46]. The fluorescence intensity is positively correlated with the magnitude of apoptosis induction [47]. As shown in Figure 5B, the majority of OV2008 cells incubated with the vehicle were primarily in quadrant I (90.86%), which contains viable cells and only 8.41% of the cells were present in quadrant II, containing apoptotic cells. After incubation with **DML6**, the percentage of live cells in quadrant I decreased to 53.39% ($p < 0.01$) for 5 μM of **DML6** and 22.37% ($p < 0.01$) for 20 μM of **DML6**. The percentage of apoptotic cells in quadrant II increased to 41.38% ($p < 0.001$) for 5 μM of **DML6** and 73.67% ($p < 0.001$) for 20 μM of **DML6** (Figure 5B). The loss of the mitochondrial membrane potential is indicated by a significant shift in the percentage of cells from quadrant I to quadrant II, and this was dependent on the concentration of **DML6**. Overall, the results indicate that **DML6** induces cell death by inducing apoptosis and MC in OV2008 cancer cells.

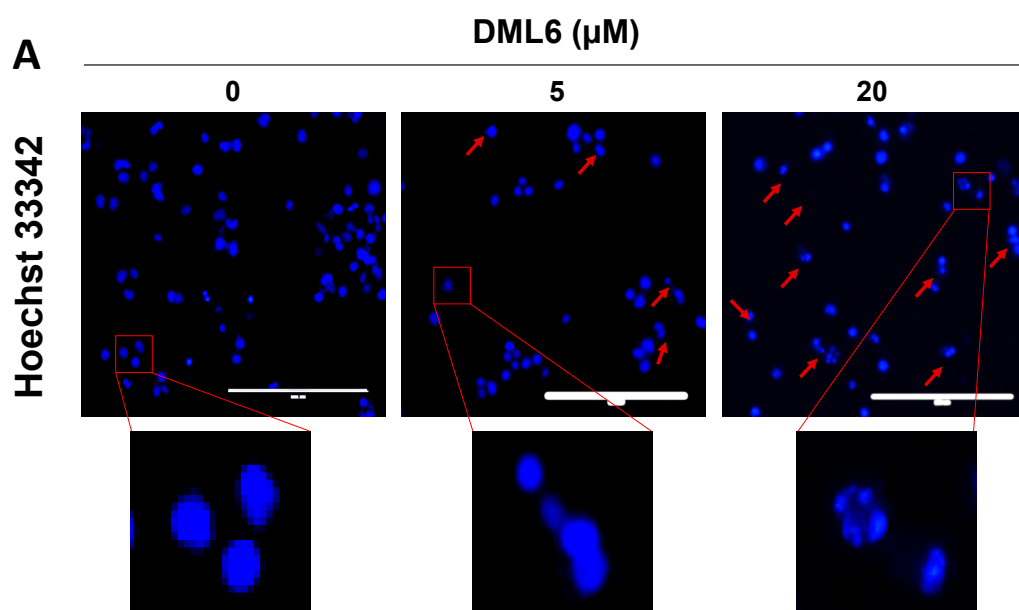


Figure 5. Cont.

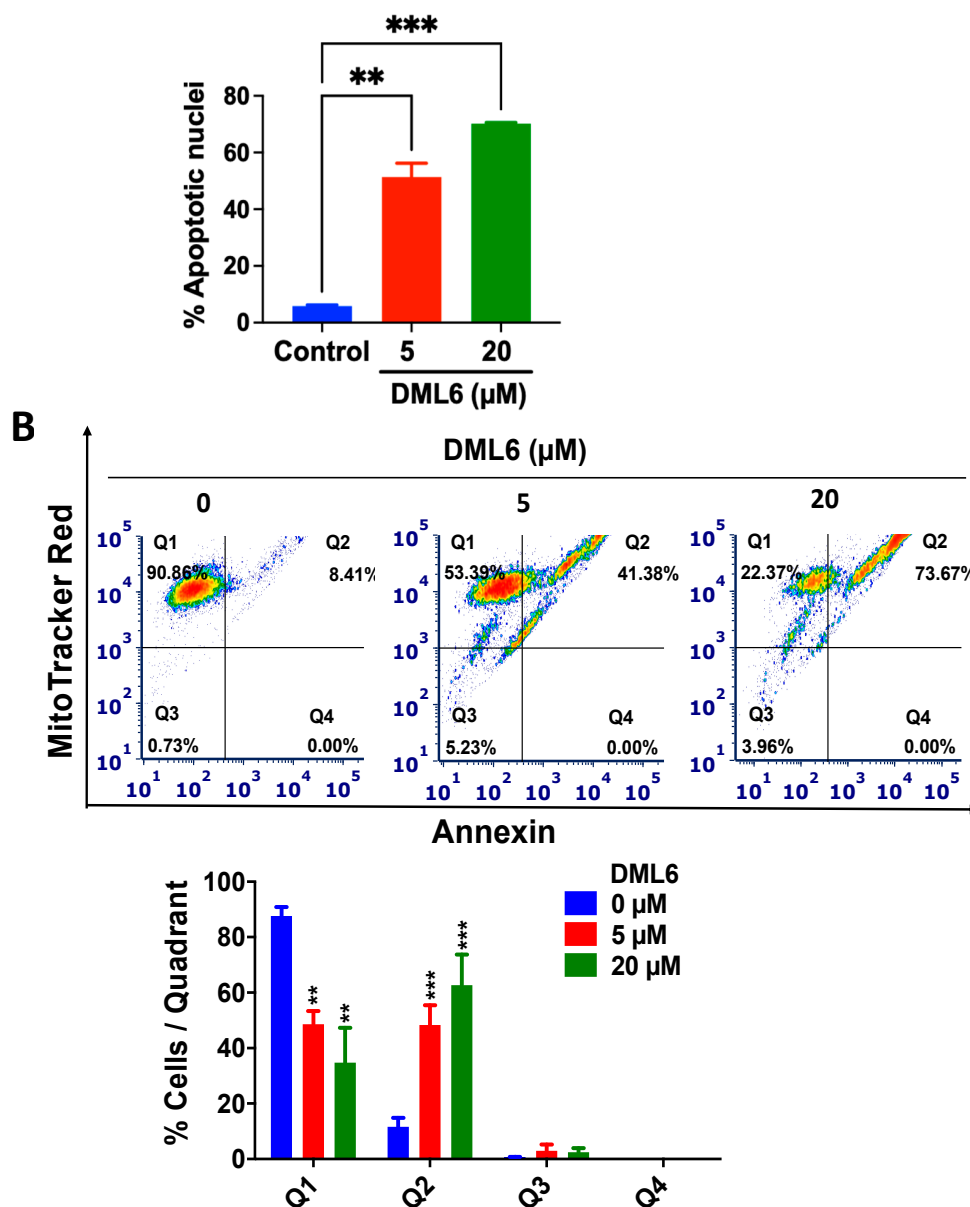


Figure 5. The effect of DML6 on apoptosis and the mitochondrial membrane potential. (A) Changes in the nuclear morphology in OV2008 cells incubated with the vehicle (0 μM), 5, or 20 μM of DML6. The cells were fixed and stained with the DNA binding dye, Hoechst 33342. The nuclear fragmentation and apoptotic chromatin condensation are indicated by red arrows. Multiple decondensed micronuclei were observed using an EVOS fluorescent microscope at 20× magnification. Scale bar represents 200 μm. A histogram quantitatively summarizing the % of apoptotic nuclei of cells incubated with 5 and 20 μM of DML6 as compared to cells incubated with the vehicle, is also shown. (B) A representative figure showing DML6 induced apoptosis. A histogram summarizing the results is also shown, ** $p < 0.01$, *** $p < 0.001$. The data represent the means \pm SEM of three independent experiments performed in triplicate.

2.7. DML6 Produces a Concentration-Dependent Increase in the Induction of Apoptosis by Activating the Intrinsic Apoptotic Pathway

Apoptosis, a form of programmed cell death that results in cell death, is one of the major mechanisms by which chemotherapeutic drugs achieve their therapeutic efficacy [48]. Morphologically, apoptosis is characterized by cytoplasmic and nuclear shrinkage, *chromatin condensation* at the nuclear periphery, nuclear fragmentations and blebbing of the plasma membrane [49]. Subsequently, this leads to the production of small apoptotic bodies

that have an intact cellular membrane and unaltered integrity of the organelles [50]. These apoptotic bodies are then released and eliminated by phagocytosis in the extracellular environment [51]. Apoptosis can occur in cells by the activation of either the extrinsic or intrinsic pathway. The intrinsic pathway, also known as the mitochondrial pathway, is activated in response to intrinsic stimuli such as DNA damage and cellular stress, and this signal is transmitted to the outer mitochondrial membrane (OMM) by proteins in the Bcl-2 family [52]. The Bcl-2 protein family consists of 3 subclasses of proteins: pro-survival/anti-apoptotic proteins, Bcl-2, Bcl-X_L, Bcl-W, A1 and Mcl-1, which bind to and sequester another class of proteins, the pore-forming proteins, Bax and Bak and pro-apoptotic BH3-only proteins, Bid, Bim, Bad, Hrk, Bik, Puma and Noxa [53,54]. The balance between the pro-apoptotic and anti-apoptotic proteins determines whether the cell dies or survives [55]. In normal cells, Bak is present in the OMM, whereas the majority of Bax is located in the cytosol and a small fraction is weakly bound to OMM [56]. Upon exposure to intrinsic stimuli, Bax is translocated from the cytosol to OMM, where Bax and Bak are oligomerized to their active conformational form [55]. This leads to the formation of pores in the mitochondria, causing OMM permeabilization and damage. As a result, several apoptogenic molecules, such as cytochrome c and DIABLO/Smac, are released from the mitochondrial membrane space to the cytosol which, in turn, activates the aspartate-specific proteases, known as caspases [51]. First, the initiator caspases, caspase-2, -8, -9, -10, are activated, followed by the subsequent cleavage and activation of the executioner caspases (caspase-3, -6, -7), which ultimately activates several cascades of proteins that produce cell death [57]. To determine whether **DML6**—induced apoptotic death in OV2008 cells occurs by activation of the intrinsic pathway, we performed a real-time quantification of apoptosis using the Caspase-3/7 Green reagent. The incubation of OV2008 cell with 5 or 20 μM of **DML6** significantly increased annexin V green fluorescence over time compared to the OV2008 cells incubated with the vehicle (Figure 6A). A significant difference in fluorescence intensity was observed between the control and **DML6** after 24 hours of incubation, indicating a significant apoptosis induction (Figure 6A). **DML6**, at 5 or 20 μM , significantly induced apoptosis in OV2008 cells in a time-dependent manner by activating caspase-3 and caspase-7, compared to cells incubated with the vehicle (5 and 20 μM , $p < 0.0001$) (Figure 6A). The lowest concentration of **DML6** (5 μM) required a longer incubation time (≈ 48 h) to induce apoptosis, compared to 20 μM of **DML6** (< 24 h; Figure 6A). These results indicate that **DML6** induces apoptotic cell death at early time points. Furthermore, we analyzed the levels of certain intrinsic apoptotic proteins using Western blotting. Our results indicate that 20 μM of **DML6** significantly decreased ($p < 0.01$) the levels of the anti-apoptotic protein, Bcl-2, and 5 and 20 μM of **DML6** significantly increased the expression of the pro-apoptotic proteins, Bax ($p < 0.05$) and Bak ($p < 0.01$). Furthermore, the incubation of OV2008 cells for 24 hours with 20 μM of **DML6** induced the cleavage of initiator caspase-9, compared to cells incubated with the vehicle. The incubation of OV2008 cells with 5 or 20 μM of **DML6** significantly increased the cleavage (and thus, the activation) of caspase-7 ($p < 0.05$) and caspase-3 ($p < 0.01$), respectively, compared to OV2008 cells incubated with the vehicle. These results indicate that **DML6** produces a significant induction of intrinsic apoptosis in OV2008 cells. Overall, these results indicate that the anticancer efficacy of **DML6** is due, in part, to the induction of intrinsic apoptosis.

Thus, our findings suggest that **DML6** may be a promising lead compound for pre-clinical development of anti-cancer agent against cervical cancer. However, there are some limitations to this study. The preliminary screening of compounds was performed in only two cervical cancer cell lines: OV2008 and HeLa cells. The cervical cancer cell line OV2008 used for this study was previously misidentified as an ovarian cancer model [58]. In 2012, genotypic profiling by Korch et. al revealed that OV2008 was identical to another cervical cancer cell line called ME-180 and was found to be HPV positive [59]. On the other hand, HeLa cells were not chosen for further in vitro experiments due to its history of cross-contamination with other cell lines [60,61]. More mechanistic studies should be conducted on more relevant cervical cancer cell lines. Similarly, in-vivo study using an

appropriate cervical cancer model is required to determine whether **DML6** is an efficacious and safe anti-cancer agent in vivo. Additionally, the nature of DNA damage (direct or indirect) induced by **DML6** was not studied in this study, its target identification and effect on DNA damage response signaling pathway along with alterations in cell cycle pathways needs further investigation.

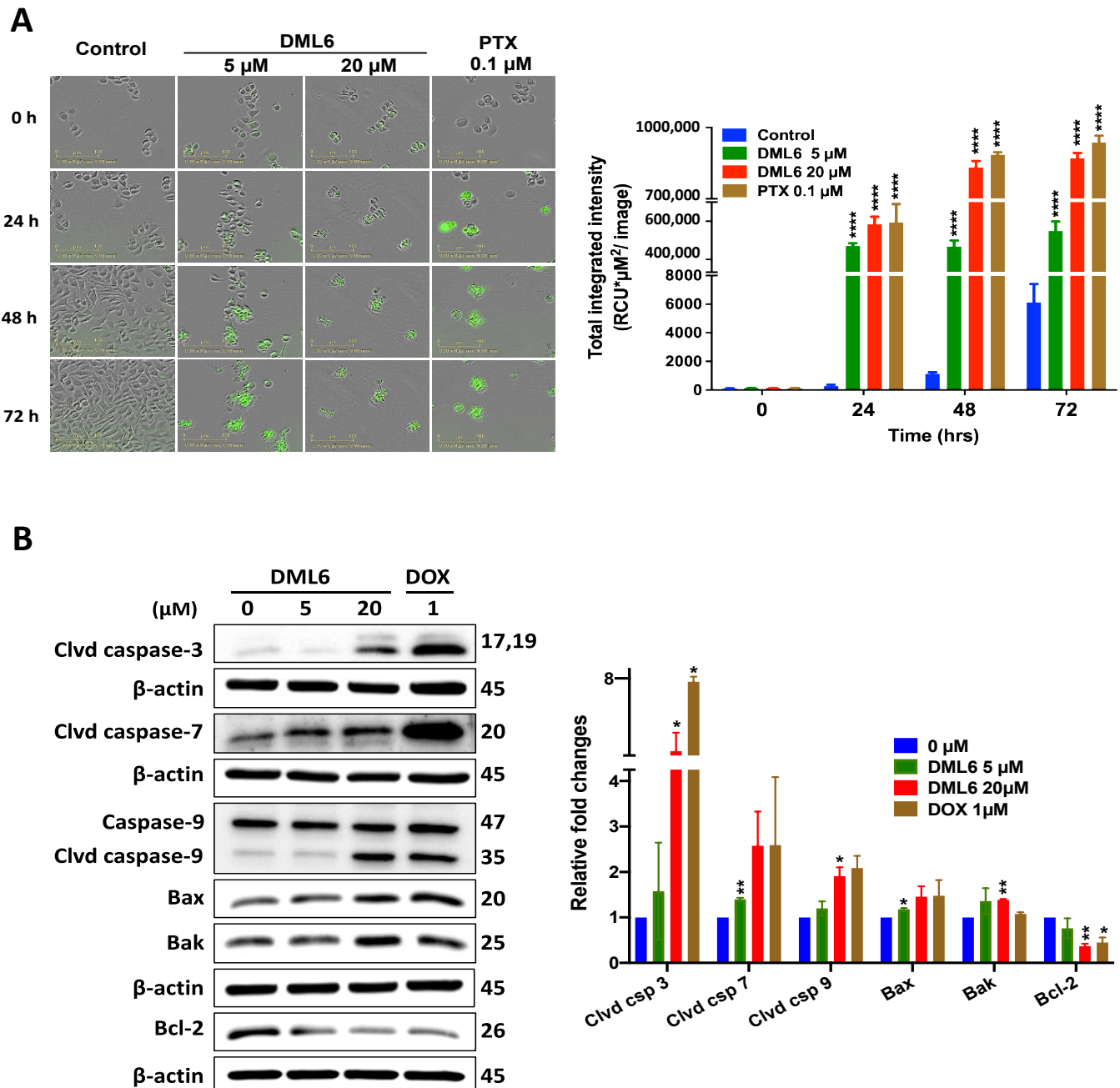


Figure 6. The effect of **DML6** on the induction of intrinsic apoptosis. **(A)** Fluorescence time-dependent experiments to measure the effect of **DML6** on the levels of apoptosis in OV2008 cells. Representative pictures of the fluorescence level of Cell Event™ Caspase-3/7 Green reagent after 24, 48, and 72 h of incubation. Bar = 100 μm . A histogram quantitatively summarizing apoptosis induction at different times for the vehicle, 5 or 20 μM of **DML6**, is also shown. The data were analyzed using a two-way ANOVA analysis of variance, followed by Bonferroni multiple comparison test; **** $p < 0.0001$. **(B)** Western blots for the proteins cleaved caspase-3, cleaved caspase-7, caspase-9, cleaved caspase-9, Bax, Bak and Bcl-2, following overnight incubation with 20 μM of **DML6**. The values of the proteins were normalized to β -actin levels. A histogram summarizing the levels of each protein is also shown. All data are presented as the means \pm SEM of four independent studies with * $p < 0.05$, ** $p < 0.01$ vs. control group. Clvd = cleaved; Csp = caspase.

3. Materials and Methods

3.1. Chemistry

All reagents and solvents used in the synthesis reactions were obtained from commercial sources and used without further purification. The progress of chemical reactions was monitored by thin layer chromatography (TLC), performed on pre-coated aluminum plates of silica gel 60 F254. The developed TLC plates were visualized for compound spots in UV light (254 nm) and/or by exposing the plates to iodine vapor. The separation of the compounds was conducted using column chromatography with silica gel (60–120 mesh). The melting points of the synthesized compounds were measured by an open capillary method on a semi-automatic digital melting point apparatus (Systonic, S-972, Panchkula, India) and the melting points were uncorrected. FTIR spectra were recorded using a spectrophotometer (Perkin Elmer, Spectrum RX-IFTIR). The $^1\text{H-NMR}$ spectra were recorded in a CDCl_3 run on a Bruker Avance-II (400 MHz) spectrometer (Bruker, Billerica, MA, USA), and tetramethylsilane (TMS) was used as the internal standard. The chemical shifts were reported in ppm relative to TMS and the coupling constants (J) were reported in Hz. The LCMS mass spectra were recorded on a Q-ToF Micro mass spectrometer with an electrospray ionization (ESI) interface (Waters, Milford, MA, USA) in the positive mode.

3.1.1. General Procedure for the Synthesis of Dialkylamino Substituted Chalcones (DML1–DML6)

Equimolar mixtures of substituted acetophenone 1a–f (15 mmol) and dialkylamino substituted benzaldehyde 2a–f (15 mmol) in ethanol (25 mL) were stirred for 10 min. Then, 40% NaOH (5 mL) was added dropwise, with continuous stirring for 2–8 h, at room temperature. Subsequently, the reaction mixture was poured into crushed ice (200 g) and neutralized with 10% HCl. The solid precipitate was filtered, washed with cold water and dried in air. The crude product was purified by recrystallization using absolute alcohol.

(*E*)-3-[4-(dimethyl amino)phenyl]-1-(pyridin-2-yl)prop-2-en-1-one (DML1). Mp: 126 °C; IR (KBr) ν (cm^{-1}): 3100, 1650, 1521, 1432, 1347; $^1\text{H NMR}$ (400 MHz, CDCl_3): δ 8.70 (s, 1H), 8.19 (d, 1H, $J = 7.5$), 8.09 (d, 1H, $J = 16.0$), 7.94 (d, 1H, $J = 16.0$), 7.85 (dd, 1H, $J = 7.0$), 7.65 (dd, 2H, $J = 8.0$), 7.44 (t, 1H, $J = 19.0$), 6.68 (dd, 2H, $J = 8.5$), 3.04 (s, 6H); ESIMS (m/z): 253.13 $[\text{M} + \text{H}]^+$.

(*E*)-3-[4-(diethyl amino)phenyl]-1-(pyridin-2-yl)prop-2-en-1-one (DML2). Mp: 142 °C; IR (KBr) ν (cm^{-1}): 3056, 1654, 1518, 1428, 1352; $^1\text{H NMR}$ (400 MHz, CDCl_3): δ 8.47 (s, 1H), 8.22 (d, 1H, $J = 7.5$), 8.14 (d, 1H, $J = 16.0$), 7.94 (d, 1H, $J = 16.0$), 7.89 (dd, 1H, $J = 7.0$), 7.62 (dd, 2H, $J = 8.0$), 7.38 (t, 1H, $J = 19.0$), 6.61 (dd, 2H, $J = 8.0$), 3.02 (s, 6H); 1.01 (m, 4H); ESIMS (m/z): 281.17 $[\text{M} + \text{H}]^+$.

(*E*)-3-[4-(dimethyl amino)phenyl]-1-(4-methoxy phenyl) prop-2-en-1-one (DML3). Mp: 118 °C; IR (KBr) ν (cm^{-1}): 3081, 1605, 1527, 1433, 1252; $^1\text{H NMR}$ (400 MHz, CDCl_3): δ 8.21 (d, 2H, $J = 8$), 8.14 (d, 1H, $J = 16.0$), 7.74 (d, 1H, $J = 16.0$), 7.59 (d, 2H, $J = 8.0$), 7.32 (d, 1H, $J = 8.0$), 6.98 (d, 1H, $J = 19.0$), 6.60 (d, 2H, $J = 8.5$), 3.90 (s, 3H), 3.01 (s, 6H); ESIMS (m/z): 282.16 $[\text{M} + \text{H}]^+$.

(*E*)-1-[3,4-dimethoxy phenyl]-3-(4-(dimethyl amino)phenyl)prop-2-en-1-one (DML4). Mp: 86 °C; IR (KBr) ν (cm^{-1}): 3052, 1622, 1540, 1429, 1238; $^1\text{H NMR}$ (400 MHz, CDCl_3): δ 8.19 (d, 2H, $J = 8$), 8.02 (d, 1H, $J = 16.0$), 7.54 (d, 1H, $J = 16.0$), 7.23 (d, 2H, $J = 8.0$), 7.02 (d, 1H, $J = 8.0$), 6.80 (d, 1H, $J = 19.0$), 6.67 (d, 2H, $J = 8.5$), 3.91 (s, 3H), 3.78 (s, 3H), 3.06 (s, 6H); ESIMS (m/z): 312.24 $[\text{M} + \text{H}]^+$.

(*E*)-1-[3,4-dimethoxy phenyl]-3-(4-(dimethyl amino)phenyl)prop-2-en-1-one (DML5). Mp: 110 °C; IR (KBr) ν (cm^{-1}): 3004, 1648, 1534, 1428, 1242; $^1\text{H NMR}$ (400 MHz, CDCl_3): δ 8.12 (d, 2H, $J = 8$), 7.89 (d, 1H, $J = 16.0$), 7.63 (d, 1H, $J = 16.0$), 7.23 (d, 2H, $J = 8.0$), 6.91 (d, 1H, $J = 8.0$), 6.87 (d, 1H, $J = 19.0$), 6.67 (d, 2H, $J = 8.5$), 3.87 (s, 3H), 3.07 (s, 4H), 1.12 (s, 6H); ESIMS (m/z): 311.2 $[\text{M} + \text{H}]^+$.

(*E*)-1-[2,4-dichloro phenyl]-3-(4-(dimethyl amino)phenyl)prop-2-en-1-one (**DML6**). Mp: 73 °C; IR (KBr) ν (cm⁻¹): 3100, 1646, 1568, 1434; ¹H NMR (400 MHz, CDCl₃): δ 8.50 (s, 1H), 8.12 (d, 1H, *J* = 7.5), 8.07 (d, 1H, *J* = 16.0), 7.84 (d, 1H, *J* = 16.0), 7.54 (dd, 1H, *J* = 7.0), 6.85 (dd, 2H, *J* = 8.0), 6.66 (dd, 2H, *J* = 8.5), 3.02 (s, 6H); ESIMS (*m/z*): 321.22 [M + H]⁺.

3.1.2. General Procedure for the Synthesis of Dialkylamino Substituted 1,3,5-Triphenyl-4,5-dihydro-1H-pyrazole (**DML7–DML12**)

The substituted chalcones **DML1–DML6** (5 mmol) and phenylhydrazine (5 mmol) in acetic acid (20 mL) were boiled under reflux for 6 h. After completion of the reaction as indicated by TLC, the reaction mixture was left to cool at room temperature. The solid separated from reaction mixture was filtered, washed with water and dried in air. The crude product was purified by recrystallization or silica-gel column chromatography in a mixture of hexane and ethyl acetate (9:1) as eluent.

N,N-dimethyl-4-[1-phenyl-5-(pyridin-2-yl)-4,5-dihydro-1H-pyrazol-3-yl]aniline (**DML7**). Mp: 179 °C: IR (KBr) ν (cm⁻¹): 3320, 1587, 1490, 1442; ¹H NMR (400 MHz, MHz, CDCl₃): δ 8.85 (d, 1H, *J* = 1.5), 8.53 (dd, 1H, *J* = 5), 8.28 (m, 1H), 7.54 (m, 1H), 7.16 (m, 4H), 7.06 (dd, 2H, *J* = 7.5), 6.94 (d, 2H, *J* = 8.5), 6.83 (t, 1H, *J* = 3), 5.36 (dd, 1H, *J* = 7), 3.78 (dd, 1H, *J* = 12.5), 3.07 (dd, 1H, *J* = 7), 2.96 (s, 6H); ESIMS (*m/z*): 343.17 [M + H]⁺.

N,N-diethyl-4-[1-phenyl-5-(pyridin-2-yl)-4,5-dihydro-1H-pyrazol-3-yl]aniline (**DML8**). Mp: 188 °C: IR (KBr) ν (cm⁻¹): 3377, 1579, 1488, 1436; ¹H NMR (400 MHz, MHz, CDCl₃): δ 8.68 (d, 1H, *J* = 1.5), 8.51 (dd, 1H, *J* = 5), 8.24 (m, 1H), 7.60 (m, 1H), 7.16 (m, 4H), 7.12 (dd, 2H, *J* = 7.5), 6.98 (d, 2H, *J* = 8.5), 6.82 (t, 1H, *J* = 3), 5.42 (dd, 1H, *J* = 7), 3.78 (dd, 1H, *J* = 12.5), 3.07 (dd, 1H, *J* = 7), 3.02 (m, 2H), 1.01 (s, 6H); ESIMS (*m/z*): 371.22 [M + H]⁺.

4-(5-[4-methoxyphenyl]-1-phenyl-4,5-dihydro-1H-pyrazol-3-yl)-*N,N*-dimethylaniline (**DML9**). Mp: 147 °C: IR (KBr) ν (cm⁻¹): 3320, 1568, 1483, 1440; ¹H NMR (400 MHz, MHz, CDCl₃): δ 7.65 (d, 2H, *J* = 1.5), 7.23 (m, 4H), 7.06 (m, 2H), 6.91 (dd, 2H, *J* = 7.5), 6.71 (d, 2H, *J* = 8.5), 6.67 (t, 1H, *J* = 3), 5.13 (dd, 1H, *J* = 7), 3.81 (s, 3H), 3.69 (dd, 1H, *J* = 7), 3.10 (s, 1H), 2.90 (s, 6H); ESIMS (*m/z*): 372.12 [M + H]⁺.

4-(5-(3,4-dimethoxyphenyl)-1-phenyl-4,5-dihydro-1H-pyrazol-3-yl)-*N,N*-dimethylaniline (**DML10**). Mp: 134 °C: IR (KBr) ν (cm⁻¹): 3316, 15548, 1478, 1442; ¹H NMR (400 MHz, MHz, CDCl₃): δ 7.49 (d, 1H, *J* = 1.5), 7.18 (m, 4H), 7.10 (m, 2H), 7.03 (dd, 1H, *J* = 7.5), 6.83 (dd, 1H, *J* = 7.5 Hz), 6.76 (t, 1H, *J* = 8.5), 6.69 (d, 2H, *J* = 7), 5.17 (dd, 1H, *J* = 7), 3.97 (s, 3H), 3.89 (s, 3H), 3.78 (m, 1H), 3.10 (m, 1H), 2.90 (s, 6H); ESIMS (*m/z*): 402.12 [M + H]⁺.

N,N-diethyl-4-(5-(4-methoxyphenyl)-1-phenyl-4,5-dihydro-1H-pyrazol-3-yl)aniline (**DML11**). Mp: 121 °C: IR (KBr) ν (cm⁻¹): 3351, 1550, 1447, 1428; ¹H NMR (400 MHz, MHz, CDCl₃): δ 7.66 (d, 2H, *J* = 7), 7.08 (m, 6H), 7.03 (dd, 2H, *J* = 7.5), 6.91 (dd, 2H, *J* = 7.5), 6.75 (t, 1H, *J* = 8.5), 6.61 (d, 2H, *J* = 7), 5.13 (dd, 1H, *J* = 7), 3.81 (s, 3H), 3.76 (m, 1H), 3.32 (m, 4H), 3.07 (m, 1H), 1.14 (s, 6H); ESIMS (*m/z*): 402.26 [M + H]⁺.

4-(5-(2,4-dichlorophenyl)-1-phenyl-4,5-dihydro-1H-pyrazol-3-yl)-*N,N*-dimethylaniline (**DML12**). Mp: 124 °C: IR (KBr) ν (cm⁻¹): 3017, 1542, 1469, 1446; ¹H NMR (400 MHz, MHz, CDCl₃): δ 7.80 (d, 1H, *J* = 7), 7.38 (d, 1H, *J* = 7), 7.23 (d, 1H), 7.18 (m, 4H), 7.07 (dd, 2H, *J* = 7.5), 6.80 (t, 1H, *J* = 8.5), 6.68 (d, 2H, *J* = 7), 5.20 (dd, 1H, *J* = 7), 3.76 (m, 1H), 3.98 (m, 1H), 3.31 (m, 1H), 2.91 (s, 6H); ESIMS (*m/z*): 410.01 [M + H]⁺.

3.2. Biological Studies

3.2.1. Cell Lines and Cell Culture

A panel of cancer cell lines, including cervical (OV2008 and HeLa), breast (MDA-MB-231), lung (A549) and colon (LOVO), prostate (DU145), human embryonic kidney cells (HEK293), human colon fibroblast cells (CRL1459), and Chinese hamster ovary cells (CHO), were grown as adherent monolayers in flasks containing Dulbecco's modified Eagle medium (DMEM), supplemented with 10% fetal bovine serum (FBS) and 1% penicillin and streptomycin, in a humidified incubator with 5% CO₂ at 37 °C.

3.2.2. MTT Assay

The cytotoxic efficacy of the novel derivatives in the cancer cell lines was determined using the 3-(4,5-dimethylthiazol-2-yl)-2,5-diphenyltetrazolium bromide (MTT) assay, as previously described [62,63]. The cells were seeded evenly (180 μL /well) in 96-well plates, at a density of 3000–5000 cells/well and incubated with serial dilutions of the compounds ranging from 0.1 to 100 μM . The MTT dye (4 mg/ml) was added after 72 h of incubation and incubated with the cells for an additional 4 h at 37 °C, allowing the viable cells to biotransform the yellow-colored MTT into dark-blue formazan crystals. Following incubation, the medium was aspirated, and the formazan crystals were dissolved by adding 100 μL of DMSO to each well. Cytation™ 5 and Cytation™ 7 multi-mode detector (Bio Tek Instruments, Winooski, VT, USA) was used to determine the absorbance readings at a wavelength of 570 nm. The IC₅₀ values were determined based on 3 separate experiments, with each experiment carried out in triplicate. The selectivity of the compounds was determined by comparing their IC₅₀ values in cervical cancer compared to the normal epithelial cell lines, HEK293, CHO, and CRL1459.

3.2.3. Time-Dependent Cytotoxicity Assays

IncuCyte™ Live-Cell Morphology Study

Real-time live cell analysis was performed as previously described [64]. In order to determine the morphological changes induced by **DML6**, OV2008 cells were seeded at 4000 cells/well in a 96-well plate and incubated overnight at 37 °C, with 5% CO₂ in an incubator. Subsequently, the cells were incubated with 1, 3 or 30 μM of **DML6** or vehicle (DMEM media with 10% FBS and 1% penicillin and streptomycin) and placed in an IncuCyte® S3 Live-Cell Analysis System (Ann Arbor, MI, USA). IncuCyte was then programmed to capture the images at different time points (0, 24, 48 and 72 h), using the integrated IncuCyte S3 software version 2020B (Essen BioScience, Ann Arbor, MI, USA).

IncuCyte™ Cytotox Green Assay

The IncuCyte cytotox green reagent (Catalog # 4633, Essen BioScience, Ann Arbor, MI, USA) was used for real time quantification of dead OV2008 cells as previously described [65]. This dye will only penetrate into cells with non-intact membranes (dead or non-viable cells). As the cells die, the increase in cell membrane permeability allows the reagent to enter the nucleus and bind to DNA, which emits green fluorescence at an excitation maximum of 491 nm and emission maximum of 509 nm. OV2008 cells were seeded (100 μL /well) in a 96-well plate and incubated overnight. The following day, **DML6** (0.1–100 μM) was prepared at 3X the final assay concentrations in diluted IncuCyte™ Cytotox Reagent and added to each well (50 μL /well). The cells were immediately placed in the IncuCyte® S3 Live-Cell Analysis System (Essen BioScience, Ann Arbor, MI, USA) and images were taken every 2 h up to 72 h and analyzed using the integrated IncuCyte S3 software version 2020B (Essen BioScience, Ann Arbor, MI, USA).

3.2.4. Time-Dependent Apoptosis Induction Study

Cell Event™ Caspase-3/7 Green Detection Reagent from (Catalog # C10423, Life Technologies, Carlsbad, CA, USA), which is a novel fluorogenic substrate for activated caspase-3/7 that is compatible with living cells, was used to determine apoptosis activation in real-time in OV2008 cells incubated with **DML6**. Briefly, OV2008 cells were seeded in 96-well plates at a density of 1×10^3 cell/well. Twenty-four hours later, the cells were incubated with the vehicle (DMEM media with 10% FBS and 1% penicillin and streptomycin), 5 or 20 μM of **DML6** for 72 h. Five micromolar of the apoptosis-detecting reagents were added to the cells immediately after **DML6** and were incubated for up to 72 h at 37 °C. Fluorescence was determined every 24h using a live cell imaging system (IncuCyte Zoom, Essen Bioscience, Ann Arbor, MI, USA, using an absorption/emission maximum of ~502/530 nm.

3.2.5. Cell Lysis and Western Blot Analysis

The OV2008 cells were lysed to obtain total cellular protein fractions using Mammalian Protein Extraction Reagent (Catalog # 78501, M-PER™, Thermo Fisher Scientific, Waltham, MA, USA). The cells were seeded in 6 mm plates at a density of 1×10^6 and incubated with 5 or 20 μM of **DML6** or 1 μM of doxorubicin (Catalog # T1-2-, TargetMol, Boston, MA, USA) (a positive control) for 24 h. The following day, the cells were washed with ice-cold PBS, scraped using a cell scraper and collected in Eppendorf tubes. The tubes were centrifuged at 1500 RPM at 4 °C for 5 min. The solution was discarded and replaced with 70 μL of the cell lysis buffer (M-PER reagent, 100 mM Sodium Orthovanadate (NaOV) at a final concentration of 2.5 mM) and a 100X protease inhibitor cocktail (Catalog # P8340, Sigma-Aldrich, St. Louis, MO, USA, final concentration of 1X, containing of aprotinin, bestatin, E-64, leupeptin and pepstatin). Thirty minutes later, the resulting solution was centrifuged at 10,000 RPM at 4 °C for 5 min and the supernatant was collected. The protein concentration of the cell extracts was determined using the bicinchoninic acid (BCA) (Catalog # 786-570, G-Biosciences, Saint Louis, MO, USA) quantification assay. The extracted proteins were loaded and separated onto a 10% tris-glycine gel and the proteins were transferred from the gel onto a 0.45 μM PVDF membrane. After blocking the membranes using 5% milk prepared in Tris-buffered saline containing Tween 20 (TBST) for 1 hour, followed by washing for 15 min, the membranes were incubated overnight with primary antibodies against Rabbit Cleaved caspase-3 (Catalog # 9664S) (1:1000), rabbit Cleaved caspase-7 (Catalog # 8438S)(1:1000), rabbit Caspase 9 (Catalog # 9502S) (1:1000), mouse Cleaved Caspase-9 (Catalog # (1:1000), rabbit Bak (Catalog # 12105T) (1:1000), rabbit Bax (Catalog # 5023T) (1:1000), mouse Bcl-2 (Catalog # 15071S) (1:1000), mouse beta-Actin (Catalog # 3700S) (1:500) (Cell Signaling Technology, Danvers, MA, USA). The following day, the membranes were washed for 30 minutes and incubated for 90 minutes with horseradish peroxidase labeled (HRP) anti-rabbit and anti-mouse secondary antibodies (1:4000 dilutions) in 5% milk prepared in TBST. Subsequently, the membranes were washed for 30 minutes with TBST and developed by SuperSignal™ West Pico PLUS Chemiluminescent Substrate (Thermo Fisher Scientific, Waltham, MA, USA). Subsequently, G:Box Chemi XX6/XX9 (Syngene, Frederick, MD, USA) was used to detect the blots. Finally, the amount of protein in each blot was quantified using the Image J software (NIH, Bethesda, MD, USA). All data were calculated as a ratio to β -actin.

3.2.6. Nuclear Staining Using Hoechst 33258 Dye

Nuclear fragmentation and chromatin condensation were detected using the Hoechst 33258 DNA dye as previously described [66]. OV2008 cells were seeded at a density of 250,000 cells/mL in 6-well plates and incubated overnight at 37 °C. The next day, the cells were incubated with the vehicle (DMEM media with 10% FBS and 1% penicillin and streptomycin), 5 or 20 μM of **DML6** and further incubated overnight at 37 °C. The cells were fixed and stained with the Hoechst 33258 DNA dye for at least 30 min. The stained nucleus fluorescence was detected using an EVOS digital microscope at wavelengths of 460–490 nm.

3.2.7. Cell Cycle Analysis

Cell cycle analysis was conducted using flow cytometry cell cycle analysis with propidium iodide (PI) as previously described [67]. OV2008 cells were plated into 6-well plates at 2.5×10^5 cells/well. The cells were incubated with the vehicle, 5 or 20 μM of **DML6** for 24 h. The next day, the cells were trypsinized with 0.25% trypsin, 2.21 mM EDTA, 1X, washed, counted, and resuspended in 1ml of ice-cold PBS. The cells were then stained with 200 μL (50 $\mu\text{g}/\text{ml}$ stock solution propidium iodide (PI) dye and incubated for at least 15 min. The distribution of the cells in each phase of the cell cycle after incubation with the vehicle or **DML6** was determined using A BD FACSCanto™ flow cytometer (BD Biosciences, Becton-Dickinson, San Jose, CA, USA) and analyzed using FCS Express 7 plus De Novo software (Glendale, CA, USA).

3.2.8. Apoptosis and Mitochondrial Membrane Potential Analysis

MitoTracker®Red and Alexa Fluor 488 annexin V kits for flow cytometry (Molecular Probes Inc., Eugene, OR, USA) were used to determine the mitochondrial membrane potential and apoptosis, respectively, in OV2008 cells, as previously described [68]. OV2008 cells were seeded in 6-well plates and incubated with the vehicle, 5 or 20 µM of **DML6** for 24 h. The following day, the cells were trypsinized using 0.25% trypsin, 2.21 mM EDTA, 1×, counted and 4 µL of 10 µM MitoTracker®Red working solution was added to 1 mL of the harvested cells. The cells were incubated at 37 °C with 5% CO₂ for 30 min. The cells were washed with ice-cold phosphate-buffered saline (PBS), followed by cell resuspension in 100 µL of the annexin binding buffer. The cell suspensions were then incubated with 5 µL of Alexa Fluor 488 annexin V for 15 min, followed by adding 400 µL of the annexin-binding buffer. Finally, flow cytometry was used to detect the fluorescence of stained cells at the following excitation/emission maximum: Alexa Fluor® 488 annexin V: 499/521 nm; MitoTracker®Red: 579/599 nm, using a flow cytometer BD FACSCanto™ (BD Biosciences, Becton-Dickinson, San Jose, CA, USA) and analyzed using FCS Express 7 plus De Novo software (Glendale, CA, USA).

3.2.9. Reactive Oxygen Species (ROS) Detection

The compound, 2',7'-dichlorofluorescein (H₂DCFDA), was used to detect ROS as previously described [69]. OV2008 cells were seeded at a density of 250,000 cells/ml. After 24 h of incubation with the vehicle, 5 or 20 µM of **DML6**, the cells were incubated with H₂DCFDA for 30 min at 37 °C. The cells were washed 3 times with 1X PBS for 5 min. The levels of reactive oxygen species were then determined based on the fluorescence level of the oxidized DCFDA dye (excitation at 485 nm and emission at 535), using a EVOS digital fluorescent microscope at 20× magnification.

3.2.10. Statistical Analysis

The data were statistically analyzed with GraphPad Prism9.1.2 software from Graph-Pad Software (San Diego, CA, USA). The MTT assay data was analyzed using one-way ANOVA, followed by Bonferroni's post-hoc analysis. The data from ROS assay and nuclear staining were analyzed using the one-way ANOVA, followed by Dunnett's post-hoc analysis. Similarly, the statistical analysis of cell cycle assay was computed using two-way ANOVA, followed by Tukey's post-hoc analysis. The mitochondrial membrane potential and time-dependent apoptosis induction study were performed using two-way ANOVA, followed by Dunnett's post-hoc analysis, respectively. Finally, the data from the Western blotting experiment were analyzed using unpaired *t*-test. All experiments were repeated in triplicate. The data are expressed as the mean ± the standard error of mean (SEM). The a priori significance level for this study was $p < 0.05$.

4. Conclusions

In conclusion, a series of 12 novel chalcone derivatives were designed, synthesized and characterized. After screening these compounds in a panel of cancer cell lines to determine their anti-proliferative efficacy, **DML6**, had the highest in vitro efficacy, with an IC₅₀ value of 7.8 µM and had selectivity for inducing cytotoxicity in the cervical carcinoma cell line, OV2008 compared to other epithelial cancer cells i.e., HEK293, LOVO, MDAMB-231, DU-145 and A549. **DML6** induced oxidative stress and arrested the cell cycle at the G2 phase. The incubation of OV2008 cells with **DML6** produced a loss of the mitochondrial membrane potential, resulting in apoptosis and mitotic catastrophe. The apoptotic efficacy of **DML6** was due to its inhibition of the anti-apoptotic protein, Bcl-2, and the upregulation of the pro-apoptotic proteins, Bax and Bak. **DML6** activated caspase-9 and cleaved caspase-3 and -7, producing apoptosis by activating the intrinsic apoptotic pathway. Overall, our results suggest that **DML6** could be a potential lead compound for the pre-clinical development of novel anti-cancer compounds.

Supplementary Materials: The following material is available online, Table S1: The antiproliferative efficacy of the DML1–DML12 compounds on the proliferation of cervical HeLa cancer cell line. Figure S1. The efficacy of DML6 in HeLa cancer cells.

Author Contributions: Conceptualization, A.K.T. and K.C.; methodology, J.M.L., S.M., N.H., K.M. and N.S.H.N.M.; software, S.M. and N.H.; validation, A.K.T., P.T. and K.C.; formal analysis, R.P., M.E. and P.T.; investigation, R.P., K.M. and P.T.; resources, A.K.T. and K.C.; data curation, S.M. and N.H.; writing—original draft preparation, S.M., N.H. and M.E.; writing—review and editing, A.K.T., K.C., M.P., D.R. and M.E.; visualization, A.K.T.; K.C. and N.S.H.N.M.; supervision, A.K.T. and K.C.; project administration, S.M.; N.H. and J.M.L.; funding acquisition, A.K.T. and K.C. All authors have read and agreed to the published version of the manuscript.

Funding: This manuscript has been supported, in part, by University of Toledo startup grants (F110760 to A.K.T.).

Institutional Review Board Statement: Not applicable.

Informed Consent Statement: Not applicable.

Data Availability Statement: The raw data presented in this study is available on request to the corresponding author. Supporting information is provided in the supplementary file.

Acknowledgments: We thank Charles R. Ashby, (St. John’s University, NY) for providing editorial assistance and David Terrero, University of Toledo, for their critical help in validating key experiments.

Conflicts of Interest: The authors declare no conflict of interest.

References

1. Sung, H.; Ferlay, J.; Siegel, R.L.; Laversanne, M.; Soerjomataram, I.; Jemal, A.; Bray, F. Global cancer statistics 2020: GLOBOCAN estimates of incidence and mortality worldwide for 36 cancers in 185 countries. *CA Cancer J. Clin.* **2021**, *71*, 209–249. [CrossRef] [PubMed]
2. World Health Organization. Human Papillomavirus (HPV) and Cervical Cancer. 2020. Available online: [https://www.who.int/en/news-room/fact-sheets/detail/human-papillomavirus-\(hpv\)-and-cervical-cancer](https://www.who.int/en/news-room/fact-sheets/detail/human-papillomavirus-(hpv)-and-cervical-cancer) (accessed on 24 June 2021).
3. Siegel, R.L.; Miller, K.D.; Fuchs, H.E.; Jemal, A. Cancer Statistics, 2021. *CA Cancer J. Clin.* **2021**, *71*, 7–33. [CrossRef]
4. Crosbie, E.J.; Einstein, M.H.; Franceschi, S.; Kitchener, H.C. Human papillomavirus and cervical cancer. *Lancet* **2013**, *382*, 889–899. [CrossRef]
5. Dunne, E.F.; Unger, E.R.; Sternberg, M.; McQuillan, G.; Swan, D.C.; Patel, S.S.; Markowitz, L.E. Prevalence of HPV infection among females in the United States. *JAMA* **2007**, *297*, 813–819. [CrossRef] [PubMed]
6. American Cancer Society. Cancer Facts and Figures. 2021. Available online: <https://www.cancer.org/content/dam/cancer-org/research/cancer-facts-and-statistics/annual-cancer-facts-and-figures/2021/cancer-facts-and-figures-2021.pdf> (accessed on 24 June 2021).
7. Bouvard, V.; Baan, R.; Straif, K.; Grosse, Y.; Secretan, B.; El Ghissassi, F.; Benbrahim-Tallaa, L.; Guha, N.; Freeman, C.; Galichet, L. A review of human carcinogens—Part B: Biological agents. *Lancet Oncol.* **2009**, *10*, 321–322. [CrossRef]
8. Serrano, B.; Brotons, M.; Bosch, F.X.; Bruni, L. Epidemiology and burden of HPV-related disease. *Best Pract. Res. Clin. Obstet. Gynaecol.* **2018**, *47*, 14–26. [CrossRef] [PubMed]
9. Pal, A.; Kundu, R. Human Papillomavirus E6 and E7: The Cervical Cancer Hallmarks and Targets for Therapy. *Front. Microbiol.* **2020**, *10*. [CrossRef] [PubMed]
10. Cohen, P.A.; Jhingran, A.; Oaknin, A.; Denny, L. Cervical cancer. *Lancet* **2019**, *393*, 169–182. [CrossRef]
11. Landoni, F.; Manes, A.; Colombo, A.; Placa, F.; Milani, R.; Perego, P.; Favini, G.; Ferri, L.; Mangioni, C. Randomised study of radical surgery versus radiotherapy for stage Ib-IIa cervical cancer. *Lancet* **1997**, *350*, 535–540. [CrossRef]
12. Rotman, M.; Sedlis, A.; Piedmonte, M.R.; Bundy, B.; Lentz, S.S.; Muderspach, L.I.; Zaino, R.J. A phase III randomized trial of postoperative pelvic irradiation in Stage IB cervical carcinoma with poor prognostic features: Follow-up of a gynecologic oncology group study. *Int. J. Radiat. Oncol. Biol. Phys.* **2006**, *65*, 169–176. [CrossRef]
13. Delgado, G.; Bundy, B.; Zaino, R.; Sevin, B.-U.; Creasman, W.T.; Major, F. Prospective surgical-pathological study of disease-free interval in patients with stage IB squamous cell carcinoma of the cervix: A Gynecologic Oncology Group study. *Gynecol. Oncol.* **1990**, *38*, 352–357. [CrossRef]
14. Josefson, D. Adding chemotherapy improves survival in cervical cancer. *BMJ Clin. Res. Ed.* **1999**, *318*, 623. [CrossRef]
15. Zhu, H.; Luo, H.; Zhang, W.; Shen, Z.; Hu, X.; Zhu, X. Molecular mechanisms of cisplatin resistance in cervical cancer. *Drug Des. Devel. Ther.* **2016**, *10*, 1885–1895. [CrossRef] [PubMed]
16. Madden, E.C.; Gorman, A.M.; Logue, S.E.; Samali, A. Tumour Cell Secretome in Chemoresistance and Tumour Recurrence. *Trends Cancer* **2020**, *6*, 489–505. [CrossRef] [PubMed]

17. Wang, L.; Dai, G.; Yang, J.; Wu, W.; Zhang, W. Cervical Cancer Cell Growth, Drug Resistance, and Epithelial-Mesenchymal Transition Are Suppressed by γ -Secretase Inhibitor RO4929097. *Med. Sci. Monit. Int. Med. J. Exp. Clin. Res.* **2018**, *24*, 4046–4053. [[CrossRef](#)]
18. Leonard, G.D.; Fojo, T.; Bates, S.E. The role of ABC transporters in clinical practice. *Oncologist* **2003**, *8*, 411–424. [[CrossRef](#)]
19. Wagner, W.; Kania, K.D.; Blauz, A.; Ciszewski, W.M. The lactate receptor (HCAR1/GPR81) contributes to doxorubicin chemoresistance via ABCB1 transporter up-regulation in human cervical cancer HeLa cells. *J. Physiol. Pharm.* **2017**, *68*, 555–564.
20. Karthikeyan, C.; Moorthy, S.H.N.; Ramasamy, S.; Vanam, U.; Manivannan, E.; Karunakaran, D.; Trivedi, P. Advances in chalcones with anticancer activities. *Recent. Pat. Anticancer Drug Discov.* **2015**, *10*, 97–115. [[CrossRef](#)] [[PubMed](#)]
21. Gao, F.; Huang, G.; Xiao, J. Chalcone hybrids as potential anticancer agents: Current development, mechanism of action, and structure-activity relationship. *Med. Res. Rev.* **2020**, *40*, 2049–2084. [[CrossRef](#)]
22. Mohamed, M.F.A.; Abu-Rahma, G.E.-D.A. Molecular targets and anticancer activity of quinoline–chalcone hybrids: Literature review. *RSC Adv.* **2020**, *10*, 31139–31155. [[CrossRef](#)]
23. Zhuang, C.; Zhang, W.; Sheng, C.; Zhang, W.; Xing, C.; Miao, Z. Chalcone: A Privileged Structure in Medicinal Chemistry. *Chem. Rev.* **2017**, *117*, 7762–7810. [[CrossRef](#)]
24. Alam, R.; Alam, M.A.; Panda, A.K.; Rahisuddin. Design, Synthesis, and Cytotoxicity Evaluation of 3-(5-(3-(aryl)-1-phenyl-1H-pyrazol-4-yl)-1-phenyl-4,5-dihydro-1H-pyrazol-3-yl)pyridine and 5-(3-(aryl)-1-phenyl-1H-pyrazol-4-yl)-3-(pyridin-3-yl)-4,5-dihydropyrazole-1-carbaldehyde Derivatives as Potential Anticancer Agents. *J. Heterocycl. Chem.* **2017**, *54*, 1812–1821. [[CrossRef](#)]
25. Alex, J.M.; Kumar, R. 4,5-Dihydro-1H-pyrazole: An indispensable scaffold. *J. Enzym. Inhib. Med. Chem.* **2014**, *29*, 427–442. [[CrossRef](#)] [[PubMed](#)]
26. Yang, W.; Hu, Y.; Yang, Y.-S.; Zhang, F.; Zhang, Y.-B.; Wang, X.-L.; Tang, J.-F.; Zhong, W.-Q.; Zhu, H.-L. Design, modification and 3D QSAR studies of novel naphthalin-containing pyrazoline derivatives with/without thiourea skeleton as anticancer agents. *Bioorganic Med. Chem.* **2013**, *21*, 1050–1063. [[CrossRef](#)] [[PubMed](#)]
27. Fang, X.; Fang, L.; Gou, S.; Cheng, L. Design and synthesis of dimethylaminomethyl-substituted curcumin derivatives/analogues: Potent antitumor and antioxidant activity, improved stability and aqueous solubility compared with curcumin. *Bioorg. Med. Chem. Lett.* **2013**, *23*, 1297–1301. [[CrossRef](#)] [[PubMed](#)]
28. D’anneo, A.; Carlisi, D.; Lauricella, M.; Puleio, R.; Martinez, R.; Di Bella, S.; Di Marco, P.; Emanuele, S.; Di Fiore, R.; Guercio, A. Parthenolide generates reactive oxygen species and autophagy in MDA-MB231 cells. A soluble parthenolide analogue inhibits tumour growth and metastasis in a xenograft model of breast cancer. *Cell Death Dis.* **2013**, *4*, e891. [[CrossRef](#)] [[PubMed](#)]
29. Kacprzak, K.M. Chemistry and Biology of Camptothecin and its Derivatives. In *Natural Products: Phytochemistry, Botany and Metabolism of Alkaloids, Phenolics and Terpenes*; Ramawat, K.G., Mérillon, J.-M., Eds.; Springer: Berlin/Heidelberg, Germany, 2013; pp. 643–682. [[CrossRef](#)]
30. Lim, M.; Otto-Duessel, M.; He, M.; Su, L.; Nguyen, D.; Chin, E.; Alliston, T.; Jones, J.O. Ligand-Independent and Tissue-Selective Androgen Receptor Inhibition by Pyrvinium. *ACS Chem. Biol.* **2014**, *9*, 692–702. [[CrossRef](#)] [[PubMed](#)]
31. Fuhrmann, U.; Hess-Stumpp, H.; Cleve, A.; Neef, G.; Schwede, W.; Hoffmann, J.; Fritzscheier, K.-H.; Chwalisz, K. Synthesis and Biological Activity of a Novel, Highly Potent Progesterone Receptor Antagonist. *J. Med. Chem.* **2000**, *43*, 5010–5016. [[CrossRef](#)]
32. Rastogi, R.P.; Singh, S.P.; Häder, D.P.; Sinha, R.P. Detection of reactive oxygen species (ROS) by the oxidant-sensing probe 2',7'-dichlorodihydrofluorescein diacetate in the cyanobacterium *Anabaena variabilis* PCC 7937. *Biochem. Biophys. Res. Commun.* **2010**, *397*, 603–607. [[CrossRef](#)]
33. Ziegler, U.; Groscurth, P. Morphological features of cell death. *Physiology* **2004**, *19*, 124–128. [[CrossRef](#)]
34. Castedo, M.; Perfettini, J.-L.; Roumier, T.; Andreau, K.; Medema, R.; Kroemer, G. Cell death by mitotic catastrophe: A molecular definition. *Oncogene* **2004**, *23*, 2825–2837. [[CrossRef](#)]
35. Kops, G.J.; Weaver, B.A.; Cleveland, D.W. On the road to cancer: Aneuploidy and the mitotic checkpoint. *Nat. Rev. Cancer* **2005**, *5*, 773–785. [[CrossRef](#)] [[PubMed](#)]
36. Yamada, H.Y.; Gorbisky, G.J. Spindle checkpoint function and cellular sensitivity to antimetabolic drugs. *Mol. Cancer Ther.* **2006**, *5*, 2963–2969. [[CrossRef](#)] [[PubMed](#)]
37. Chang, B.-D.; Broude, E.V.; Dokmanovic, M.; Zhu, H.; Ruth, A.; Xuan, Y.; Kandel, E.S.; Lausch, E.; Christov, K.; Roninson, I.B. A senescence-like phenotype distinguishes tumor cells that undergo terminal proliferation arrest after exposure to anticancer agents. *Cancer Res.* **1999**, *59*, 3761–3767. [[PubMed](#)]
38. Vakifahmetoglu, H.; Olsson, M.; Zhivotovsky, B. Death through a tragedy: Mitotic catastrophe. *Cell Death Differ.* **2008**, *15*, 1153–1162. [[CrossRef](#)] [[PubMed](#)]
39. Kobayashi, D.; Shibata, A.; Oike, T.; Nakano, T. One-step protocol for evaluation of the mode of radiation-induced clonogenic cell death by fluorescence microscopy. *J. Vis. Exp. JoVE* **2017**, *128*, 56338. [[CrossRef](#)] [[PubMed](#)]
40. Castedo, M.; Kroemer, G. Mitotic catastrophe: A special case of apoptosis. *J. Soc. Biol.* **2004**, *198*, 97–103. [[CrossRef](#)] [[PubMed](#)]
41. Reed, J.C. Cytochrome c: Can't live with it—Can't live without it. *Cell* **1997**, *91*, 559–562. [[CrossRef](#)]
42. Wong, R.S. Apoptosis in cancer: From pathogenesis to treatment. *J. Exp. Clin. Cancer Res.* **2011**, *30*, 87. [[CrossRef](#)]
43. Chipuk, J.E.; Bouchier-Hayes, L.; Green, D.R. Mitochondrial outer membrane permeabilization during apoptosis: The innocent bystander scenario. *Cell Death Differ.* **2006**, *13*, 1396–1402. [[CrossRef](#)]
44. Mariño, G.; Kroemer, G. Mechanisms of apoptotic phosphatidylserine exposure. *Cell Res.* **2013**, *23*, 1247–1248. [[CrossRef](#)] [[PubMed](#)]

45. Pistritto, G.; Trisciuglio, D.; Ceci, C.; Garufi, A.; D'Orazi, G. Apoptosis as anticancer mechanism: Function and dysfunction of its modulators and targeted therapeutic strategies. *Aging* **2016**, *8*, 603. [CrossRef] [PubMed]
46. Lizarbe, M.A.; Barrasa, J.I.; Olmo, N.; Gavilanes, F.; Turnay, J. Annexin-phospholipid interactions. Functional implications. *Int. J. Mol. Sci.* **2013**, *14*, 2652–2683. [CrossRef]
47. Vermes, I.; Haanen, C.; Steffens-Nakken, H.; Reutellingsperger, C. A novel assay for apoptosis flow cytometric detection of phosphatidylserine expression on early apoptotic cells using fluorescein labelled annexin V. *J. Immunol. Methods* **1995**, *184*, 39–51. [CrossRef]
48. Fink, S.L.; Cookson, B.T. Apoptosis, pyroptosis, and necrosis: Mechanistic description of dead and dying eukaryotic cells. *Infect. Immun.* **2005**, *73*, 1907–1916. [CrossRef]
49. Prokhorova, E.A.; Egorshina, A.Y.; Zhivotovsky, B.; Kopeina, G.S. The DNA-damage response and nuclear events as regulators of nonapoptotic forms of cell death. *Oncogene* **2020**, *39*, 1–16. [CrossRef]
50. Galluzzi, L.; Vitale, I.; Aaronson, S.A.; Abrams, J.M.; Adam, D.; Agostinis, P.; Alnemri, E.S.; Altucci, L.; Amelio, I.; Andrews, D.W.; et al. Molecular mechanisms of cell death: Recommendations of the Nomenclature Committee on Cell Death 2018. *Cell Death Differ.* **2018**, *25*, 486–541. [CrossRef]
51. Elmore, S. Apoptosis: A review of programmed cell death. *Toxicol. Pathol.* **2007**, *35*, 495–516. [CrossRef]
52. Dewson, G.; Kluck, R.M. Mechanisms by which Bak and Bax permeabilise mitochondria during apoptosis. *J. Cell Sci.* **2009**, *122*, 2801–2808. [CrossRef]
53. Shamas-Din, A.; Kale, J.; Leber, B.; Andrews, D.W. Mechanisms of action of Bcl-2 family proteins. *Cold Spring Harb. Perspect. Biol.* **2013**, *5*, a008714. [CrossRef]
54. Lomonosova, E.; Chinnadurai, G. BH3-only proteins in apoptosis and beyond: An overview. *Oncogene* **2008**, *27* (Suppl. 1), S2–S19. [CrossRef]
55. Westphal, D.; Dewson, G.; Czabotar, P.E.; Kluck, R.M. Molecular biology of Bax and Bak activation and action. *Biochim. Biophys. Acta BBA Mol. Cell Res.* **2011**, *1813*, 521–531. [CrossRef]
56. Takahashi, Y.; Karbowski, M.; Yamaguchi, H.; Kazi, A.; Wu, J.; Sebti, S.M.; Youle, R.J.; Wang, H.-G. Loss of Bif-1 suppresses Bax/Bak conformational change and mitochondrial apoptosis. *Mol. Cell. Biol.* **2005**, *25*, 9369–9382. [CrossRef] [PubMed]
57. Parrish, A.B.; Freil, C.D.; Kornbluth, S. Cellular mechanisms controlling caspase activation and function. *Cold Spring Harb. Perspect. Biol.* **2013**, *5*, a008672. [CrossRef]
58. International Cell Line Authentication Committee. Register of Misidentified Cell Lines. Available online: <https://iclac.org/databases/cross-contaminations/> (accessed on 24 June 2021).
59. Korch, C.; Spillman, M.A.; Jackson, T.A.; Jacobsen, B.M.; Murphy, S.K.; Lessey, B.A.; Jordan, V.C.; Bradford, A.P. DNA profiling analysis of endometrial and ovarian cell lines reveals misidentification, redundancy and contamination. *Gynecol. Oncol.* **2012**, *127*, 241–248. [CrossRef]
60. Kniss, D.A.; Summerfield, T.L. Discovery of HeLa Cell Contamination in HES Cells: Call for Cell Line Authentication in Reproductive Biology Research. *Reprod. Sci. Thousand Oaks Calif.* **2014**, *21*, 1015–1019. [CrossRef] [PubMed]
61. Capes-Davis, A.; Theodosopoulos, G.; Atkin, I.; Drexler, H.G.; Kohara, A.; MacLeod, R.A.; Masters, J.R.; Nakamura, Y.; Reid, Y.A.; Reddel, R.R. Check your cultures! A list of cross-contaminated or misidentified cell lines. *Int. J. Cancer* **2010**, *127*, 1–8. [CrossRef]
62. Manivannan, E.; Amawi, H.; Hussein, N.; Karthikeyan, C.; Fetcenko, A.; Narayana Moorthy, N.S.H.; Trivedi, P.; Tiwari, A.K. Design and discovery of silybin analogues as antiproliferative compounds using a ring disjunctive—Based, natural product lead optimization approach. *Eur. J. Med. Chem.* **2017**, *133*, 365–378. [CrossRef]
63. Hussein, N.; Amawi, H.; Karthikeyan, C.; Hall, F.S.; Mittal, R.; Trivedi, P.; Ashby, C.R.; Tiwari, A.K. The dopamine D3 receptor antagonists PG01037, NGB2904, SB277011A, and U99194 reverse ABCG2 transporter-mediated drug resistance in cancer cell lines. *Cancer Lett.* **2017**, *396*, 167–180. [CrossRef] [PubMed]
64. Tukaramrao, D.B.; Malla, S.; Saraiya, S.; Hanely, R.A.; Ray, A.; Kumari, S.; Raman, D.; Tiwari, A.K. A Novel Thienopyrimidine Analog, TPH104, Mediates Immunogenic Cell Death in Triple-Negative Breast Cancer Cells. *Cancers* **2021**, *13*, 1954. [CrossRef]
65. Amawi, H.; Hussein, N.A.; Ashby Jr, C.R.; Alnafisah, R.; Sanglard, L.M.; Manivannan, E.; Karthikeyan, C.; Trivedi, P.; Eisenmann, K.M.; Robey, R.W. Bax/tubulin/epithelial-mesenchymal pathways determine the efficacy of silybin analog HM015k in colorectal cancer cell growth and metastasis. *Front. Pharmacol.* **2018**, *9*, 520. [CrossRef] [PubMed]
66. Karthikeyan, C.; Amawi, H.; Viana, A.G.; Sanglard, L.; Hussein, N.; Saddler, M.; Ashby, C.R.; Moorthy, N.H.N.; Trivedi, P.; Tiwari, A.K. 1H-Pyrazolo [3, 4-b] quinolin-3-amine derivatives inhibit growth of colon cancer cells via apoptosis and sub G1 cell cycle arrest. *Bioorg. Med. Chem. Lett.* **2018**, *28*, 2244–2249. [CrossRef]
67. Amawi, H.; Hussein, N.; Boddu, S.H.; Karthikeyan, C.; Williams, F.E.; Ashby, C.R.; Raman, D.; Trivedi, P.; Tiwari, A.K. Novel thienopyrimidine derivative, RP-010, induces β -catenin fragmentation and is efficacious against prostate cancer cells. *Cancers* **2019**, *11*, 711. [CrossRef]
68. Al-Oudat, B.A.; Ramapuram, H.; Malla, S.; Audat, S.A.; Hussein, N.; Len, J.M.; Kumari, S.; Bedi, M.F.; Ashby, C.R.; Tiwari, A.K. Novel Chrysin-De-Allyl PAC-1 Hybrid Analogues as Anticancer Compounds: Design, Synthesis, and Biological Evaluation. *Molecules* **2020**, *25*, 3063. [CrossRef] [PubMed]
69. Amawi, H.; Karthikeyan, C.; Pathak, R.; Hussein, N.; Christman, R.; Robey, R.; Ashby, C.R.; Trivedi, P.; Malhotra, A.; Tiwari, A.K. Thienopyrimidine derivatives exert their anticancer efficacy via apoptosis induction, oxidative stress and mitotic catastrophe. *Eur. J. Med. Chem.* **2017**, *138*, 1053–1065. [CrossRef] [PubMed]

See discussions, stats, and author profiles for this publication at: <https://www.researchgate.net/publication/356596129>

Gallic acid analogues with antibreast cancer and antioxidant action: synthesis and pharmacological assessment

Article in *Acta pharmaceutica Hungarica* · November 2021

DOI: 10.33892/aph.2021.91.53-66

CITATIONS

0

READS

99

3 authors:



Naveen Dhingra

Medi-Caps University

46 PUBLICATIONS 144 CITATIONS

[SEE PROFILE](#)



Rajesh Sharma

Devi Ahilya University, Indore

140 PUBLICATIONS 1,238 CITATIONS

[SEE PROFILE](#)



Anand Kar

Devi Ahilya University, Indore

142 PUBLICATIONS 4,770 CITATIONS

[SEE PROFILE](#)

Some of the authors of this publication are also working on these related projects:



Synthesis of New Schiff base and their complexes with main group elements [View project](#)



Cancer Biology [View project](#)

Gallic acid analogues with antibreast cancer and antioxidant action: synthesis and pharmacological assessment

NAVEEN DHINGRA^{1*}, RAJESH SHARMA², ANAND KAR³

¹Department of Bioscience, School of Liberal Arts and Science, Mody University, Laxmangarh-332311, Rajasthan, India

²School of Pharmacy, Devi Ahilya University, Takshashila Campus, Khandwa Road, Indore-452001 (M.P.), India

³School of Life Sciences, Devi Ahilya University, Takshashila Campus, Khandwa Road, Indore-452001 (M.P.), India

*Corresponding author: Naveen Dhingra

E-mail: navlifescience@gmail.com

Received: 16 May 2021 / Revised: 14 June 2021 / Accepted: 28 June 2021

Abstract: Breast cancer is one of the important public health problems today and recent treatments have not been found to be very effective for advanced-stage metastatic disease of the breast. In the present study ten 3,4,5- trihydroxybenzohydrazone derivatives (AR 01- AR 10) were synthesized by two different methods viz. reflux and stirring. It was observed that compounds synthesized by stirring method acquire good yield and require less time in comparison to reflux method. Further cytotoxicity activity performed on two breast cancer cell lines viz. MDA-MB-468 and MCF-7 revealed moderate activity in all compounds at 40 µg/mL and 80 µg/mL which has the highest in samples AR 01 and AR 10 for both cell lines. Considerably all compounds have shown potent antioxidant activity at 50 µg/mL and above concentrations. Tumor in mice treated with compound AR 01 was found to be smaller in comparison to control and AR 10. Findings revealed that compound having electron donating group showed more potent activity against breast cancer cell lines both in vitro and in vivo. Cytotoxicity activity also correlates with QSAR study and showed that compounds having donating group showed positive contribution towards the toxicity. These findings suggest that gallic acid derivatives were potent cytotoxic against breast cancer cell lines and may provide potent therapeutic effects against breast cancer.

Keywords: Gallic acid derivatives; cytotoxicity; antioxidant; in vivo; QSAR

1. INTRODUCTION

Polyphenols constitute an important class of chemopreventive agents because of its ROS and RNS quenching and preventing nature [1]. The underlying mechanism for the quenching behaviour of polyphenolic compounds is the characteristic of benzene rings because of both their acidity (ability to donate protons) and their delocalized π -electrons (ability to transfer electrons while remaining relatively stable) [2]. Gallic acid (3,4,5-trihydroxybenzoic acid) is a well-known naturally occurring compound. It is present as hydrolysable tannins in various natural products with various biological activities these are antioxidant, anticarcinogenic, antimutagenic, antibacterial, antifungal, antiviral, neuroprotective, anti-inflammatory, induces apoptosis of tumor cells, direct inhibition of several enzyme activities [3-14].

In recent years there is much attention in the development of synthetic gallic acid derivatives with description of their pharmacological and biological activities. Various pharmacological activities have been evaluated of gallic acid derivatives in-

cluding antioxidant, anticancer and neuroprotective activities. Indanone derivatives of gallic acid was found to be cytotoxic against various human cancer cell lines viz. KB403 (oral and mouth cancer cells), WRL68 (liver cancer cells), CaCO2 (colon cancer cells), HepG2 (liver cells) and MCF7 (hormone-dependent breast cancer cells) [15-17]. Gallic hydrazones containing an indole moiety exhibited antioxidant and cytotoxicity activities against human colon cancer cell line (HCT-116) and estrogen dependent human breast cancer cell line (MCF-7) [18]. One of the reviews reported the antitumoral properties of alkyl esters of gallic acid against various tumor cell lines [19].

Various mechanisms have been reported for anticancer activity of gallic acid. Some studies revealed that apoptosis is one of the reasons of inducing cancer cell death without harming normal cells [12, 20, 21]. Subramanian et al., reviewed that anticancer activity derivatives of gallic acid is related to generation of reactive oxygen species, regulation of apoptotic and anti-apoptotic proteins, suppression of oncogenes and regulation of cell cycle by arresting it [22]. One of the reviews re-

ported that high antioxidant activity with ability to inhibit lipid peroxidation and metal ion chelation is a responsible cause of anticancer activity of gallic acid derivatives [23]. Effect of gallic acid derivatives on drug metabolizing enzyme through inhibition of cytochrome P450 activation of indirectly acting mutagens and/or by scavenging of metabolically generated mutagenic electrophiles is one of the causes as anticancer agent [24].

Computer-aided drug discovery/design methods have played powerful tools in the development of therapeutically important small molecules for the study of structure-activity relationships (SAR) [25]. Recently many Quantitative Structure Activity Relationship (QSAR) techniques have been introduced, among them the Free-Wilson analysis (2D QSAR) is a simple and convenient method that is suitable for analyzing compounds with the same parent structure having small set of compounds [26]. The method can distinguish the different contributions of each substituent to each position, and can offer useful information about the mode of action for selected compounds. Beside the QSAR study; *in silico* study comprises of docking study. Molecular docking is used for predicting the preferred orientation of ligands with large biomolecules, predicting the strength of the bonding forces and finding the best geometrical arrangements [27].

Further they were evaluated for *in vitro* cytotoxicity study on two breast cancer cell lines *viz.* estrogen receptor positive (MCF-7) and estrogen receptor negative (MDA-MB-468) and *in vivo* study on CH3/Jax mice tumor model. Free Wilson (2D QSAR) was analyzed through Valstat software for cytotoxicity study on both breast cancer cell lines. Additionally, different antioxidant activities (DPPH, scavenging of superoxide and iron chelating) of synthesized compounds were investigated.

2. MATERIALS AND METHODS

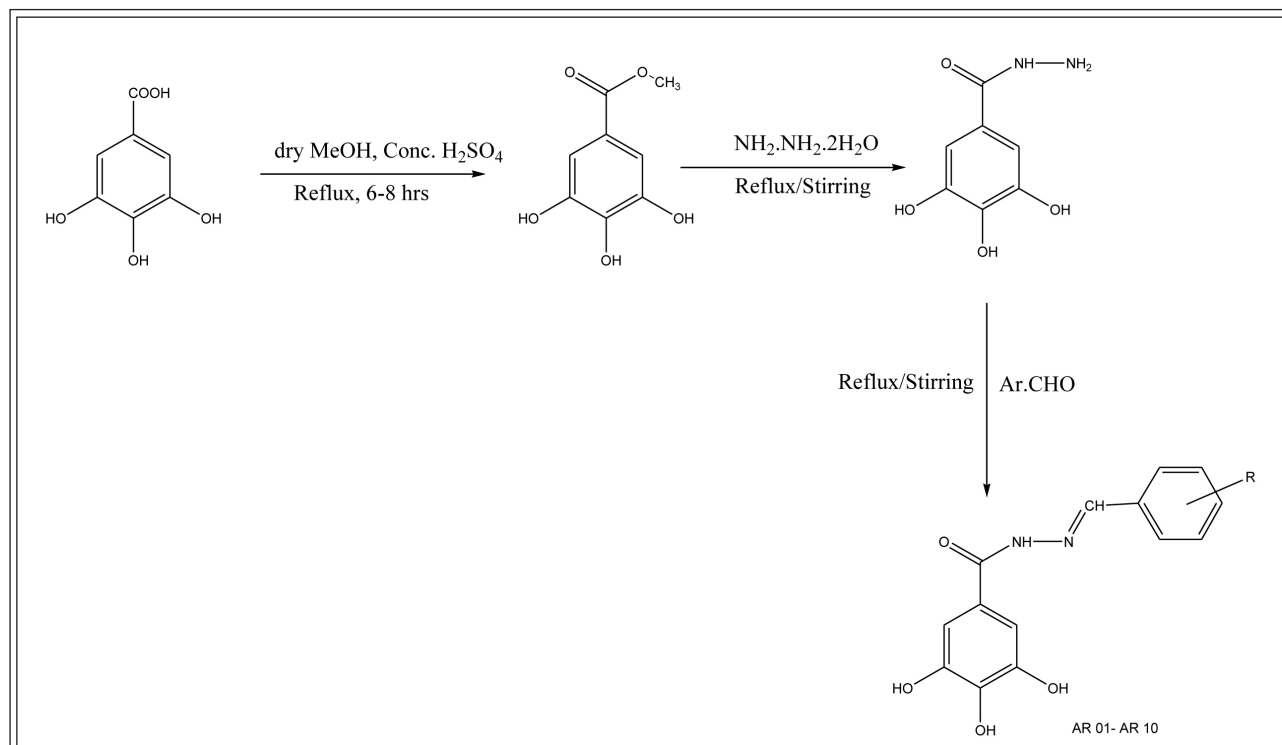
2.1. Chemicals

Synthetic materials and reagents were purchased from Sigma Chemicals Co., St. Louis, USA. All solvents were procured from Merck, Mumbai, India. All chemicals used were of analytical grade.

2.2 Synthesis method (Scheme 1)

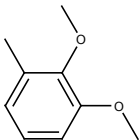
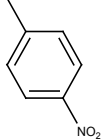
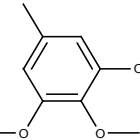
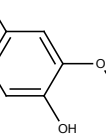
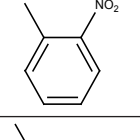
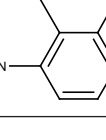
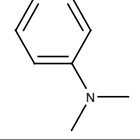
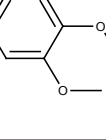
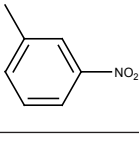
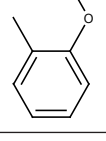
Step I: Synthesis of methyl 3,4,5-trihydroxybenzoate

The selected compounds were synthesized by 3 steps reaction. Structures of compounds with their code are depicted in Table I.



Scheme 1 Synthesis of 3,4,5-Trihydroxybenzohydrazones (AR 01- AR-10)

Table I Structure of synthesized compounds with their IUPAC name

Compounds No.	IUPAC name	Substituent (R)	Compounds No.	IUPAC name	Substituent (R)
AR 01	3,4,5-trihydroxy-N'-[(1E)-(2,3-dimethoxyphenyl)methylidene]benzohydrazide		AR 06	3,4,5-trihydroxy-N'-[(1E)-(4-nitrophenyl)methylidene]benzohydrazide	
AR 02	3,4,5-trihydroxy-N'-[(1E)-(3,4,5-trimethoxyphenyl)methylidene]benzohydrazide		AR 07	3,4,5-trihydroxy-N'-[(1E)-(4-hydroxy-3-methoxyphenyl)methylidene]benzohydrazide	
AR 03	3,4,5-trihydroxy-N'-[(1E)-(2-nitrophenyl)methylidene]benzohydrazide		AR 08	3,4,5-trihydroxy-N'-[(1E)-(2-chloro-5-nitrophenyl)methylidene]benzohydrazide	
AR 04	3,4,5-trihydroxy-N'-[(1E)-[4-(dimethylamino)phenyl]methylidene]benzohydrazide		AR 09	3,4,5-trihydroxy-N'-[(1E)-(3,4-dimethoxyphenyl)methylidene]benzohydrazide	
AR 05	3,4,5-trihydroxy-N'-[(1E)-(3-nitrophenyl)methylidene]benzohydrazide		AR 10	3,4,5-trihydroxy-N'-[(1E)-(3-methoxyphenyl)methylidene]benzohydrazide	

A mixture of gallic acid (6.0 g, 10.8 mM), dry MeOH (120 mL) and Conc. H₂SO₄ (1.20 mL) in a round bottom (RB) flask were heated under reflux for 6-8 h. After completion of the reaction, the solvent was evaporated under pressure in vacuum and extracted with ethyl acetate followed by washing with sufficient amount of water. The organic layer was concentrated in vacuum giving the crude methyl gallate. Recrystallization was done in hot water to obtain pure methyl gallate.

In the second and third step 3,4,5-trihydroxybenzohydrazide and 3,4,5-trihydroxybenzohydrazone derivatives respectively were synthesized by two methodology *viz.* reflux (*method A*) and stirring (*method B*). In *method A* reflux was used whereas, in *method B* only stirring was performed to synthesiz the same compounds.

Step II: Synthesis of 3,4,5-trihydroxybenzohydrazide

Method A

Methyl 3,4,5-trihydroxybenzoate (9.2 g, 50 mmol) and hydrazine hydrate (45 mL) were taken in RB flask and stirred under room temperature until mixed completely. Ethanol (250 mL) was added to the mixture and was stirred under reflux for 6-8 h

and then kept overnight under room temperature. The separated white solid was collected on a Buchner funnel filtered, washed with ethanol and dried over silica gel.

Method B

The synthesis of 3,4,5-trihydroxybenzohydrazide was tried under stirring conditions at room temperature methyl 3,4,5-trihydroxybenzoate (9.2 g, 50 mM) and hydrazine hydrate (45 ml) were taken in 100 mL conical flask and 40 mL of 50 % ethanol was added and the reaction mixture was allowed to stir for 1.5-2 h. The separated white precipitate was collected on a Buchner funnel filtered, dried and recrystallized from 50 % ethanol and dioxane mixture.

Step III: Synthesis of 3,4 5- trihydroxybenzohydrazone derivatives

Method A

3,4,5-trihydroxybenzohydrazide (0.8 mmol) was refluxed with various aromatic aldehydes (0.8 mmol) in 20 mL of 50% ethanol and one drop of glacial acetic acid for about 1-1.5 h. The reaction mixture was poured into excess crushed ice. The solid separated was filtered, washed with water and recrystallized from suitable solvent.

Method B

The synthesis of various 3,4,5-trihydroxybenzohydrazone was tried under stirring conditions at room temperature. 3,4,5-trihydroxybenzohydrazide (0.8 mmol) was allowed to stir with various aromatic aldehydes (0.8 mmol) in 20 mL of 50 % ethanol and one drop of glacial acetic acid for about 40-50 min. The reaction mixture was poured into excess crushed ice. The solid separated was filtered, washed with water and recrystallized from suitable solvent.

2.3 *In vitro* cytotoxicity assay

The *in vitro* cytotoxicity of the extract was determined using sulforhodamine-B (SRB) on estrogen receptor positive (MCF-7) and estrogen receptor negative (MDA-MB-468) breast cancer cell lines as described previously (Dhingra et al., 2016). Briefly, cell lines were pre-incubated in Dulbecco's Modified Eagle Medium (DMEM) for 24 h at 37 °C in 5% v/v CO₂ and compounds were added and incubated for another 48 h in four different concentrations (10 µg/mL, 20 µg/mL, 40 µg/mL and 80 µg/mL). After incubation, sulforhodamine B was added and plates were incubated at room temperature for 30 min. Finally, the optical density was recorded on ELISA reader at wavelength of 540 nm using 690 nm as reference wavelength. Percent growth was calculated on a plate-by-plate basis for test wells relative to control wells.

$$\% \text{ Growth} = [A_1 / A_0] \times 100$$

where A_1 is the average absorbance of the test well and A_0 is the average absorbance of the control well.

2.4 *In vivo* activity of potent cytotoxic synthesized compounds

2.4.1 Maximum tolerated dose (MTD) assessment in C3H/Jax mice

For each drug C3H/Jax mice were randomly divided into groups (6/group) and received a single i.p. injection of compounds in DMSO at dose levels specified in the results. Three doses of compounds were given on every third day to the group of mice with the initial dose of 150 mg/kg. The dose was increased on the basis of the mortality of mouse/mice. With the single mortality of the mouse the MTD was decided.

2.4.2 *In vivo* study

The animal use and care protocol was approved by the Anti-Cancer Drug screening facility (ACDSF) at ACTREC, Tata Memorial Centre, Navi Mumbai. The animals tumors were divided into various treatment groups and a control group (6 mice/group). The untreated control group received the vehicle only. Compounds were dissolved in the vehicle, and were given i.p. at dose of 50 mg/kg thrice a week for four weeks. Relative tumor volume, tumor/control from relative tumor volume, animal body weights (in g), survival of number of mice were measured for the next 30 days. The body weight data obtained was then converted to percentage body weight changes. The length and width of tumors were measured and the volume (v) was calculated using the formula $v = (\text{width})^2 \times (\text{length}/2)$ ¹⁴. Relative tumor volume was calculated by the following formula:

Relative Tumor Volume (RTV) = Tumor volume on day of measurement/Tumor volume on day 1. Percentage tumor growth was calculated as T/C by the following formula:

$$T/C = (T_n - T_0 / C_n - C_0) \times 100$$

$$\text{If } (T_n - T_0) < 0, \text{ then } T/C = (T_n - T_0) / T_0 \times 100$$

$C_0(C_n)$: Tumor weight of day 0 (day n) in the control group

$T_0(T_n)$: Tumor weight of day 0 (day n) in the treated group

2.5 QSAR Study

Free Wilson approach has been applied for QSAR study. Different functional groups on substituted aldehydes were used for the preparation of the matrix. Free and Wilson derived a mathematical model that describes presence and absence of certain structural features i.e., functional group at different position (ortho, meta and para) were represented by 1 and 0 respectively with biological activity values (Table II).

$$\text{Log } 1/C = \sum a_i + \mu$$

The values of a_i in equation are the biological activity groups contributing of the substituents X1, X2.....Xi in the different positions p of compound and μ is the biological activity values of the refer-

Table II Free-Wilson structural matrix for the compounds

Compounds No.	ortho				para			meta				
	H	OCH ₃	NO ₂	Cl	H	OCH ₃	NO ₂	H	OCH ₃	N(CH ₃) ₂	NO ₂	OH
AR 01	1	1	0	0	1	1	0	1	0	0	0	0
AR 02	1	0	0	0	0	1	0	0	1	0	0	0
AR 03	1	0	1	0	1	0	0	1	0	0	0	0
AR 04	1	0	0	0	1	0	0	0	0	1	0	0
AR 05	1	0	0	0	1	0	1	1	0	0	0	0
AR 06	1	0	0	0	1	0	0	0	0	0	1	0
AR 07	1	0	0	0	1	1	0	0	0	0	0	1
AR 08	1	0	0	1	1	0	1	1	0	0	0	0
AR 09	1	0	0	0	1	1	0	0	1	0	0	0
AR 10	1	0	0	0	1	1	0	1	0	0	0	0

ence compound, most often the unsubstituted parent structure of a series.

2.6 Antioxidant activities

2.6.1. DPPH radical scavenging activity

The DPPH radical-scavenging activity was determined using the method proposed by Dhingra et al., (2016). Briefly, DPPH solution (100 μM) was added to 1 ml of polyphenol extracts with 1 mL of methanol. The mixture was shaken vigorously and allowed to stand at room temperature in the dark for 10 min. The decrease in absorbance of the resulting solution was monitored at 517 nm at 10 min. Butylated hydroxytoluene (BHT) was used as standard control [28]. The percent of DPPH discoloration of the sample was calculated according to the equation:

$$\% \text{ Scavenging [DPPH]} = [(A_0 - A_1) / A_0] \times 100$$

where A_0 is the absorbance of the control and A_1 is the absorbance in the presence of the samples or standard.

2.6.2. ABTS assay

For ABTS assay, the procedure followed was taken from that of Arnao et al. (2001) with some modifications. Compounds (1 mL) were allowed to react with 1 mL of the ABTS⁺ solution for 2 hrs. in dark condition [29]. Then the absorbance was taken at 734 nm using the spectrophotometer. The percent of ABTS radicals of the sample was calculated according to the equation:

$$\% \text{ inhibition [ABTS]} = [(A_0 - A_1) / A_0] \times 100$$

where A_0 is the absorbance of the control and A_1 is

the absorbance in the presence of the samples and standard. The results were expressed as IC₅₀ (μg/mL).

2.6.3. Scavenging of superoxide

The effect of the extract on superoxide anion radicals was estimated according to the method described previously [28]. The reaction mixture contained 1 mL each of riboflavin (3.3×10 mol L⁻¹), methionine (0.01 mol L⁻¹), NBT (4.6×10 mol L⁻¹) each. After adding 1 mL of sample of different concentrations, the reaction mixture was illuminated at 4000 lx and 25 °C for 30 min. BHT was used as standard. The absorbance of the reaction mixture was measured at 560 nm with a spectrophotometer and the scavenging percentage was calculated according to the following formula:

$$\% \text{ Scavenging} = [(A_0 - A_1) / A_0] \times 100$$

where A_0 is the absorbance of the control and A_1 is the absorbance of the sample/standard.

3. RESULTS

3.1. Synthesis study

Synthesis of 3,4,5-trihydroxybenzohydrazide (step II)

According to literature the synthesis of 3, 4, 5-trihydroxybenzohydrazide was carried out by refluxing methyl 3,4,5-trihydroxybenzoate and hydrazine hydrate in ethanol under reflux for 6-8 h. In an attempt to increase the yield and to save the time we performed the same reaction under stirring condition at room temperature for only 1.5-2 h and the yield was increased from 52 to 74 % (Table III).

Table III Physical and analytical data of the synthesized intermediates and derivatives

Steps/Compounds No.	Molecular Formula	M.P. (°C)	Yield (%)		R _f Value	Solvent for recrystallization
			A	B		
I	C ₈ H ₈ O ₅	201-203	56	-	0.52*	Hot Water
II	C ₇ H ₈ N ₂ O ₄	167-169	52	74	0.61*	Methanol
AR 01	C ₁₆ H ₁₆ N ₂ O ₆	169-171	76	87	0.78*	Ethyl acetate + Chloroform
AR 02	C ₁₇ H ₁₈ N ₂ O ₇	171-173	76	88	0.73*	Ethyl acetate + Chloroform
AR 03	C ₁₄ H ₁₁ N ₃ O ₆	170-171	77	86	0.51**	Ethyl acetate
AR 04	C ₁₆ H ₁₇ N ₃ O ₄	176-177	74	83	0.68*	Ethyl acetate + Chloroform
AR 05	C ₁₄ H ₁₁ N ₃ O ₆	171-172	69	78	0.76**	Ethyl acetate
AR 06	C ₁₄ H ₁₁ N ₃ O ₆	171-172	78	87	0.80**	Ethyl acetate
AR 07	C ₁₅ H ₁₄ N ₂ O ₆	171-173	77	92	0.75*	Ethyl acetate + Chloroform
AR 08	C ₁₄ H ₁₀ ClN ₃ O ₆	168-169	82	88	0.62**	Ethyl acetate
AR 09	C ₁₆ H ₁₆ N ₂ O ₆	168-169	77	86	0.81*	Ethyl acetate + Chloroform
AR 10	C ₁₅ H ₁₄ N ₂ O ₅	171-173	82	87	0.48*	Ethyl acetate + Chloroform

A, reflux condition; B, stirring condition; R_f, retardation factor; *Solvent system, Pet ether: Acetone; ** Solvent system CHCl₃: MeOH

Synthesis of 3,4,5-trihydroxybenzohydrazone derivatives (III)

The synthesis of compounds AR 01-10 was carried out by refluxing for 1.5-2 h. The yields obtained were in the range of 69-82 %. The same reaction was performed under stirring condition 40-50 min. The reaction was successful and the products were compared with the earlier products. The yield obtained was in the range of 78-92%. Hence the modified procedure was found to better one in respect of saving time and yield (Table III).

3.2. In vitro cytotoxicity study

For MCF-7 cells at the lowest concentrations tested (10 and 20 µg/mL) none of the compounds

showed activity whereas at 40 µg/mL out of 10 synthesized compounds three compounds viz. AR 01, AR 03 and AR 10 showed cytostatic effect and showed <50 % of growth in comparison to growth. At the highest concentration tested (80 µg/mL) 7 compounds viz. AR 01, AR 02, AR 03, AR 07, AR 08, AR 09 and AR 10 showed potent activity and showed < 50 % control growth whereas, at the same concentration AR 03 showed cytotoxic effect. Among all the compounds, AR 05 and AR 06 were found to be least active (Figure 1a). Growth inhibition of 50 % (GI₅₀) of cells with drug concentration resulting in a 50% reduction in the net protein increase was observed for all the compounds. AR 03 and AR 10 was found to show lowest GI₅₀ values of 33.7 and 34.8 µg/mL respectively whereas, other

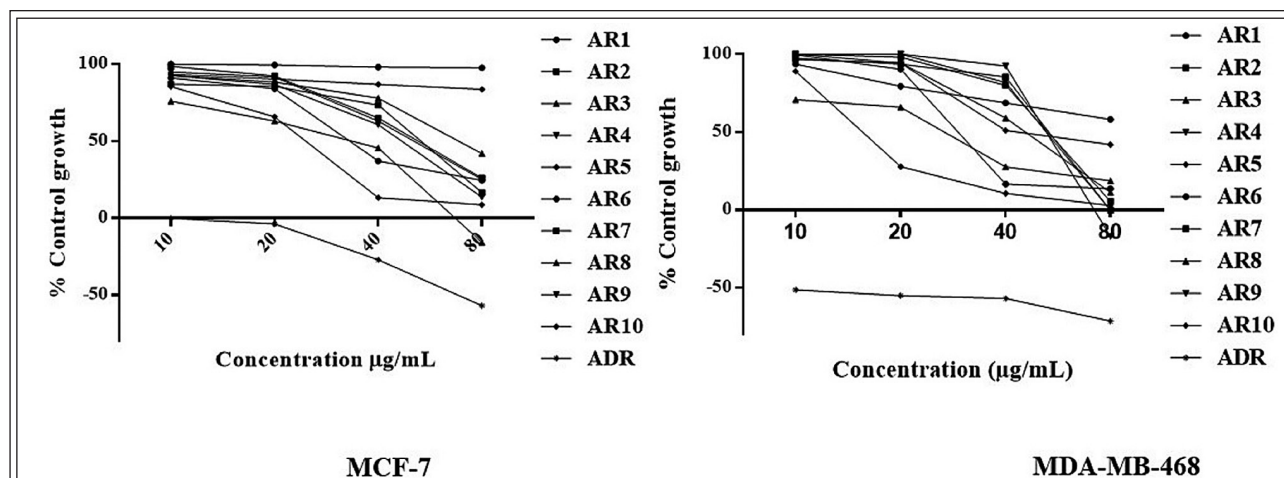


Figure 1 Percent control growth of synthesized compounds and standard (ADR) on (a) estrogen receptor positive (MCF-7), (b) estrogen receptor positive negative (MDA-MB-468) cell lines.

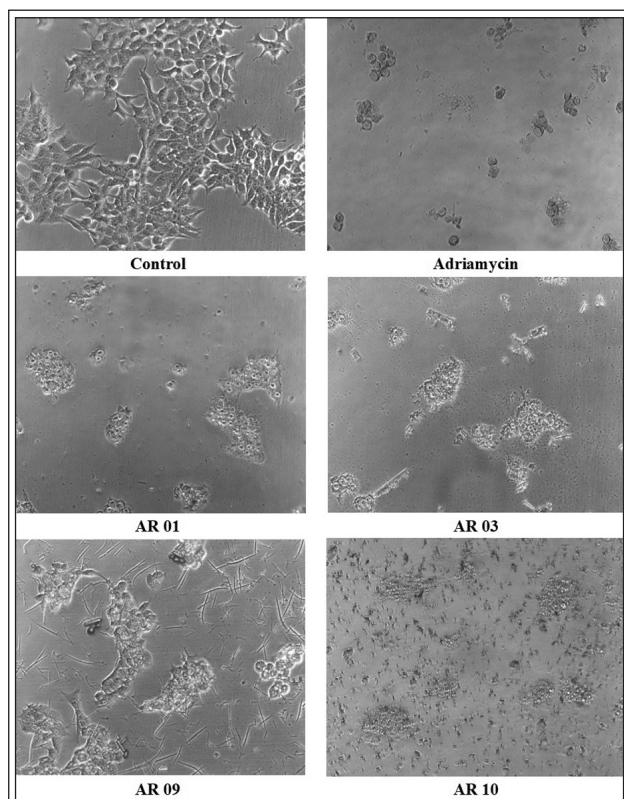


Figure 2 Cell morphology of MCF-7 cell line.

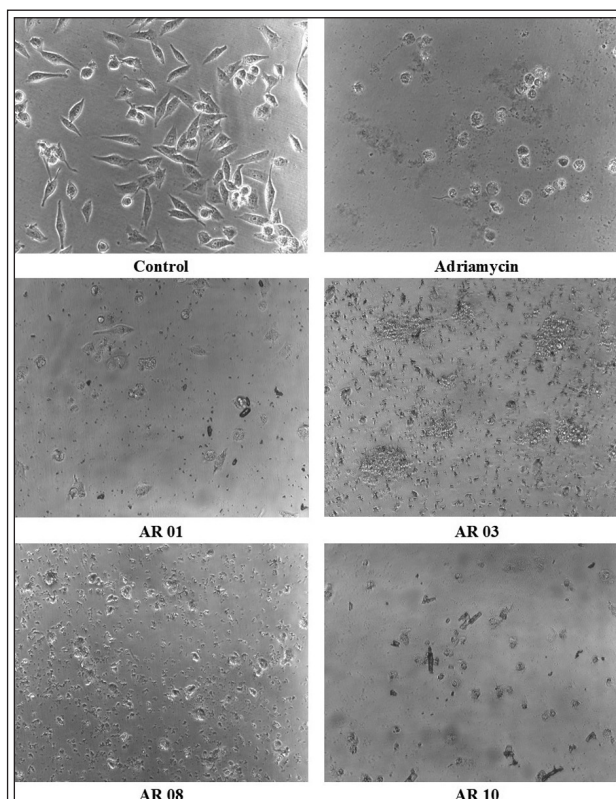


Figure 3 Cell morphology of MDA-MB-468 cell line

compounds gave the value in range of 48.0 – 73.0 $\mu\text{g/mL}$. AR 05 and AR 06 showed GI_{50} of > 80 $\mu\text{g/mL}$. Most cytotoxic compounds which change the cell morphology of MCF-7 cells is shown in Figure 2 AR 10 causes the cytotoxic effect and reduces the number of the cells. AR 10 was found to change the morphology at the best followed by AR 01, AR 03 and AR 09.

At the highest concentration tested (80 $\mu\text{g/mL}$) all the compounds showed 50 % control growth of MDA-MB-468 cells and thus are cytostatic in nature. AR-09 was found to be the most potent at the highest concentration tested and showed cytotoxic effect. At 40 $\mu\text{g/mL}$, AR 01, AR 02, AR 05 and AR 10 were found to be cytostatic, where-

as, at 20 $\mu\text{g/mL}$ only AR 10 was found to be potent and showed cytostatic effect. AR 06 was found to be least active among all, compounds towards MDA-MB-468 cells (Figure 1b). AR 10 was found with lowest GI_{50} value followed by AR 08 with values of 27.7 and 37.8 $\mu\text{g/mL}$ respectively. AR 10, AR 01 and AR 08 were found to be most potent in respect of IC_{50} with lowest values of 32.91, 40.66 and 40.95 $\mu\text{g/mL}$ respectively whereas, other compounds showed moderate activity with values in range of > 40 and ≤ 50 $\mu\text{g/mL}$. Similar to MCF-7, AR 10 was found to be most potent and changes the morphology of MDA-MB-468 cells followed by AR 01, AR 08 and AR 03 (Figure 3).

Table IV Maximum Tolerated Dose evaluated for the most potent cytotoxic compounds

Drug	Maximum dose used	Number of animals dead / Total	% death	Toxicity Criteria	Further dose for MTD
AR-01	150 mg/Kg	0/6	0	Well tolerated	300 mg/kg
AR-01	300 mg/Kg	0/6	0	Well tolerated	450 mg/kg
AR-01	450 mg/Kg	0/5	0	Well tolerated	600 mg/kg
AR-01	600 mg/kg	1/6	16.7		Dose Selected
AR-10	150 mg/Kg	0/6	0	Well tolerated	300 mg/kg
AR-10	300 mg/Kg	0/6	0	Well tolerated	450 mg/kg
AR-10	450 mg/Kg	0/6	0	Well tolerated	600 mg/kg
AR-10	600 mg/Kg	1/6	16.7		Dose Selected

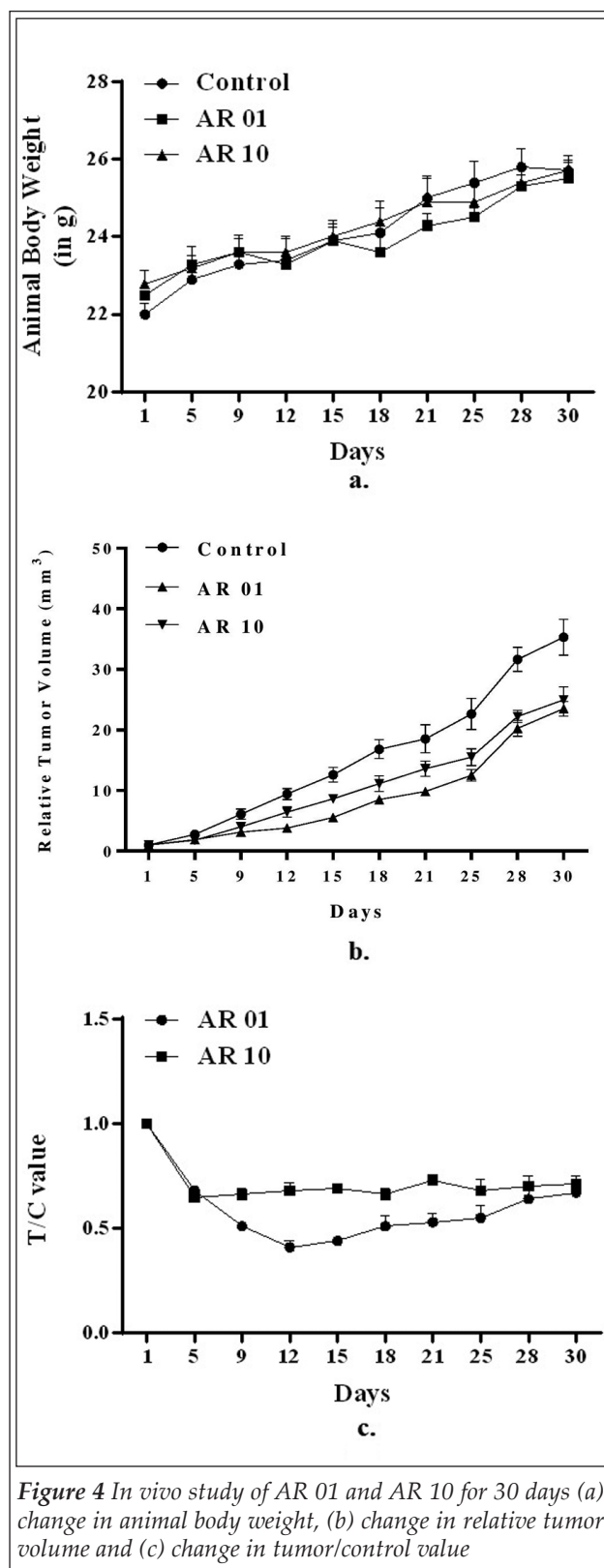


Figure 4 In vivo study of AR 01 and AR 10 for 30 days (a) change in animal body weight, (b) change in relative tumor volume and (c) change in tumor/control value

3.3. In vivo study

Maximum tolerable dose (MTD) of compounds AR 01 and AR 10 in mice was found to be 600 mg/kg

(Table IV). No obvious evidence of toxicity was observed in treated animals by comparing the body weight as there was no change in body weight of mice for both the compounds (Figure 4a). Tumor volumes of all the mice for control, AR 01 and AR 10 were observed and mean relative tumor was calculated (Figure 4b).

Relative tumor volume of compounds in comparison to control is shown in Figure 4b. It was observed that on 18th, 21st and 25th day there was significant difference ($p < 0.05$) between the relative tumor volume of control and AR 01 whereas, on 28th and 30th day there was highly significant ($p < 0.01$) difference between the tumor volume of control and AR 01 and significant ($p < 0.05$) difference between control and AR 10. Relative tumor volume on 28th day for control, AR 01 and AR 10 was 31.66, 20.29 and 22.23 respectively. However, on 30th day it was 35.31, 23.53 and 24.98 for control, AR 01 and AR 10 respectively (Figure 4b).

Tumor by control (T/C) ratio was measured and it was observed that AR 01 showed less T/C value in comparison to AR 10. From 9th to 25th day there was reduction in T/C value of AR 01 in comparison to AR 10 whereas, for 28th and 30th day there was no change in T/C value for both compounds (Figure 4c). Tumor in treated vs. by control was expressed as T/C ratio was less in AR 01 as compared to AR 10. From 9th to 25th day there was reduction in T/C value of AR 01 in comparison to AR 10, whereas, for 28th and 30th day there was no change in T/C value for both the compounds (Figure 7). Tumor in mice treated with compound AR 01 was smaller in comparison to control and AR 10.

3.4. QSAR study (Free-Wilson approach)

QSAR study was performed for cytotoxicity activity for both cell lines. Two best models were selected out of 10 different generated models. The best QSAR model built using multiple linear regression (MLR) method is represented by the following equation:

For MCF-7

Model 1:

$$\text{BA} = 4.333 - m\text{-NO}_2 (0.418) - p\text{-NO}_2 (1.5280) \\ (n = 10, r = 0.968, r^2 = 0.936, \text{variance} = 0.021, \\ \text{SD} = 0.143, F = 51.771, \text{FIT} = 739.582, q^2 = 0.822) \quad (1)$$

Model 2:

$$\text{BA} = 4.1385 + m\text{-OCH}_3 (0.1829) - p\text{-NO}_2 (1.3335) \\ (n = 10, r = 0.922, r^2 = 0.849, \text{variance} = 0.048, \text{SD} = \\ 0.221, F = 19.779, \text{FIT} = 282.570, q^2 = 0.752) \quad (2)$$

For MDA-MB-468

Model 1:

$$BA = 4.30575 + m\text{-OCH}_3(0.06245) - p\text{-NO}_2(0.22875)$$

($n = 10, r = 0.798, r^2 = 0.638, \text{variance} = 0.006, SD = 0.076, F = 6.154, FIT = 87.914, q^2 = 0.462$) (3)

Model 2:

$$BA = 4.35386 - m\text{-NO}_2(0.0604) - p\text{-NO}_2(0.276857)$$

($n = 10, r = 0.781, r^2 = 0.611, \text{variance} = 0.006, SD = 0.078, F = 5.488, FIT = 78.394, q^2 = 0.407$) (4)

where, n is the number of observations, r is the correlation coefficient, r^2 is the squared correlation coefficient, SD is the standard error of estimate, p is the statistical significance with Fisher's statistic F , q^2 is cross-validated square correlation coefficient.

Model generated for MCF-7 cells cytotoxicity was statistically highly significant in comparison to MDA-MB-468 cells. The high correlation coefficient r (0.96 and 0.9217) indicates the susceptibility of descriptors to form the above model (1 and 2). Squared correlation coefficient (r^2) of 0.94 and 0.85 explains 94% and 85% variance in biological activity of the tested compounds. It also indicates the statistical significance >99.9% with F values (51.778 and 19.779). Cross-validated square correlation coefficient (q^2) by LOO technique was 0.82 and 0.75 which showed a good internal predictive ability of the model 1 and 2 respectively.

From the contribution values for both MCF-7 and MDA-MB-468 activity it is clear that the electron-donating group on the phenyl ring had posi-

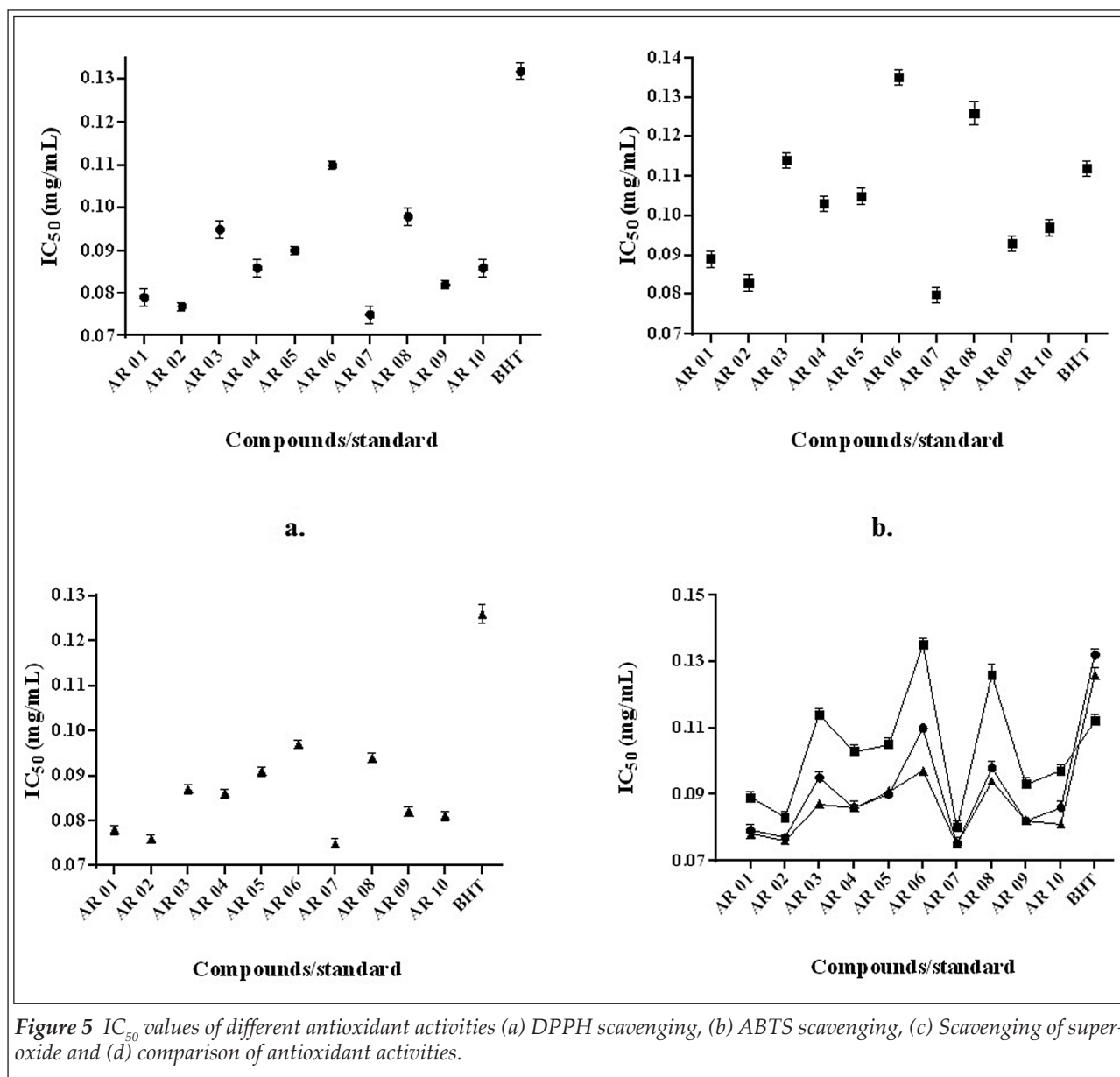


Figure 5 IC₅₀ values of different antioxidant activities (a) DPPH scavenging, (b) ABTS scavenging, (c) Scavenging of superoxide and (d) comparison of antioxidant activities.

Table V Experimental and predicted values from QSAR models for MCF-7 and MDA-MB-468 cell lines activity

Compounds No.	MCF-7		MDA-MB-468	
	Experimental $pI_{C_{50}}$	Predicted pIC_{50}	Experimental pIC_{50}	Predicted pIC_{50}
AR 01	4.324	4.333	4.391	4.368
AR 02	4.284	4.333	4.314	4.368
AR 03	4.466	4.333	4.321	4.306
AR 04	4.258	4.333	4.314	4.305
AR 05	3.693	3.915	4.199	4.305
AR 06	2.804	2.805	4.077	4.077
AR 07	4.246	4.333	4.296	4.368
AR 08	4.138	3.915	4.388	4.305
AR 09	4.317	4.333	4.356	4.368
AR 10	4.436	4.333	4.482	4.368

tive contribution and electron withdrawing group had negative contribution toward the activity. Compounds having nitro group at ortho position contribute positively toward the activity. The experimental and predicted values for both the activities are given in [Table V](#).

3.5. Antioxidant activities

3.5.1. DPPH scavenging

DPPH scavenging capacities of synthesized compounds have been expressed in IC_{50} values ([Figure 6a](#)). All the compounds showed potent activity in comparison to standard BHT and showed IC_{50} value n range of 0.075-0.110 mg/mL. AR 07 was found to be most potent followed by AR 02 and AR 01 with IC_{50} value of 0.075 ± 0.002 , 0.077 ± 0.001 and 0.079 ± 0.002 mg/mL. The values of IC_{50} for compounds AR 09, AR 10, AR 04, AR 05, AR 03, AR 08, AR 06 and BHT were 0.082 ± 0.001 , 0.086 ± 0.002 , 0.086 ± 0.002 , 0.090 ± 0.001 , 0.095 ± 0.002 , 0.098 ± 0.002 , 0.110 ± 0.001 and 0.132 ± 0.002 mg/mL respectively. The DPPH scavenging of compounds in respect of their IC_{50} values were in the order of AR 07 > AR 02 > AR 01 > AR 09 > AR 10 ~ AR 04 > AR 05 > AR 03 > AR 08 > AR 06 > BHT.

At the highest concentration (200 μ g/mL) AR 07, AR 02, AR 01 and AR 09 scavenged > 90% of DPPH. AR 10, AR 04, AR 05 and AR 03 scavenged > 80 % and < 90% whereas; AR 08, AR 06 and BHT scavenged > 70 % and < 80% of DPPH ([Figure 6a](#)).

3.5.2. ABTS scavenging

The IC_{50} values of all the compounds are depicted in [Figure 5b](#). The order of IC_{50} values of all the

synthesized compounds is AR 07 > AR 02 > AR 01 > AR 09 > AR 10 > AR 04 > AR 05 > BHT AR 03 > AR 08 > AR 06. The IC_{50} values of all compounds and standard are in the range of 0.080-0.135 mg/mL. AR 07 exhibited ABTS scavenging activity followed by AR 02 and AR 01 with IC_{50} value of 0.080 ± 0.002 , 0.083 ± 0.002 and 0.089 ± 0.002 mg/mL respectively. AR 06 showed lowed ABTS scavenging activity with IC_{50} value of 0.126 ± 0.003 mg/mL.

At the highest concentration (200 μ g/mL), AR 07 and AR 02 scavenged > 90 % of ABTS, AR 01, AR 09, AR 10 scavenged > 80 % and < 90 % whereas, AR 04, AR 05, AR 03 and BHT scavenged > 70 % and < 80 % of ABTS. AR 08 and AR 06 showed moderate activity with scavenging of > 50 % and < 70 % of ABTS ([Figure 6b](#)).

3.5.3. Scavenging of superoxide

All the compounds significantly scavenged the superoxide radical in dose-dependent manner. All compounds showed potent superoxide scavenging activity in comparison to standard BHT. Similar to the previous antioxidant activities, AR 07 exhibited highest superoxide scavenging with IC_{50} value of 0.075 ± 0.001 mg/mL followed by, AR 02 and AR 01 with IC_{50} value of 0.076 ± 0.001 and 0.078 ± 0.001 mg/mL respectively. The scavenging of compounds in respect of their IC_{50} values were in the order of AR 07 > AR 02 > AR 01 > AR 10 > AR 09 > AR 04 > AR 03 > AR 05 > AR 08 > AR 06 > BHT ([Figure 5c](#)). Correlation of IC_{50} values of all antioxidant activities is depicted in [Figure 5d](#).

At the highest concentration (200 μ g/mL) AR 07, AR 02, AR 01 AR 10 and AR 09 scavenged >

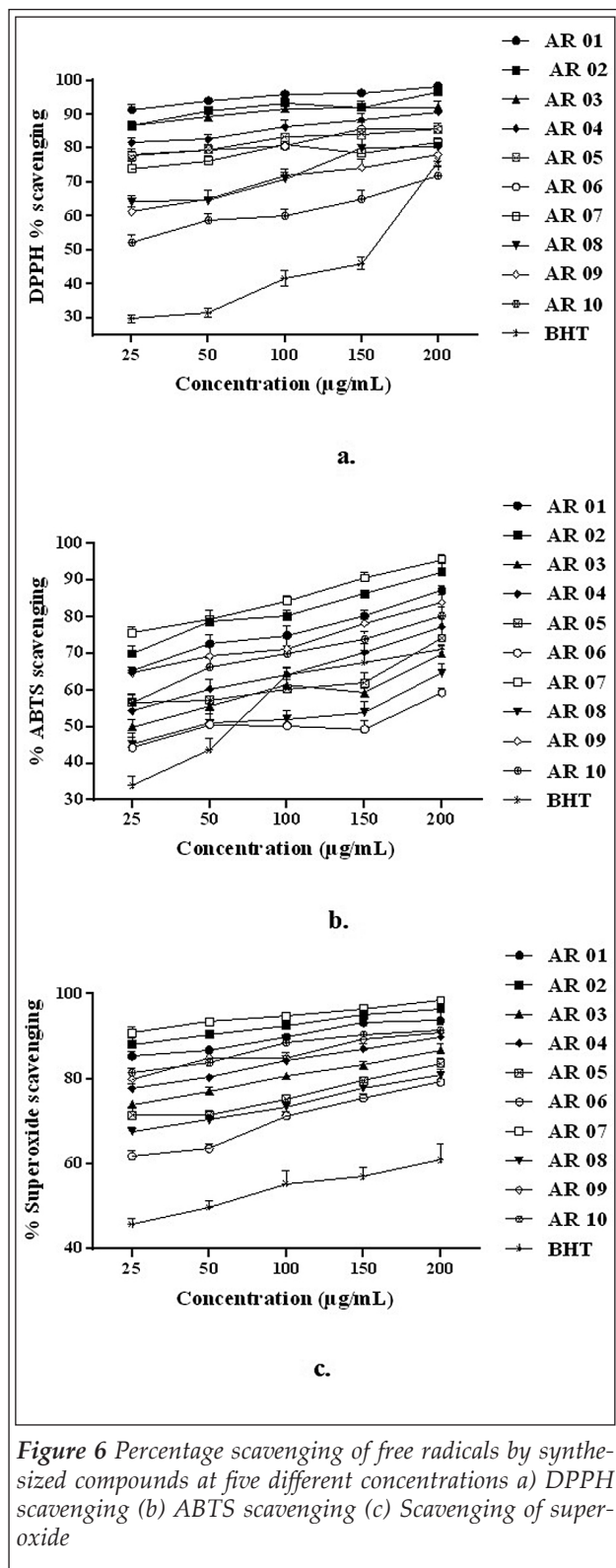


Figure 6 Percentage scavenging of free radicals by synthesized compounds at five different concentrations a) DPPH scavenging (b) ABTS scavenging (c) Scavenging of superoxide

90% of superoxide whereas, AR 04, AR 03, AR 05 AR 06 and AR 08 scavenged > 75 % and < 90 % superoxide, BHT showed lowest activity with scavenging of 60 % of superoxide radicals (Figure 6c).

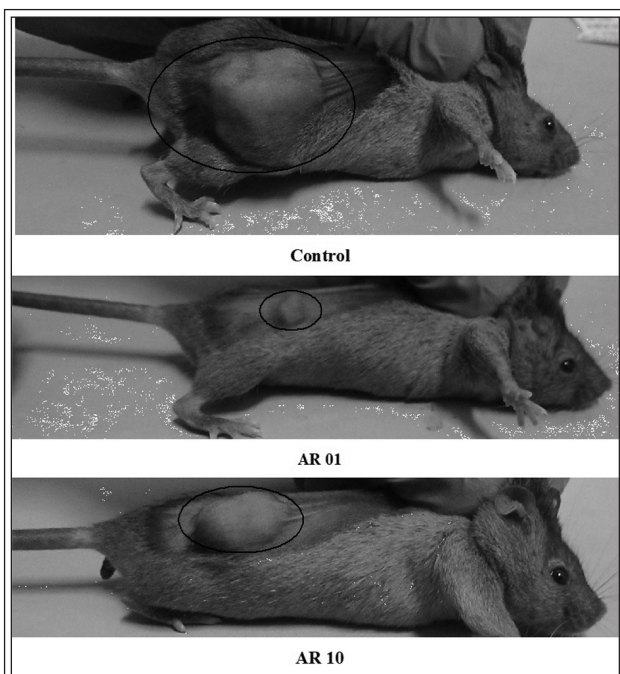


Figure 7 Implanted tumor tissue in control, AR 01 and AR 10.

4. DISCUSSION

Gallic acid, a natural phytochemical, present in various fruits, vegetables and nuts. It is known to possess various biological activities such as anti-tumor, antioxidant and anti-inflammatory cardio-protective, neuroprotective and anti-ageing [30, 31]. It has been reported that antitumor activity of gallic acid is associated with the anti-oxidative stress nature [32]. Because of its natural origin and various beneficial activities, the interest in the synthesized derivatives of gallic acid is still there. Studies have reported that derivatives of gallic acid such as schiff base, indanone, hydrazones derivatives and azo exhibited anticancer, antioxidant ability and neuroprotective effect, scavenging of free radicals, induction of apoptosis of cancer cells, etc. [16, 18, 33].

Out of the two methods (reflux and stirring) to synthesize 3,4,5-trihydroxybenzohydrazone derivatives, stirring method was found to be more effective with respect of yield, time and energy. In the reaction, methyl 3,4,5-trihydroxybenzoate underwent a nucleophilic substitution reaction with hydrazine hydrate to result in the synthesis of 3,4,5-trihydroxybenzohydrazide. The possible mechanism that the acid hydrazide underwent Schiff reaction with various aromatic aldehydes to yield various Schiff bases. This reaction first of all requires protonation of carbonyl oxygen of aldehyde by acetic acid. The nitrogen of free amino

group of acid hydrazide attacks the electron deficient carbonyl carbon of protonated aldehyde to form an intermediate known as a carbinolamine. This carbinolamine is again protonated by acetic acid, followed by deprotonation and dehydration to yield the Schiff bases.

There are several studies investigating the cytotoxicity effects of gallic acid derivatives on various cancer types. Alkyl esters of gallic acid are effective against various cancer cell lines HL60RG (human promyelocytic leukemia), P388-D1 (mouse lymphoid neoplasm), HeLa (human epithelial carcinoma), dRLh-84 (rat hepatoma), PLC/PRF/5 (human hepatoma), and KB (human epidermoid carcinoma) cells and these compounds exhibited low toxicity *in vivo* and a relative selectivity to tumor cells, exhibiting potential antitumor activity [19, 34]. Jara et al. reported that alkyl gallate triphenylphosphonium lipophilic cations showed selective cytotoxicity mouse mammary adenocarcinoma TA3/Ha cell line. Gallic acid based indanone derivatives exhibited potential cytotoxicity against various human cancer cell lines *viz.* cell lines *i.e.*, KB403 (oral and mouth cancer cells), WRL68 (liver cancer cells), CaCO2 (colon cancer cells), HepG2 (liver cells) and MCF7 (hormone-dependent breast cancer cells) [16,35]. Different mechanisms have been proposed for the anticancer activity of gallic acid derivatives. One of the papers reported that hydrophobic moiety of alkyl gallic acid derivatives seem to contribute greatly to the activity, presumably by increasing affinity for cell membranes and permeability [35]. Jara et al. (2014) reported that mitochondrial membrane potential might be one of the mechanisms underlying the anticancer activity. *In vivo* activity of alkyl gallate triphenylphosphonium cation at the dose of 10 mg of on CAF1-Jax mice showed resulted in a survival rate of mice without significant differences compared with the control group [35]. Van et al. (1986) reported that gallic acid is non-toxic, even when administered at 120 mg/kg/day in rats [37].

In the given study gallic acid derivatives were found to be cytotoxic against breast cancer cell lines. *In vivo* activity of our compounds showed that at 600 mg/kg of dose they were not toxic. Majority of the electron donating groups is found to be more potent against breast cancer cell lines and thus intracellular antioxidant activity of the compounds might be the reason of their cytotoxicity. Compounds which comprise of methoxy group are found to be more potent as compared to compounds containing nitro group. Previously it has

been reported that compounds having hydroxyl and methoxy group inhibits more growth of ovarian cell than compounds having nitro group. Compounds having methoxy group at meta position are found to be more cytotoxic than compounds having methoxy at para position whereas, in case of nitro group substituted compounds ortho nitro is considered to be more potent than meta and para nitro substituted compounds. Similar results were observed for colon cancer too [38]. Our results concord with the given studies. For MCF-7 cell line compounds having nitro at para position and methoxy at meta position were found to be most potent with least IC_{50} value whereas for MDA-MB-468 compounds methoxy at meta position and di methoxy at ortho and meta position were more effective. Compounds having nitro at meta and para position were found to be least active with highest IC_{50} value for both MCF-7 and MDA-MB-468 cell lines.

The correlation between various descriptors with biological activity is the most important means of structure–activity relationship (SAR) study. Equation is generated with minimum number of descriptors to obtain best fit. By interpreting the resulting descriptors from the equations generated, it is possible to gain some insight into factors that are likely to govern the cytotoxic activity. In the given study free Wilson approach was performed which incorporates the contributions made by various structural fragments to the overall biological activity [39-41].

In the given study all the donating group *viz.* p-OH, o-OCH₃, m-OCH₃, p-OCH₃ and p-N(CH₃)₂ on phenyl ring had positive contribution to toxicity. Majority of the compounds are positioned at 3rd, 4th or 5th position and thus -O will be easy available to form hydrogen bond with binding site. It is clear from the equation that o-OCH₃ showed very low contribution towards cytotoxicity activity. Group o-NO₂ showing positive contribution towards cytotoxicity activity for both cell lines, could be due to “penetrating effect” which causes a great change on the electronic cloud on -OH group [42].

The DPPH and ABTS radical-scavenging assays are tow common assays to access antioxidant activities. Both assays work on the principle of redox functioned proton ion for unstable free radicals and thus stabilize the harmful free radicals in the human body [43]. Mechanism behind both the activities is the reduction of unstable free radicals by hydrogen-donating antioxidants to a stable

free radical [44-46]. Mechanism behind superoxide scavenging is that, superoxide anion, being weak oxidant, produces dangerous hydroxyl radicals as well as singlet oxygen, both of which contribute to oxidative stress. It is known that donating group, particularly hydroxyl group plays one of the major reasons for the antioxidant activity [47]. The ortho and para hydroxyl substitution is commonly regarded as important for the radical scavenging activities. In our study compound AR 07 possessed highest antioxidant activity due to the presence of hydroxyl group at para position and one methoxy group at meta position. It is reported that presence of hydroxyl group in place of methoxy group is prone to make compound more antioxidant and thus compound AR 02 (three methoxy group) exhibited less antioxidant activity than AR 07. Compounds AR 05, AR 06 and AR 08 are found to be with least antioxidative activity due to the presence of electron withdrawing group ($-\text{NO}_2$). In the given study compounds with electron donating group are found to be potent antioxidant in nature.

Conclusion

A total of ten gallic acid analogues were synthesized and were screened for cytotoxicity on breast cancer cell lines and various antioxidant activities. It was observed that compounds synthesized by stirring method acquires more yield and requires less time. All synthesized compounds showed potent antioxidant activity at 50 $\mu\text{g}/\text{mL}$ and above whereas, compound AR 01 and AR 10 showed potent cytotoxic activity at 40 $\mu\text{g}/\text{mL}$ and 80 $\mu\text{g}/\text{mL}$ for both cancer cell lines. Further cytotoxicity activity with QSAR study showed that compounds having donating group showed positive contribution towards the toxicity. Development of these cytotoxic agents against breast cancer cell lines with significant antioxidant property might be useful for anticancer drug development in the future.

Conflict of Interest

There is no conflict of interest among authors.

Acknowledgements

Financial assistance from the Department of Science and Technology, India for the award of IN-SPIRE-DST SRF to Naveen Dhingra (IF110047) is gratefully acknowledged.

References

1. Pandey KB, Rizvi SI (2009) Plant polyphenols as dietary antioxidants in human health and disease. *Oxid Med Cell Longev.* 2:270-278. <https://doi.org/10.4161/oxim.2.5.9498>
2. Escarpa A, González MC (2001) Approach to the Content of Total Extractable Phenolic Compounds from Different Food Samples by Comparison of Chromatographic and Spectrophotometric Methods. *Analytica Chimica Acta* 427:119-127. [https://doi.org/10.1016/S0003-2670\(00\)01188-0](https://doi.org/10.1016/S0003-2670(00)01188-0)
3. Osborne LC, Peeler JT, Archer DL (1981) Reduction in antiviral activity of human beta interferon by gallic acid. *Infect Immun.* 33:769-774. <https://doi.org/10.1128/iai.33.3.769-774.1981>
4. Kroes BH, van den Berg AJ, Quarles van Ufford HC, van Dijk H, Labadie RP (1992) Anti-inflammatory activity of gallic acid. *Planta Med* 58:499-504. <https://doi.org/10.1055/s-2006-961535>
5. Soong, Y, Barlow PJ (2004) Antioxidant activity and phenolic content of selected fruit seeds. *Food Chem* 88:411-417. <https://doi.org/10.1016/j.foodchem.2004.02.003>
6. Nikolic K (2006) Theoretical study of phenolic antioxidants properties in reaction with oxygen-centered radicals. *Journal of Molecular Structure THEOCHEM* 774:95-105. <https://doi.org/10.1016/j.theochem.2006.07.017>
7. Faried A, Kurnia D, Faried LS et al. (2007) Anticancer effects of gallic acid isolated from Indonesian herbal medicine, *Phaleria macrocarpa* (Scheff.) Boerl, on human cancer cell lines. *Int J Oncol* 30:605-613. <https://doi.org/10.3892/ijo.30.3.605>
8. Bin-Chuan J, Wu-Huei H, Jai-Sing Y, et al (2009). Gallic Acid Induces Apoptosis via Caspase-3 and Mitochondrion-Dependent Pathways in Vitro and Suppresses Lung Xenograft Tumor Growth in Vivo. *J Agric Food Chem* 57:7596-7604. <https://doi.org/10.1021/jf901308p>
9. Cheng-Zhen L, Xin Z, Hao L, et al Gallic Acid Induces the Apoptosis of Human Osteosarcoma Cells In Vitro and In Vivo via the Regulation of Mitogen-Activated Protein Kinase Pathways. *Cancer Biotherapy & Radiopharmaceuticals* 27:701-710. <https://doi.org/10.1089/cbr.2012.1245>
10. Borges A, Ferreira C, Saavedra MJ, Simões M. (2013) Antibacterial activity and mode of action of ferulic and gallic acids against pathogenic bacteria. *Microb Drug Resist* 19:256-265. <https://doi.org/10.1089/mdr.2012.0244>
11. Mansouri MT, Farbood Y, Sameri MJ, et al. (2013) Neuroprotective effects of oral gallic acid against oxidative stress induced by 6-hydroxydopamine in rats. *Food Chem* 138:1028-1033. <https://doi.org/10.1016/j.foodchem.2012.11.022>
12. Wang K, Zhu X, Zhang K, (2014). Investigation of gallic acid induced anticancer effect in human breast carcinoma MCF-7 cells. *J Biochem Mol Toxicol* 28:387-93. <https://doi.org/10.1002/jbt.21575>
13. Ji-Hye L, Mi O, Jong Hyeon S, et al. (2016) Antiviral Effects of Black Raspberry (*Rubus coreanus*) Seed and Its Gallic Acid against Influenza Virus Infection. 8:157-169. <https://doi.org/10.3390/v8060157>
14. Zahra S, Batoul P, Pezhman B, Moein S. (2016) Gallic Acid Inhibits Proliferation and Induces Apoptosis in Lymphoblastic Leukemia Cell Line (C121). *Iranian Journal of Medical Sciences* 41:525-530.
15. Zhongbing L, Guangjun N, Peter SB, Huihu T, Baolu Z, (2006) Structure-activity relationship analysis of anti-

- oxidant ability and neuroprotective effect of gallic acid derivatives. *Neurochemistry International* 48:263-274. <https://doi.org/10.1016/j.neuint.2005.10.010>
16. Saxena HO, Faridi U, Srivastava S, et al. (2008) Gallic acid-based indanone derivatives as anticancer agents. *Bioorg Med Chem Lett*. 18:3914-3918. <https://doi.org/10.1016/j.bmcl.2008.06.039>
 17. Veena SK, Suvarna AK, Dhiraj M, (2009) Rupali Wagh, Mahalaxmi Mohan, Sanjay B. Kasture. Antioxidant and Antiparkinson Activity of Gallic Acid Derivatives. *Pharmacologyonline* 1:385-395.
 18. Khaledi H, Alhadi AA, Yehye WA, Ali HM, Abdulla MA, Hassandarvish P (2011) Antioxidant, cytotoxic activities, and structure-activity relationship of gallic acid-based indole derivatives. *Arch Pharm (Weinheim)*. 344:703-709. <https://doi.org/10.1002/ardp.201000223>
 19. Locatelli C, Filippin-Monteiro FB, Creczynski-Pasa TB (2013). Alkyl esters of gallic acid as anticancer agents:a review. *Eur J Med Chem* 60:233-239. <https://doi.org/10.1016/j.ejmech.2012.10.056>
 20. Inoue M, Suzuki R, Koide T, Sakaguchi N, Ogihara Y, Yabu Y (1994). Antioxidant, gallic acid, induces apoptosis in HL-60RG cells. *Biochem Biophys Res Commun*. 204:898-904. <https://doi.org/10.1006/bbrc.1994.2544>
 21. Subramanian V, Venkatesan B, Tumala A, Vellaichamy E. (2014) Topical application of Gallic acid suppresses the 7,12-DMBA/Croton oil induced two-step skin carcinogenesis by modulating anti-oxidants and MMP-2/MMP-9 in Swiss albino mice. *Food Chem Toxicol* 66:44-55. <https://doi.org/10.1016/j.fct.2014.01.017>
 22. Subramanian AP, John A. A., Vellayappan MV, et al (2015). Gallic acid:prospects and molecular mechanisms of its anticancer activity. *RSC Advances* 45:6-11. <https://doi.org/10.1039/C5RA02727F>
 23. Badhani B, Sharma N, Kakkar R. (2015) ChemInform Abstract:Gallic Acid:A Versatile Antioxidant with Promising Therapeutic and Industrial Applications. *RSC Advances* 35:27540-27557 <https://doi.org/10.1039/C5RA01911G>
 24. Ow YY, Stupans I. (2003) Gallic acid and gallic acid derivatives:effects on drug metabolizing enzymes. *Curr Drug Metab* 4:241-8. <https://doi.org/10.2174/1389200033489479>
 25. Hughes JP, Rees S, Kalindjian SB, Philpott KL. (2011) Principles of early drug discovery. *Br J Pharmacol*. 162:1239-1249. <https://doi.org/10.1111/j.1476-5381.2010.01127.x>
 26. Hongming C, Lars C, Mats E, et al (2013) Beyond the Scope of Free-Wilson Analysis:Building Interpretable QSAR Models with Machine Learning Algorithms. *J Chem Inf Model* 536:1324-1336 <https://doi.org/10.1021/ci4001376>
 27. Lengauer T, Rarey M (1996). Computational methods for biomolecular docking. *Curr Opin Struct Biol* 6:402-406. [https://doi.org/10.1016/S0959-440X\(96\)80061-3](https://doi.org/10.1016/S0959-440X(96)80061-3)
 28. Dhingra N, Sharma R, Kar A (2014) Towards further understanding on the antioxidative activities of Prunus persica fruit:A comparative study with four different fractions. *Spectrochimica Acta Part A:Molecular and Biomolecular Spectroscopy* 132:582- 587 <https://doi.org/10.1016/j.saa.2014.05.008>
 29. Arnao MB, Cano A, Alcolea JF, Acosta M. (2001) Estimation of free radical-quenching activity of leaf pigment extracts. *Phytochem Anal* 2001 12:138-43. <https://doi.org/10.1002/pca.571>
 30. Karamać M, Kosińska A, Pegg RB. (2005) Comparison of radicalscavenging activities of selected phenolic acids. *Pol J Food Nutr Sci*. 14:165-70.
 31. Kaur S, Michael H, Arora S, Härkönen PL, Kumar S (2005). The in vitro cytotoxic and apoptotic activity of Triphala--an Indian herbal drug. *J Ethnopharmacol* 97:15-20. <https://doi.org/10.1016/j.jep.2004.09.050>
 32. Tzu-Rong S, Jen-Jie L, Chi-Chu T, et al. (2013) Inhibition of Melanogenesis by Gallic Acid:Possible Involvement of the PI3K/Akt, MEK/ERK and Wnt/ β -Catenin Signaling Pathways in B16F10 Cells. *Int J Mol Sci*. 14:20443-20458. <https://doi.org/10.3390/ijms141020443>
 33. Sheetal A, Honnegowda S, Mandapati R. (2007) Isolation and TLC Densitometric Quantification of Gallicin, Gallic Acid, Lupeol and β -Sitosterol from *Bergia suffruticosa*, a Hitherto Unexplored Plant. *Chromatographia*. 66:725-734. <https://doi.org/10.1365/s10337-007-0389-1>
 34. Inoue M, Suzuki R, Sakaguchi N, Li Z, Takeda T, Ogihara Y, Jiang BY, Chen Y (1995) Selective induction of cell death in cancer cells by gallic acid. *Biol Pharm Bull*. 18:1526-30. <https://doi.org/10.1248/bpb.18.1526>
 35. Jara JA, Castro-Castillo V, Saavedra-Olavarría J et al. (2014) Antiproliferative and uncoupling effects of delocalized, lipophilic, cationic gallic acid derivatives on cancer cell lines. Validation in vivo in syngenic mice. *J Med Chem* 57:2440-2454. <https://doi.org/10.1021/jm500174v>
 36. Saeki K, Yuo A, Isemura M, et al. (2000) Apoptosis-inducing activity of lipid derivatives of gallic acid. *Biol Pharm Bull* 23:1391-134. <https://doi.org/10.1248/bpb.23.1391>
 37. Van der H, Janssen CA, Strik PJCM, (1986) Toxicology of gallates:a review and evaluation. *Food and Chem Tox* 24:1067-1070. [https://doi.org/10.1016/0278-6915\(86\)90290-5](https://doi.org/10.1016/0278-6915(86)90290-5)
 38. Rodrigues P, Macaya I, Bazzocco S, et al. (2014) RHOA inactivation enhances Wnt signalling and promotes colorectal cancer. *Nat Commun*. 21:5458-5480 <https://doi.org/10.1038/ncomms6458>
 39. Free SM, Wilson JW. (1964) A Mathematical Contribution to Structure-Activity Studies. *J Med Chem* 1964, 7:395-399. <https://doi.org/10.1021/jm00334a001>
 40. Kubinyi H (1979). Lipophilicity and drug activity. *Prog Drug Res*. 23:97-198. https://doi.org/10.1007/978-3-0348-7105-1_5
 41. Franke, R. In Nauta, W.Th.; Rekker, R.F., Eds.1984. *Theoretical Drug Design Methods*, Elsevier, New York, pp. 256.
 42. Zhiyuan Z, Danhui L, Wanrun J, Zhigang W (2018) The electron density delocalization of hydrogen bond systems. *Advances in Physics:X* 3:298-315 <https://doi.org/10.1080/23746149.2018.1428915>
 43. Aruoma OI. (1998) Free radicals, oxidative stress, and antioxidants in human health and disease. *Journal of the American Oil Chemists' Society*. 1998, 75:199-212. <https://doi.org/10.1007/s11746-998-0032-9>
 44. Re R, Pellegrini N, Proteggente A, et al. (1999) Antioxidant activity applying an improved ABTS radical cation decolorization assay. *Free Radic Biol Med*. 26:1231-1237. [https://doi.org/10.1016/S0891-5849\(98\)00315-3](https://doi.org/10.1016/S0891-5849(98)00315-3)
 45. Ozcelik B, Lee JH, Min DB. (2003) Effects of Light, Oxygen, and pH on the Absorbance of 2,2-Diphenyl-1-picrylhydrazyl. *Journal of Food Science*. 68:487-490. <https://doi.org/10.1111/j.1365-2621.2003.tb05699.x>
 46. bVillano D, Fernández-Pachón MS, Moyá ML, (2007) Troncoso AM, García-Parrilla MC. Radical scavenging ability of polyphenolic compounds towards DPPH free radical. *Talanta*. 71:230-235. <https://doi.org/10.1016/j.talanta.2006.03.050>
 47. Nishikimi M, Appaji N, Yagi K. (1972) The occurrence of superoxide anion in the reaction of reduced phenazine methosulfate and molecular oxygen. *Biochem Biophys Res Commun*. 46:849-54. [https://doi.org/10.1016/S0006-291X\(72\)80218-3](https://doi.org/10.1016/S0006-291X(72)80218-3)

Formulation and Characterization of Chitosan coated Liposome for Sustained Release of bio-actives

RAJESH SHARMA^{1*}, MAHENDRA CHOUHAN¹, KAMLESH DASHORA²

¹School of Pharmacy, Devi Ahilya Vishwavidhyalaya, Indore-452001, Madhya Pradesh, India.

²Institute of Pharmacy, Vikram University, Ujjain-456001, Madhya Pradesh, India

*Corresponding Author.

Email ID: rbsm73@yahoo.co.in

Received: 10.02.21, Revised: 04.03.21, Accepted: 05.04.21

ABSTRACT

The aim of current study was to assess the potential Chitosan coated liposomes formulation. Modified ethanol injection method was adopted and inspects the vesicle morphology. Average particle size was found to be 303.6 nm & entrapment efficiency 78±5 %. In vitro release pattern followed 63.5±0.18 in 24hrs. Prepared formulations have received considerable attention in pharmaceutical and biomedical application, specifically achieving sustained release controlled formulation. Thus, it is a useful method for prolonging drug release from dosage forms, reducing adverse effects and to deliver drugs in a controlled manner.

Keywords: Liposomes, Chitosan, Release rate, stability, sustain release

1. INTRODUCTION

Novel drug delivery systems is an essential requirements, which delivers drug against the causative agent of the disease being treated by carrier based drug loaded system and transported to site of action. The Chitosan coated drug delivery system like liposome decodes challenges against micro-organism related disease. Liposomes are bilayer round or oval

vesicles composed of aqueous volume portion covered by lipid bilayered. They comprises of natural or synthetic phospholipids. Liposomes are colloidal, vesicular structure based on phospholipids bilayers. Their characteristics depend on the manufacturing protocol and choice of bilayer components. They range from 20 nm to 100 nm diameter¹.

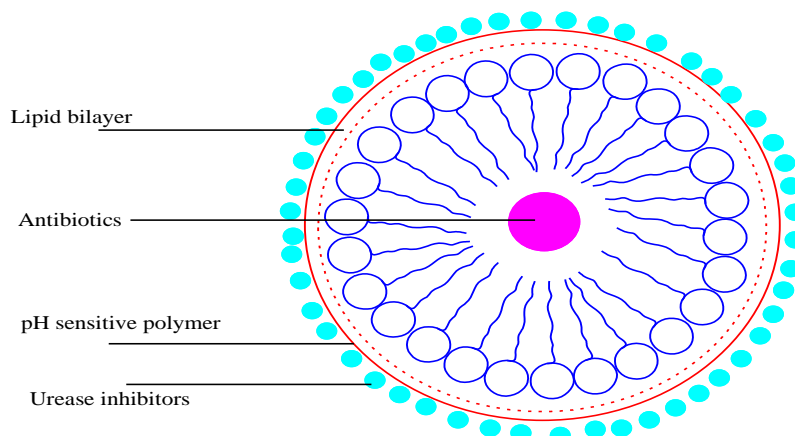


Fig.1 Schematic representation of liposome containing antibiotic at the core and covered with pH sensitive polymer linked with Urease inhibitor

Liposomes has number of components however phospholipids and cholesterol being the main components. It is apparent from the above facts that liposome is a model drug delivery system for mucoadhesive preparations incorporating drug moiety. The coating by Chitosan is required for more adhesion to the membrane and Urease inhibitor use to inhibit Urease synthesis, finally stop the growth of bacteria. Chitosan is a

polycationic, nontoxic, mucoadhesive polymer, which has been proven to be safe.²⁻⁴ Chitosan proposed has gastric retentive property, linked with the electrostatic interactions between the cationic amine groups of chitosan and the gastric mucins that are negatively charged at the stomach acidic pH.^{5, 6} Acetohydroxamic acid (AHA) displays bacteriostatic and bactericidal effects on *H. pylori* through competitive inhibitory

binding site^{7,8}. The present study was to prepare and investigated acquire particle size with the help of Zeta-seizer. Behaviour mechanism including Invitro drug release profile having highest regression coefficient values for Higuchi's model. Performance of prepared formulation was examined by stability testing. In future prepared formulation can be further used as medicated product.

2. MATERIAL AND METHODS

2.1 Materials

Generous gift of Chitosan (Fisher Company), & Amoxicillin (Ranbaxy, Dewas). Acetohydroxamic acid (AHA) & Lecithin was procured from Sigma-Aldrich USA. Cholesterol, Ethanol, Glacial acetic

acid, all other chemical used in present work is of Analytical or HPLC grade.

2.2 PREPARATION OF LIPOSOMES

Chitosan coated sustained release preparation based on modified ethanol injection method were fabricated according to the procedure suggestive karn et.al. 2011⁹ (fig2). Ethanolic solution was prepared and homogeneously mixed in Lecithin: cholesterol mixture. Simultaneously Chitosan solution was prepared in glacial acetic acid. Both solutions were slowly injected in PBS (pH7.4) buffer solution at stirring speed 300rpm for 4hrs using mechanical stirrer (Remi, India). Chitosan coated Liposomes suspension were collected by washing three times and dried at room temperature for 24 hrs.

METHOD OF PREPARATION

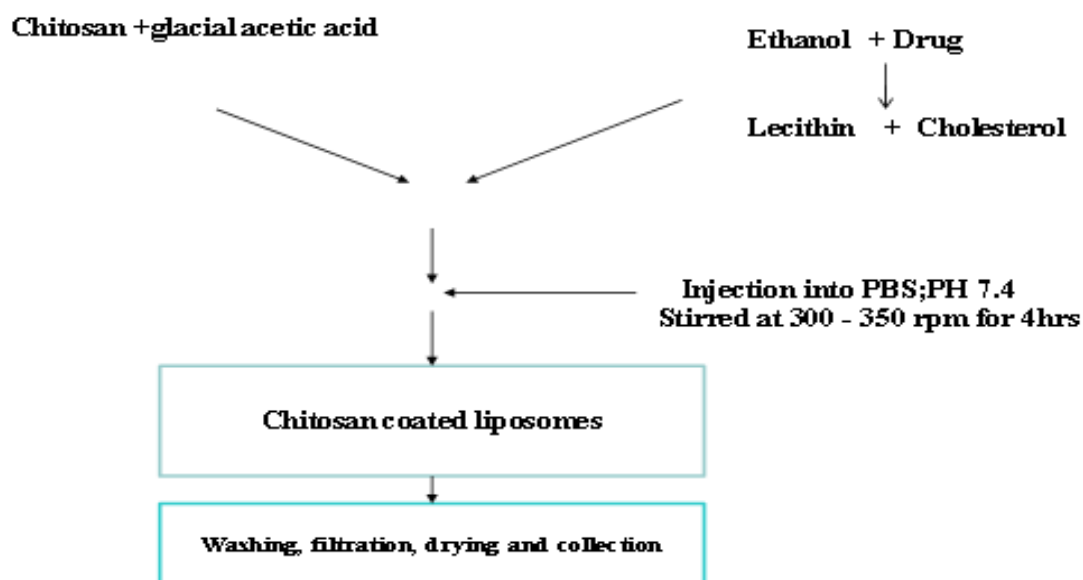


Fig.2-Schematic Presentation of Prepared Liposomes

2.3 Characterization of prepared liposomes

2.3.1 Particle size and size distribution

Particle size and size distribution were calculated microscopically with calibrated ocular micrometer. Least count of the ocular micrometer was considered as 16.2 μm around 100 particles from each formulation. Zeta potential was observed by Malvern Zeta seizer (Malvern Instrument, UK) and the observed data for each formulation were recorded.

2.3.2 Shape and surface morphology

Drops of prepared liposomes placed on glass slide were observed under optical microscopy (Leitz-Biomed, Germany) and scanning electron microscope (SEM, Hitachi, Japan) to examine their shape. In order to examine the surface

morphology, the formulations were viewed under scanning electron microscope. Prepared Liposomes powders in double adhesive tape were lightly shake and then trapped to an aluminium stub. The stubs were then coated with gold to a thickness of about 300 \AA using a sputter water. The samples were then randomly scanned for studying surface morphology but show the images of coating to prove internal surface.

2.3.3 Entrapment efficiency

Prepared Liposome 100 mg formulation was distributed in 100 ml in PBS solution; (pH 7.4) and shaken vigorously for 10 min. and supernatant was kept aside. Similarly, the

sediment was again treated in the same manner and second supernatant was mixed with first supernatant. Formulations were dissolved in 20 ml in PBS solution; (pH 7.4) for 2 hrs centrifuged at 3000 rpm for 5 min^{5,6} and then filtered through 0.45µm syringe filter (Millipore Millex HN, USA) Sample withdrawn at regular interval and absorbance was taken on Shimadzu UV-Spectrometry at λmax 228nm. The free drug detected in supernatant and the percent drug entrapped was calculated.

2.3.4 Drug release In vitro study in biological fluids

The dissolution test of prepared Liposomes was conceded by the paddle type dissolution apparatus specified in USP XXIII^{7, 8}. 10mg prepared formulation precisely mixed with 100 ml of dissolution medium maintain perfect sink condition. The content was rotated at 100 rpm thermostatically controlled at 37±0.5°C. Biological media SGF (pH 1.2) and PBS (pH 7.4) used to classify release rate of prepared formulation. The samples were withdrawn and equivalent amount of fresh medium was added to

release medium. The collected samples were filtered through 0.45µm-syringe filter (Millipore millex HN) and analyzed spectrophotometrically.

2.3.5 Stability studies

The Stability of Prepared liposomes is crucial for market point of view. The formulations developed were tested for their stability by storing them in amber coloured glass bottles at 4°C and 27±2°C for 90 days. Formulation was dissolved in PBS (pH 7.4) (1:1 v/v) solutions. The product was filtered and then it was analysed for drug content using spectrophotometric techniques.

RESULT AND DISCUSSION:

The surface and particle morphology of prepared formulation was evaluated. The particle attained plain & spherical surface morphology as depicted in figure 4.

The average Particle size attributes for Prepared Liposome was 303.6 nm in figure 3. Zeta potential factor contain Electrophoretic cell supporting with electric field were found 2.80±0.20mV indicate stability and mucoadhesive of the formulation.

Size Distribution Report by Volume

v2.1



Sample Details

Sample Name: CCL01 1
SOP Name: aman 1.sop
General Notes:

File Name: CCL01.dts
Record Number: 1
Material RI: 1.59
Material Absorbtion: 0.010
Dispersant Name: Water
Dispersant RI: 1.330
Viscosity (cP): 0.8872
Measurement Date and Time: Monday, March 12, 2018 12:...

System

Temperature (°C): 25.0
Count Rate (kcps): 317.8
Cell Description: Disposable sizing cuvette
Duration Used (s): 120
Measurement Position (mm): 4.65
Attenuator: 8

Results

Z-Average (r.nm):	PdI:	Intercept:	Result quality:	Size (r.nm):	% Volume	Width (r.nm):
303.6	0.471	0.845	Good	Peak 1: 567.5	92.9	247.9
				Peak 2: 2348	7.1	491.5
				Peak 3: 0.000	0.0	0.000

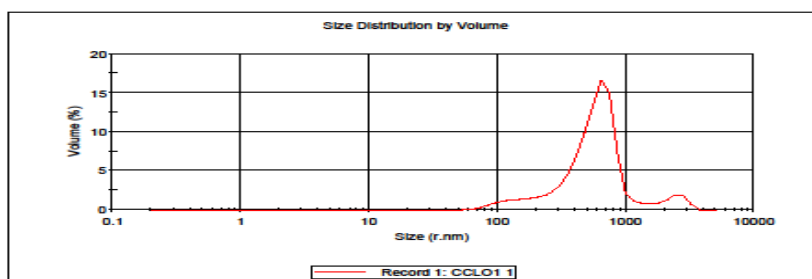


Fig.3: Average particle size assessment of prepared liposomes

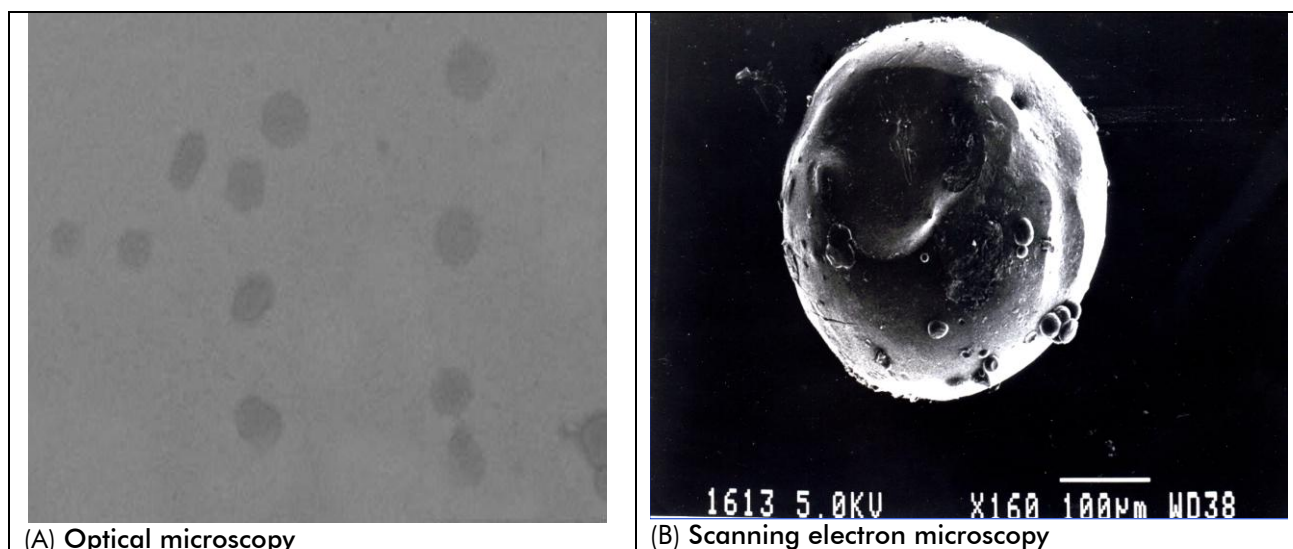


Fig.4:Microscopic assessment of prepared liposomes

Entrapment efficiency:

The finding suggested physical mechanism for drug into Chitosan coated liposomes. The formulation were analyzed UV-Spectrometer and result was found to be $78 \pm 5\%$.

In-vitro Drug Release:

In figure 5, in-vitro drug release profile of the prepared formulations was presented graphically. Dialysis method was used to conclude the drug release and it was found that at 6 hrs the percent of drug released of formulations was $48.3 \pm 0.23\%$. After 24 hrs the drug release was

found to be $63.5 \pm 0.18\%$. In vitro drug release was carried out in simulated gastrointestinal fluids of different pH (1.2 & 7.4). It was observed that the release rate of Amoxicillin from the prepared formulation was significantly slower than the conventional dosage forms. The in vitro drug release study performed in (pH 1.2 & Ph 7.4) respectively to confirm that prepared formulation resulted in sustained and prolonged release of drug in the GIT fluids.

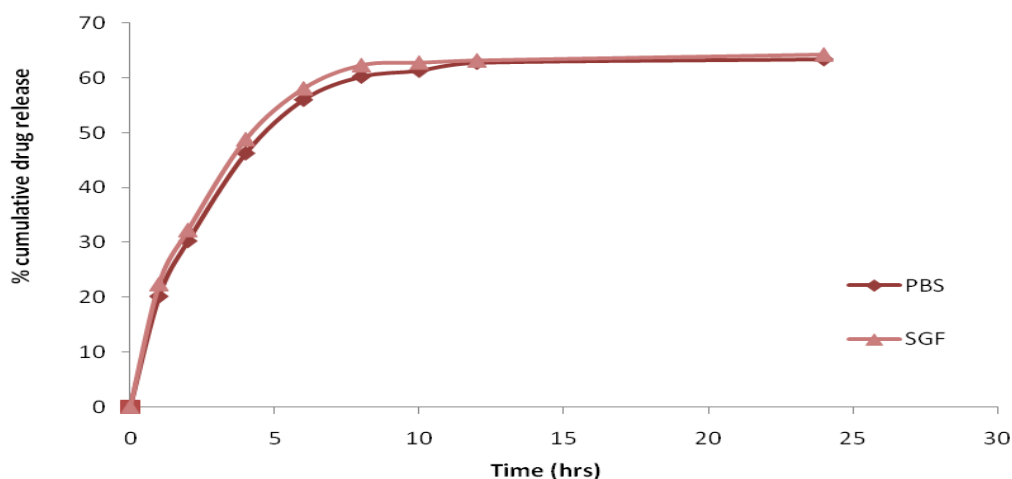


Fig.5: Percentage cumulative drug release of prepared liposomes

Stability study

Prepared formulation was stored at $04 \pm 1^\circ\text{C}$, $25 \pm 1^\circ\text{C}$ and at $40 \pm 1^\circ\text{C}$ and the residual drug content of the formulation was measured after 15, 45 and 90 days. The percent residual drug content of the selected formulation is presented

in table 2. It was observed that the formulation stored at $04 \pm 1^\circ\text{C}$ and $25 \pm 1^\circ\text{C}$ was quite stable as very less drug was degraded on storage for 30days while it was quite unstable at $40 \pm 1^\circ\text{C}$ as the residual drug content was

less after storage at 40±1°C for 90 days.

Table 2 Stability study of prepared liposomes

Parameters	Initial observation (0 day)			Initial observation (45 day)			Initial observation (90 day)		
	4 ^{0C}	25 ^{0C}	40 ^{0C}	4 ^{0C}	25 ^{0C}	40 ^{0C}	4 ^{0C}	25 ^{0C}	40 ^{0C}
Particle size(nm)	302±04.23	302±04.23	321±03.42	303±03.22	303±04.32	332±02.59	308±04.23	329±03.59	336±02.49
Residual drug content (%)	NA	NA	NA	83±09	82±03	56±08	83±09	69±04	52±07
Surface morphology	-	-	-	-	-	++	-	+	++

Note: - =No change, + =slight change ++ = moderate change

Funding Acknowledgement:

The authors are thankful to the Head, School of Pharmacy, Devi Ahilya University, Indore, Madhya Pradesh, India, for providing financial assistance and facilities to work.

Authors contribution statement:

Mr. Mahendra Chouhan had collected the data, prepare a liposome novel drug delivery system and further estimation done with various techniques. Dr. Rajesh Sharma and Dr.Kamlesh Dashor reviewed these data and provided suggestions to improve the designing of coated liposome formulation. All authors collectively contributed to methodology and resulted in parts of the final manuscript.

Conflict of interest:

Conflict of interest declared none.

REFERENCES:

1. Kulkarni PR, Yadav J, Vaidya KA. Liposomes, A Novel Drug Delivery System, *Int. J. Curr. Pharm, Res* 2011; (2):10-18.
2. Mansouri S, Cuie Y, Winnik F, Shi Q, Lavigne P, Benderdour M, Beaumont E, Fernandes JC, Characterization of folate-chitosan-DNA nanoparticles for gene therapy, *Biomaterials*, 2006; (27): 2060-2065.
3. Jin J, Song M, Hourston D, Novel chitosan-based films cross-linked by genipin with improved physical properties, *Biomacromolecules*, 2004; (5):162-168.
4. Sogias IA, Williams AC, Khutoryanskiy VV, Why is chitosan mucoadhesive, *Biomacromolecules*, 200;(9):1837-1842.
5. Deacon M, Mcgurk S, Roberts C, Williams P, Tendler S, Davies M, Davis S, Harding S, Atomic

- force microscopy of gastric mucin and chitosan mucoadhesive systems, *Biochem J*, 2000; (348) : 557-563.
6. Phillips K, Munster D, Allardyce R, Bagshaw P, Antibacterial action of the urease inhibitor acetohydroxamic acid on *Helicobacter pylori*, *Journal of clinical pathology*, 1993; (46): 372-373.
7. Ohta T, Shibata H., Kawamori T, Iimuro M, Sugimura T, Wakabayashi K, Marked Reduction of *Helicobacter pylori* Induced Gastritis by Urease Inhibitors, Acetohydroxamic Acid and Flurofamide, in Mongolian Gerbils, *Biochemical and biophysical research communications*, 2001; (285):728-733.
8. Todd MJ, Hausinger R, Competitive inhibitors of *Klebsiella aerogenes* urease: Mechanisms of interaction with the nickel active site, *Journal of Biological Chemistry* 1989;(264):15835-15842.
9. Karn P R, Vanic Z, Pepic I, Basnet NS, They were studied that the mucoadhesive liposomal delivery systems: the choice of coating material, *Drug Development and Industrial Pharmacy* 2011;(37):482-488.
10. Blumenthal M, Goldberg, A, Brinkmann J, Herbal Medicine. *Integrative Medicine Communications*, Newton 2000



Syntheses, biological evaluation of some novel substituted benzoic acid derivatives bearing hydrazone as linker

Ganesh Prasad Mishra^{1,2} · Rajesh Sharma¹ · Mukul Jain³ ·
Debdutta Bandyopadhyay³

Received: 18 May 2021 / Accepted: 22 July 2021

© The Author(s), under exclusive licence to Springer Nature B.V. 2021

Abstract

On the basis of rational drug design fourteen novel compounds having benzoic acid as acidic head, hydrazone as linker and substituted diaryl sulfanyl/aryl-cyclohexylsulfanyl as a hydrophobic tail were synthesized and characterized by physico-chemical and spectrophotometric (FTIR, Mass, ¹HNMR and ¹³CNMR) analysis. The spectral data were satisfactory with their structures. The designed compounds were docked against peroxisome proliferated activated receptors (PPAR γ) and further evaluated for in vitro PPAR γ agonist activity and in vivo hypoglycemic activity in wistar strain of albino rats. Compound **3k** and **3m** exhibited potent anti-diabetic activity without ulcerogenic toxicity and minimum side effects as weight gain. Therefore these compounds would be considered as promising agents for the development of novel antidiabetic agents.

Keywords PPAR γ agonists · Benzoic acid derivatives · Hydrazone · Thioether · Anti-diabetic · Ulcerogenic toxicities

Introduction

PPAR(peroxisome proliferator activated receptor) γ is a member of the peroxisome proliferator activated receptor family and has been the subject of extensive research for mechanistic importance in glucose and lipid homeostasis [1]. The receptor is widely distributed in the spleen, colon, adipose tissue and macrophages, and found to a lesser extent in the liver, pancreas and skeletal

✉ Ganesh Prasad Mishra
gm25mishra@gmail.com

¹ School of Pharmacy, Devi Ahilya Vishwavidyalaya, Takshshila Campus, Khandwa Road, Indore, M.P. 452001, India

² Kharvel Subharti College of Pharmacy, Swami Vivekanand Subharti University, Subhartipuram, NH-58, Delhi-Haridwar Bypass Road, Meerut, U.P. 250002, India

³ Zydus Research Centre, Sarkhej-Bavla N.H 8A, Moraiya, Ahmedabad 382210, India

muscle [2]. PPAR γ agonist actions are known to improve hyperglycemia and hyperlipidemia, and to reduce cardiovascular risk factors such as atherosclerosis, arterial hypertension and inflammatory mediators. Hyperlipidemia is usually associated with hyperglycemia and frequently leads to the development of type-2 diabetes mellitus (T2DM) and cardiovascular disease [3], thus posing a substantial worldwide economic burden [4].

PPAR γ agonists, such as thiazolidinediones (TZDs) have proven to be efficacious as insulin sensitizing agents in the treatment of persistent hyperglycemia [5–9]. Due to unwanted adverse effects of long term administered TZDs, such as weight gain and fluid retention, search of new PPAR γ agonists without adverse effects is essential in the development of new antidiabetic agents.

Literature was reported that benzoic acid derivatives stimulated expression and exhibited PPAR γ agonistic activity [10–12]. Benzoic acid possesses a simple skeleton that belong to open chain acidic group in place of close chain acidic TZD and that binds comfortably in the active site of PPAR γ [13, 14]. These findings prompted us to search novel benzoic acid derivatives containing different hydrophobic tail part as PPAR γ agonists.

Design

Compounds having trifunctional unit (acidic head part, hydrophobic tail part and a connecting part as linker) have been shown good PPAR γ agonistic activity [15]. Keeping these structural features in mind novel benzoic acid derivatives were designed. The different hydrophobic tail parts are conveniently selected according to physicochemical properties such as hydrophobicity and electronic distribution. The hydrophobic tail part which differs in the compounds is of major interest. In designed compound, the benzoic acid as acidic head part is linked with substituted aryl/cyclohexylsulfanyl via hydrazone moiety as linker (Fig. 1). Earlier hydrazone was effectively evaluated as anti-diabetic agents [16, 17].

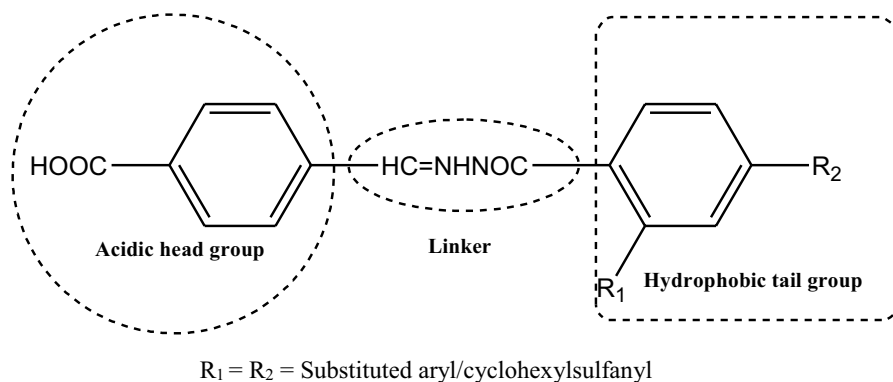


Fig. 1 Design of benzoic acid derivatives

Experimental section

Molecular docking

The Program Molegro Virtual Docker (MVD 2012. 5.5, Molegro Bioinformatics, Aarhus C, Denmark) was employed to generate grid, calculate dock score and evaluate conformers [18]. The compounds were docked using PPAR γ protein coordinates. Protein coordinates were downloaded from the Protein Data Bank, accession code 2PRG [19]. Chain A was prepared for docking within the MVD by removing chain B and all water molecules. Maximum number of cavities was fixed to 5 for detection of possible binding cavities, grid resolution was 0.60 Å with center at coordinates $x=(-17.45)$, $y=(-16.26)$ and $z=(18.04)$ Å, and the binding site radius was set to 16 Å, while other parameters was set as default. All compounds were stored in a MVD file and an original conformation was generated for each compound. Compounds were docked into the protein coordinates and the highest scoring pose was selected for each of the compounds. The best docking poses are predicted to be the most stable conformation of each compound for binding to the PPAR γ receptor. The validation of the docking process was performed and determines whether the molecular docking algorithm is able to recover the crystallographic.

position with root mean square distance value less than 2.0 Å [see Supplementary File 1].

Synthetic materials and methods

All synthetic starting material, reagents, and solvents were procured from Sigma Aldrich and Merck and used without further purification. Thin-layer chromatography (TLC) and column chromatography was used to reach the completion of the reaction and purity of the compounds synthesized respectively. Melting points were recorded using an open capillary tube electrothermal melting point apparatus and are uncorrected. IR spectra were obtained in KBr discs on a Shimadzu 8400S Fourier-transform infrared (FTIR) spectrophotometer. ^1H NMR spectra were recorded on a FT NMR (400 MHz) and ^{13}C NMR were recorded at 100 MHz on a BRUKER AVANCE II 400 NMR spectrometer; DMSO- d_6 was used as a solvent. Chemical shifts are reported as δ (ppm). The Mass spectra were recorded on a Waters Q-TOF Micro mass spectrometer. Elemental analysis was performed using EURO Vector EA 3000 analyzer. The spot on sample loaded TLC (E-Merck pre-coated plates) plates were identified by exposing to UV light and iodine vapour. The CsF-Celite reagent was prepared by stirring an aqueous solution of CsF with celite 521 at room temperature for 20 min [20].

Preparation of intermediates

Procedure for preparation of ester

A mixture of substituted benzoic acid (1.0 mmol), methanol (10 mmol) and few drops of Conc. sulfuric acid as catalyst was refluxed at 70 °C for 4–5 h. and reaction

was monitored by TLC. After completion of reaction, the reaction mixture was cooled and filtered. The solid residue (IM1) was washed with distilled water and dried.

Procedure for preparation of thioether

A mixture of aryl/acylthiol (100 mmol) and CsF-Celite as a solid base (150 mmol) in 20 ml of acetonitrile containing substituted ester (200 mmol) was refluxed at 80 °C for 03–18 h and the progress of the reaction was monitored by TLC. After completion of reaction, the reaction mixture was cooled at room temperature and filtered. The CsF-Celite was separated as residue and thioether as filtrate. The filtrate was evaporated to get desired product (IM2).

Procedure for preparation of hydrazide

Hydrazide intermediates were obtained from reaction of the substituted thioether (10 mmol) with excess of hydrazine 90% (10 mmol) under reflux at 110 °C for 45 min. The solid was obtained by cooling the reaction vessels, filtered off and washed with distilled water and dried to get desired products (IM3).

General method for the preparation of compounds (3a–3n)

The compounds were synthesized by reacting equimolar proportion of substituted aryl hydrazides (IM3; 10 mmol) and p-formyl benzoic acid (10 mmol) in absolute ethanol (25 mL) under reflux at 78 °C for 40 min. The precipitate was filtered off and washed with distilled water and finally recrystallized with dimethylformamide to obtain **3a–3n**.

(1) 4-[[2-(4-Chloro-phenylsulfanyl)-benzoyl]-hydrazonomethyl]-benzoic acid (3a)

White solid; Yield: 83%; mp: 219–221 °C; IR (KBr, ν cm^{-1}): 3348(NH), 3059(CH), 2988(OH), 1749(C=O), 1680 (C=O), 1530(C=C), 1058(C–Cl), 680(C–S). ^1H NMR (DMSO- d_6): δ 12.13(s, 1H, COOH), 11.56(s, 1H, NH), 10.10 (*s*, 1H, –N=CH), 7.95–7.92(*d*, J =7.37 Hz, 2H), 7.73–7.70 (*d*, J =6.70 Hz, 2H), 7.59–7.54 (*m*, 6H), 7.39–7.35. (*d*, J =8.62 Hz, 2H). ^{13}C NMR (DMSO- d_6): δ 192.35, 171.53, 164.98, 145.32, 138.15, 137.46, 135.33, 129.92, 125.70, 125.19, 125.30, 125.21, 125.19, 125.09, 124.90, 124.84, 124.53, 124.31, 124.17, 124.11, 124.05. MS: m/z . 412.70 ($\text{M}^+ + 2$). Anal. Calcd for $\text{C}_{21}\text{H}_{15}\text{ClN}_2\text{O}_3\text{S}$: C, 61.40; H, 3.69; N, 6.83; S, 7.80. Found: C, 61.37; H, 3.53; N, 6.70; S, 7.47.

(2) 4-[[2-(4-Fluoro-phenylsulfanyl)-benzoyl]-hydrazonomethyl]-benzoic acid (3b)

White solid; Yield: 93%; mp: 229–231 °C; IR(KBr, ν cm^{-1}): 3391(NH), 3077(CH), 3019(OH), 1747(C=O), 1698(C=O), 1527(C=C), 1157(C–F), 683(C–S). ^1H NMR (DMSO- d_6): δ 12.14(*s*, 1H, COOH), 11.65(*s*, 1H, NH), 10.13

(s, 1H, -N=CH), 7.89–7.86 (*d*, $J=8.93$ Hz, 2H), 7.74–7.71(*d*, $J=7.05$ Hz, 2H), 7.59–7.50 (*m*, 6H), 7.46–7.42(*d*, $J=7.23$ Hz, 2H). ^{13}C NMR (DMSO-*d*₆): δ 192.96, 171.34, 166.53, 145.76, 140.34, 138.62, 135.77, 129.88, 125.70, 125.10, 124.47, 124.29, 124.23, 124.21, 124.17, 124.11, 124.07, 124.01, 123.83, 123.76, 123.65. MS: m/z 395.43 (M^+). Anal. Calcd for $\text{C}_{21}\text{H}_{15}\text{FN}_2\text{O}_3\text{S}$: C, 63.94; H, 3.84; N, 7.11; S, 8.13. Found: C, 63.85; H, 3.64; N, 7.02; S, 8.08.

(3) 4-[[2-(4-Bromo-phenylsulfanyl)-benzoyl]-hydrazonomethyl]-benzoic acid (3c)

White solid; Yield: 81%; mp: 230–232 °C; IR(KBr, ν cm^{-1}): 3388(NH), 3113(CH), 3013(OH), 1758(C=O), 1683 (C=O), 1514(C=C), 1041(C–Br), 669(C–S), ^1H NMR (DMSO-*d*₆): δ 12.13(*s*, 1H, COOH), 11.64(*s*, 1H, NH), 10.09(*s*, 1H, -N=CH), 7.84–7.81(*d*, $J=7.19$ Hz, 2H), 7.73–7.70(*d*, $J=7.81$ Hz, 2H), 7.61–7.55(*m*, 6H), 7.47–7.43 (*d*, $J=8.01$ Hz, 2H). ^{13}C NMR (DMSO-*d*₆): δ 192.21, 171.11, 165.82, 145.47, 139.46, 135.71, 131.19, 126.47, 125.21, 125.13, 125.01, 124.93, 124.61, 124.18, 124.11, 124.03, 124.95, 124.61, 124.33, 124.13, 124.11. MS: m/z 456.63 ($\text{M}^+ + 2$). Anal. Calcd for $\text{C}_{21}\text{H}_{15}\text{BrN}_2\text{O}_3\text{S}$: C, 55.39; H, 3.32; N, 6.15; S, 7.08. Found: C, 55.35; H, 3.04; N, 6.12; S, 7.03.

(4) 4-[[2-(*p*-Tolylsulfanyl)-benzoyl]-hydrazonomethyl]-benzoic acid (3d)

Off-white solid; Yield: 78%; mp: 224–226 °C; IR(KBr, ν cm^{-1}): 3331(NH), 3121(CH), 3008(OH), 1751(C=O), 1689 (C=O), 1521(C=C), 691(C–S). ^1H NMR (DMSO-*d*₆): δ 2.08(*s*, 1H, COOH), 11.56(*s*, 1H, NH), 10.11(*s*, 1H, -N=CH), 7.88–7.85(*d*, $J=7.03$ Hz, 2H), 7.65–7.63(*d*, $J=7.12$ Hz, 2H), 7.59–7.53(*m*, 6H), 7.39–7.35 (*d*, $J=7.33$ Hz, 2H), 2.22 (*s*, 3H). ^{13}C NMR (DMSO-*d*₆): δ 191.02, 171.51, 165.21, 145.74, 138.52, 135.43, 129.94, 125.71, 125.58, 125.53, 125.33, 125.21, 125.10, 125.03, 124.93, 124.77, 124.71, 124.11, 123.33, 123.09, 122.70, 21.42. MS: m/z 391.10 ($\text{M}^+ + 1$). Anal. Calcd for $\text{C}_{22}\text{H}_{18}\text{N}_2\text{O}_3\text{S}$: C, 67.69; H, 4.65; N, 7.17; S, 8.22. Found: C, 67.35; H, 4.64; N, 7.12; S, 8.18.

(5) 4-[[2-(4-Methoxy-phenylsulfanyl)-benzoyl]-hydrazonomethyl]-benzoic acid (3e)

Off white solid; Yield: 89%; mp: 261–263 °C; IR (KBr, ν cm^{-1}): 3359(NH), 3100(CH), 2991(OH), 2831(OCH₃), 1733(C=O), 1687(C=O), 1530(C=C), 684(C–S). ^1H NMR (DMSO-*d*₆): δ 12.10(*s*, 1H, COOH), 11.63(*s*, 1H, NH), 10.11(*s*, 1H, -N=CH), 7.84–7.82(*d*, $J=7.83$ Hz, 2H), 7.69–7.67(*d*, $J=6.71$ Hz, 2H), 7.60–7.50(*m*, 4H), 7.41–7.37(*d*, $J=5.22$ Hz, 2H), 3.43(*s*, 3H). ^{13}C NMR (DMSO-*d*₆): δ 191.91, 170.40, 167.15, 157.46, 144.97, 138.29, 135.74, 129.52, 125.89, 125.31, 125.28, 125.19, 125.17, 125.14, 125.07, 124.92, 124.71, 124.57, 124.38, 124.17, 124.07, 55.36. MS: m/z 407.08 ($\text{M}^+ + 1$). Anal. calcd for $\text{C}_{22}\text{H}_{18}\text{N}_2\text{O}_4\text{S}$: C, 65.05; H, 4.48; N, 6.89; S, 7.89. Found: C, 64.95; H, 4.34; N, 6.42; S, 7.68.

(6) 4-[[2-(2,4-Dimethyl-phenylsulfanyl)-benzoyl]-hydrazonomethyl]-benzoic acid (3f)

White solid; Yield: 81%; mp: 205–207 °C; IR (KBr, ν cm^{-1}): 3369(NH), 3122(CH), 3011(OH), 1724(C=O), 1681(C=O), 1516(C=C), 659(C–S). ^1H NMR (DMSO-*d*₆): δ 12.09(*s*, 1H, COOH), 11.61(*s*, 1H, NH), 10.12(*s*, 1H, -N=CH), 7.85–7.83(*d*, $J=6.22$ Hz, 2H), 7.77–7.73(*d*, $J=5.19$ Hz, 2H), 7.61–7.56(*m*, 5H), 7.42–7.39(*d*, $J=7.57$ Hz, 2H), 2.46(*s*, 6H). ^{13}C NMR (DMSO-*d*₆): δ 191.29, 171.23, 165.41, 145.33, 137.43, 135.46, 130.45, 126.91, 125.62, 125.33, 125.30, 125.21, 125.11, 125.01, 124.73, 124.33, 124.24, 124.17, 124.09, 123.82, 123.71, 22.37, 21.13. MS: m/z 405.13 ($\text{M}^+ + 1$). Anal. calcd for $\text{C}_{23}\text{H}_{20}\text{N}_2\text{O}_3\text{S}$: C, 68.32; H, 4.95; N, 6.93; S, 7.94. Found: C, 68.03; H, 4.64; N, 6.62; S, 7.78.

(7) 4-[(2-Cyclohexylsulfanyl-benzoyl)-hydrazonomethyl]-benzoic acid (3 g)

White solid; Yield: 67%; mp: 209–211 °C; IR (KBr, ν cm^{-1}): 3311(NH), 3113(CH), 2941(OH), 1733(C=O), 1684(C=O), 1525(C=C), 621(C–S). ^1H NMR (DMSO-*d*₆): δ 11.98 (*s*, 1H, COOH), 11.41(*s*, 1H, NH), 10.04(*s*, 1H, -N=CH), 7.84–7.82(*d*, $J=7.20$ Hz, 2H), 7.66–7.64(*d*, $J=5.28$ Hz), 7.36–7.33(*d*, $J=5.43$ Hz, 2H), 7.11–7.06(*m*, 2H), 3.33(*m*, 1H), 1.63–1.39(*m*, 10 H) ^{13}C NMR (DMSO-*d*₆): δ 190.08, 170.03, 164.93, 144.42, 137.12, 135.37, 129.41, 125.61, 125.05, 124.39, 124.33, 124.23, 124.13, 124.09, 123.08, 43.15, 39.43, 39.42, 26.45, 25.19, 25.18. MS: m/z 383.33 ($\text{M}^+ + 1$). Anal. Calcd for $\text{C}_{21}\text{H}_{22}\text{N}_2\text{O}_3\text{S}$: C, 65.94; H, 5.81; N, 7.33; S, 8.38. Found: C, 65.83; H, 5.64; N, 7.12; S, 8.08.

(8) 4-[[4-(4-Chloro-phenylsulfanyl)-benzoyl]-hydrazonomethyl]-benzoic acid (3 h)

White solid; Yield: 84%; mp: 278–280 °C; IR (KBr, ν cm^{-1}): 3359(NH), 3101(CH), 2989(OH) 1733(C=O), 1697(C=O), 1518(C=C), 1069(C–Cl), 683(C–S). ^1H NMR (DMSO-*d*₆): δ 12.13(*s*, 1H, COOH), 11.57(*s*, 1H, NH), 10.08(*s*, 1H, -N=CH), 7.93–7.91(*d*, $J=7.02$ Hz, 2H), 7.72–7.70(*d*, $J=8.73$ Hz, 2H), 7.58–7.54(*m*, 6H), 7.37–7.33(*d*, $J=6.88$ Hz, 2H). ^{13}C NMR (DMSO-*d*₆): δ 192.32, 171.46, 165.93, 145.72, 139.46, 138.40, 135.33, 129.92, 126.71, 125.60, 125.39, 125.33, 125.21, 125.11, 125.09, 124.48, 124.27, 124.11, 124.03, 123.81, 123.76. MS: m/z 412.94 ($\text{M}^+ + 2$). Anal. Calcd for $\text{C}_{21}\text{H}_{15}\text{ClN}_2\text{O}_3\text{S}$: C, 61.40; H, 3.69; N, 6.83; S, 7.80. Found: C, 61.31; H, 3.64; N, 6.60; S, 7.71.

(9) 4-[[4-(4-Fluoro-phenylsulfanyl)-benzoyl]-hydrazonomethyl]-benzoic acid (3i)

White solid; Yield: 93%; mp: 270–272 °C; IR (KBr, ν cm^{-1}): 3402(NH), 3049(CH), 3023(OH), 1741(C=O), 1701(C=O), 1529(C=C), 1148(C–F), 689(C–S). ^1H NMR (DMSO-*d*₆): δ 12.14 (*s*, 1H COOH), 11.63. (*s*, 1H, NH), 10.13(*s*, 1H, -N=CH), 7.88–7.85(*d*, $J=7.17$ Hz, 2H), 7.73–7.71(*d*, $J=7.06$ Hz, 2H), 7.59–7.54(*m*, 6H), 7.43–7.39(*d*, $J=8.07$ Hz, 2H). ^{13}C NMR (DMSO- *d*₆): δ 192.90, 171.74, 166.51, 145.73, 140.12, 138.40, 135.77, 130.31, 126.70, 125.58, 125.41, 125.30, 125.23, 125.11, 124.59, 124.44, 124.31, 124.25, 124.23, 124.19,

124.10. MS: m/z 395.14 ($M^+ + 1$). Anal. Calcd for $C_{21}H_{15}FN_2O_3S$: C, 63.94; H, 3.84; N, 6.83; S, 8.13. Found: C, 63.83; H, 3.74; N, 6.70; S, 8.01.

(10) 4-[4-(4-Bromo-phenylsulfanyl)-benzoyl]-hydrazonomethyl]-benzoic acid (3j)

White solid; Yield: 82%; mp: 279–281 °C; IR (KBr, ν cm^{-1}): 3349 (NH), 3101 (CH), 2999 (OH), 1719 (C=O), 1682 (C=O), 1522 (C=C), 1051 (C–Br), 661 (C–S). 1H NMR (DMSO- d_6): δ 12.12 (s, 1H, COOH), 11.62 (s, 1H, NH), 10.09 (s, 1H, –N=CH), 7.85–7.83 (d, $J=7.20$ Hz, 2H), 7.73–7.70 (d, $J=8.03$ Hz, 2H), 7.60–7.54 (m, 6H), 7.47–7.42 (d, $J=6.91$ Hz, 2H). ^{13}C NMR (DMSO- d_6): δ 192.21, 170.11, 165.41, 145.07, 138.40, 136.72, 135.12, 129.91, 125.91, 125.59, 125.41, 125.30, 125.26, 125.18, 125.15, 124.80, 124.61, 124.55, 124.30, 124.09, 124.01. MS: m/z 456.61 ($M^+ + 2$). Anal. calcd for $C_{21}H_{15}BrN_2O_3S$: C, 55.39, H, 3.32, N, 6.15, S, 7.08. Found: C, 55.27, H, 3.14, N, 6.12, S, 7.06.

(11) 4-[4-p-Tolylsulfanyl-benzoyl]-hydrazonomethyl]-benzoic acid (3k)

Off-white solid; Yield: 76%; mp: 256–258 °C; IR (KBr, ν cm^{-1}): 3341 (NH), 3103 (CH), 2943 (OH), 1721 (C=O), 1681 (C=O), 1527 (C=C), 663 (C–S). 1H NMR (DMSO- d_6): δ 12.10 (s, 1H, COOH), 11.58 (s, 1H, NH), 10.12 (s, 1H, –N=CH), 7.88–7.85 (d, $J=6.20$ Hz, 2H), 7.67–7.65 (d, $J=5.01$ Hz, 2H), 7.61–7.56 (m, 6H), 7.37–7.34 (d, $J=4.97$ Hz, 2H), 2.23 (s, 3H). ^{13}C NMR (DMSO- d_6): δ 192.19, 171.10, 166.41, 145.77, 138.40, 135.30, 129.94, 126.71, 125.69, 125.41, 125.33, 125.23, 125.11, 125.05, 124.93, 124.84, 124.71, 124.51, 124.33, 123.19, 123.10, 20.42. MS: m/z 391.02 ($M^+ + 1$). Anal. calcd for $C_{22}H_{18}N_2O_3S$: C, 67.68; H, 4.65; N, 7.18; S, 8.21. Found: C, 67.51; H, 4.64; N, 7.02; S, 8.05.

(12) 4-[4-(4-Methoxy-phenylsulfanyl)-benzylidene-hydrazinocarbonyl]-benzoic acid (3l)

Off white solid; Yield: 88%; mp: 285–287 °C; IR (KBr, ν cm^{-1}): 3359 (NH), 3107 (CH), 2979 (OH), 2833 (OCH₃), 1733 (C=O), 1687 (C=O), 1533 (C=C), 684 (C–S). 1H NMR (DMSO- d_6): δ 12.10 (s, 1H, COOH), 11.61 (s, 1H, NH), 10.15 (s, 1H, –N=CH), 7.86–7.82 (d, $J=7.10$ Hz, 2H), 7.70–7.67 (d, $J=7.03$ Hz, 2H), 7.60–7.57 (m, 6H), 7.41–7.38 (d, $J=6.73$ Hz, 2H), 3.44 (s, 3H). ^{13}C NMR (DMSO- d_6): δ 191.66, 170.40, 166.44, 157.34, 144.77, 138.44, 130.44, 125.61, 125.30, 125.22, 125.20, 125.18, 125.11, 125.05, 124.93, 124.80, 124.71, 124.51, 124.23, 124.09, 123.95, 55.48. MS: m/z 407.21 ($M^+ + 1$). Anal. calcd for $C_{22}H_{18}N_2O_4S$: C, 65.05; H, 4.48; N, 6.89; S, 7.90. Found: C, 65.00; H, 4.34; N, 6.42; S, 7.61.

(13) 4-[4-(2,4-Dimethyl-phenylsulfanyl)-benzoyl]-hydrazonomethyl]-benzoic acid (3m)

White solid; Yield: 79%; mp: 259–261 °C; IR (KBr, ν cm^{-1}): 3311 (NH), 3094 (CH), 2981 (OH), 1715 (C=O), 1680 (C=O), 1531 (C=C), 653 (C–S). 1H NMR (DMSO- d_6):

δ 12.09(s, 1H, COOH), 11.61(s, 1H, NH), 10.11(s, 1H, -N=CH), 7.84–7.82(*d*, $J=6.77$ Hz, 2H), 7.79–7.77(*d*, $J=7.03$ Hz, 2H), 7.61–7.56(*m*, 5H), 7.51–7.47(*d*, $J=5.54$ Hz, 2H), 2.43(*s*, 6H). ^{13}C NMR (DMSO-*d*6): δ 191.11, 171.16, 165.33, 145.75, 138.40, 130.35, 125.94, 125.71, 125.49, 125.33, 125.21, 125.20, 125.11, 125.05, 124.93, 124.74, 124.61, 124.41, 124.23, 124.09, 123.90, 21.62, 20.50. MS: m/z 405.31($\text{M}^+ + 1$). Anal. calcd for $\text{C}_{23}\text{H}_{20}\text{N}_2\text{O}_3\text{S}$: C, 68.30; H, 4.95; N, 6.92; S, 7.94. Found: C, 68.17; H, 4.64; N, 6.62; S, 7.78.

(14) 4-[(4-Cyclohexylsulfanyl-benzoyl)-hydrazonomethyl]-benzoic acid (3n)

White solid; Yield: 63%; mp: 252–254 °C; IR (KBr, ν cm^{-1}): 3313(NH), 3104(CH), 2953(OH), 1742(C=O), 1681 (C=O), 1517(C=C), 648(C–S). ^1H NMR (DMSO-*d*6): δ 12.01(*s*, 1H COOH), 11.44(*s*, 1H, NH), 10.02(*s*, 1H, -N=CH), 7.86–7.83(*d*, $J=4.26$ Hz, 2H), 7.68–7.65(*d*, $J=5.73$ Hz, 2H), 7.39–7.35(*d*, $J=5.88$ Hz, 2H), 7.15–7.09(*m*, 2H), 3.41(*m*, 1H), 1.76–1.43(*m*, 10H). ^{13}C NMR (DMSO-*d*6): δ 190.10, 170.06, 163.53, 145.72, 138.45, 135.33, 129.52, 125.71, 124.28, 124.21, 124.15, 124.01, 123.12, 123.01, 122.77, 44.14, 39.39, 39.40, 26.43, 25.20, 25.21. MS: m/z 383.43 ($\text{M}^+ + 1$). Anal. Calcd for $\text{C}_{21}\text{H}_{22}\text{N}_2\text{O}_3\text{S}$: C, 65.90; H, 5.80; N, 7.31; S, 8.40. Found: C, 65.67; H, 5.64; N, 7.23; S, 8.11.

Biological studies

Wistar strain of albino rats (normal and hyperglycemic; 150–190 g) were maintained under standard conditions, i.e., room temperature (25 ± 2 °C) and photoperiod of 12 h day/night cycles each day for 1 week before and during the experiment. The rats were allowed free access to tap water and pellet diet. Rats were divided into following five groups for evaluation of intraday, interday hypoglycemic activity, biochemical parameters and body weight measurement:

Group	Description
Group I	Normal control rats treated with vehicles (10% Tween 80 suspension)
Group II	Hyperglycemic control rats treated with vehicles (10% Tween 80 suspension)
Group III	Normal control rats treated with compound 3m (3m in 10% Tween 80 suspension at a dose of 28 mg/kg)
Group IV	Hyperglycemic rats treated with rosiglitazone (Rosiglitazone in 10% Tween 80 suspension at a dose of 10 mg/kg)
Group V	Hyperglycemic rats treated with synthesized compounds (Synthesized compounds in 10% Tween 80 suspension at a dose of 28 mg/kg)

Intraday blood glucose level was measured at 0th, 1st, 3rd and 6th hrs duration after the administration of vehicle, standard drug (rosiglitazone) and test compounds (**3a–3n**). For evaluation of the effect of compound **3k** and **3m** on interday study of blood glucose, biochemical parameters (TC, TG, HDL, LDL, AP), the same rats were continued with the same dose of test compounds, standard drug and vehicle once daily for 3 week (21 days). Standard kit (Beacon Diagnostics, India) were used

to determined TC, TG, HDL, LDL and AP after period of 21 days. All the procedures were performed in accordance with guidelines of institutional animal ethics committee, CPCSEA, Government of India. All values were expressed as mean \pm S.E.M. Statistical significance was estimated by analysis of variance (ANOVA).

Induction of hyperglycemia

Hyperglycemia was induced in overnight fasted rats by a single intraperitoneal injection of 65 mg/kg streptozotocin in citrate buffer (pH 4.5), 15 min after the intraperitoneal administration of 110 mg/kg.

of nicotinamide. Blood glucose level was checked after 72 h by one touch Accu-check glucometer. Rats with blood glucose levels greater than 250 mg/dl were considered hyperglycemic and were used for the study [21].

Intraday evaluation of hypoglycemic activity of benzoic acid derivatives in normal and STZ induce rats

After overnight fasted rats, intraday blood glucose level was measured at 0th, 1st, 3rd and 6th hrs duration after the administration of vehicle, standard drug (rosiglitazone) and test compounds (**3a–3n**) through gastric intubation using a force feeding needle. Blood samples were collected from the tail vein and blood glucose level was determined with one touch Accucheck glucometer.

Interday evaluation of hypoglycemic activity of benzoic acid derivatives in normal and STZ induce rats

The vehicle, standard drug and test compounds (**3k–3m**) were administered into the rats of the respective groups every day morning for 21 days by gastric intubation using force feeding needle. Blood samples were collected for the measurement of blood glucose from the tail vein at 1st day, 7th, 14th and 21st day duration after the administration of vehicle, standard drug and test compounds (**3k** and **3m**) and blood glucose levels were determined with basic one touch Accucheck glucometer.

Effects of compound 3k and 3m on biochemical parameters of normal and STZ induce rats at 21 days

Biochemical parameters such as TC, TG, HDL, LDL and AP were also estimated on overnight fasted rats at the end of 21st day by using Biochemistry Analyzer Chem-7 (Erba Mannheim) [22–25].

Effects of compound 3k and 3m on body weight of normal and STZ induce rats at 21 days

At the beginning (1st day) and at the end of study (21st day), overnight fasted rats were subjected to weight measurement).

Gastro-ulcerogenic toxicity studies

Albino rats of wistar strain (150–200gm) of both sexes were divided into different groups, control, test and standard (containing six animals each). The test group, control group and standard group were received test drug, vehicle and standard drug respectively. The test compounds and standard compound were suspended in 10% tween-20 and administered orally to each animal by using gastric gavage needle. The control group animals, however received the same volume of vehicle. In this study, the animals were administered a 28 mg/kg (body weight) dose of the test drugs and 10 mg/kg (body weight) dose of standard drug (indomethacin) [26].

Results and Discussion

Molecular docking

Figure 2 illustrates the best docking pose of the most active compound **3m** with amino acid residues of PPAR γ . The compound **3m** showed hydrogen bond interaction with Tyr473, Ser289, His323, and Cys285. This hydrogen bonding pattern is conserved in most PPAR γ agonist complex structures and essential for the activity of the compound [14, 27]. The crystal form of 2PRG [19] consists 2 molecules in the asymmetric unit, denoted A and B. Chain A was chosen for the PPAR γ agonist docking study. The redocking results with chain A gave most reliable docked conformation for the synthesized compound- protein interactions. This is reason behind selection of chain A over chain B. The crystal structure of the 2PRG complex was re-docked for validation.

Chemistry of synthesized compounds

A simple and convenient synthetic route has been developed for synthesis of designed compounds [28–31]. In the first step, the starting material was esterified in strongly acidic conditions and obtained intermediates (**IM1**) were subjected to thioetherification (**IM2**). Thioetherification follows an addition–elimination two-step reaction; in the first step, aryl/cyclohexylsulfanyl as nucleophile attacks on aryl ring bearing chloride leaving group. In the second step, elimination of the chloride leads to generation of thioethers. Here, the utility of cesium fluoride-celite (CsF-Celite) was to activation of the aryl halide groups by the lewis acid type effect. In next step **IM2** were subjected to ammonolysis to get hydrazides (**IM3**) which on further reaction with absolute ethyl alcohol containing 4-formylbenzoic acid yielded desired compounds **3a–3n**. This reaction condition is essential for nucleophilic addition of the amino group to the carbonyl function of the aldehyde. The synthesized compounds (**3a–3n**) were confirmed by FTIR, ^1H NMR, ^{13}C NMR, Mass and Elemental analysis. The FT-IR spectrum of intermediates clearly indicated the desired substitution in the intermediates. The absence of OH group, SH

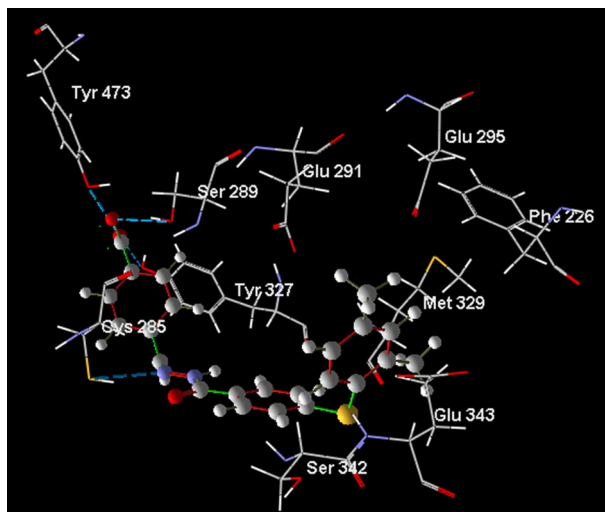
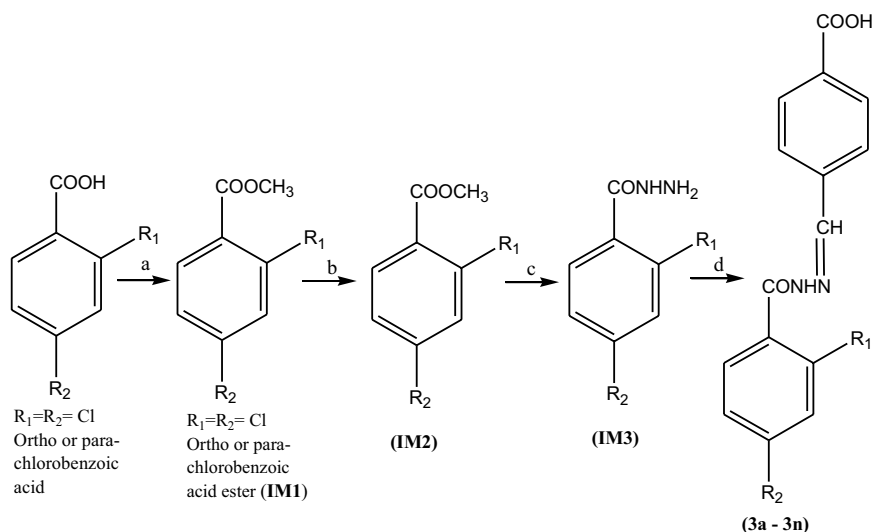


Fig. 2 The most active compound **3m** (ball and stick tube) is interacted with Phe226, Glu291, Glu295, Met329, Ser 342 and Glu343 of amino acid residues in the active binding sites of the receptor. H-bond interactions with key amino acids Tyr473, Ser289, His323 (not appeared) and Cys285 are shown in magenta dashed lines

group absorption and sharp decrease in C=O stretching of hydrazide in the FT-IR spectra of the **IM1**, **IM2** and **IM3** respectively confirmed the reactions of esterification, thioetherification and ammonolysis (Scheme 1).

The FT-IR spectra of synthesized compounds **3a–3n** showed absorption bands around 3023–2943 cm^{-1} for OH (COOH), 3402–3311 cm^{-1} for NH hydrazone, while the distinguished absorption peaks C=O for acid was observed in the range 1758–1715 cm^{-1} , C=O for hydrazone was observed in the range 1701–1680 cm^{-1} and C–S for the thioether was observed in the range of 691–621 cm^{-1} . ^1H NMR spectrum revealed the lack of –SH signal and the presence of characteristic singlets around δ 12.14–11.98 for carboxylic acid protons, around δ 11.65–11.41 for the NH protons of hydrazone while condensation of p-formyl benzoic acid with various substituted aryl hydrazides was confirmed by downfield region of δ 10.15–10.02 observed as singlet for =CH group at phenyl ring. In addition, the ^1H NMR spectra of compounds **3a–3n** showed aromatic group protons as three doublets around δ 7.93–7.82, 7.77–7.63 and 7.51–7.33. On the other hand, the spectrum of **3d**, **3f**, **3k** and **3m** exhibited singlets for CH_3 groups at δ 2.23, 2.43, 2.22 and 2.46 respectively. The ^1H NMR spectroscopic data of compound **3e** and **3l** showed the presence of singlet at δ 3.44 and 3.43 respectively for three protons in the methoxy group. The compound **3g** and **3n** showed the presence of multiplets around δ 7.15–1.39 for aromatic and aliphatic protons. Moreover, compounds **3a–3f** and **3h–3m** showed the presence of a multiplets around δ 7.61–7.50 for aromatic protons. ^{13}C NMR spectra, which were in conformity with the assigned structures, displayed most characteristic signals appearing at around δ 192.96–190.10 ppm for carbonyl carbon peak, δ 171.74–170.03 ppm for carboxylic acid carbon peak, δ



- (1) **IM2**, **IM3** and **3a** : $R_1 = 4-Cl-C_6H_4S-$, $R_2 = H$ (8) **IM2**, **IM3** and **3h** : $R_1 = H$, $R_2 = 4-Cl-C_6H_4S-$
- (2) **IM2**, **IM3** and **3b** : $R_1 = 4-F-C_6H_4S-$, $R_2 = H$ (9) **IM2**, **IM3** and **3i** : $R_1 = H$, $R_2 = 4-F-C_6H_4S-$
- (3) **IM2**, **IM3** and **3c** : $R_1 = 4-Br-C_6H_4S-$, $R_2 = H$ (10) **IM2**, **IM3** and **3j** : $R_1 = H$, $R_2 = 4-Br-C_6H_4S-$
- (4) **IM2**, **IM3** and **3d** : $R_1 = 4-CH_3-C_6H_4S-$, $R_2 = H$ (11) **IM2**, **IM3** and **3k** : $R_1 = H$, $R_2 = 4-CH_3-C_6H_4S-$
- (5) **IM2**, **IM3** and **3e** : $R_1 = 4-OCH_3-C_6H_4S-$, $R_2 = H$ (12) **IM2**, **IM3** and **3l** : $R_1 = H$, $R_2 = 4-OCH_3-C_6H_4S-$
- (6) **IM2**, **IM3** and **3f** : $R_1 = 2,4-(CH_3)_2-C_6H_3S-$, $R_2 = H$ (13) **IM2**, **IM3** and **3m** : $R_1 = H$, $R_2 = 2,4-(CH_3)_2-C_6H_3S-$
- (7) **IM2**, **IM3** and **3g** : $R_1 = C_6H_{11}S-$, $R_2 = H$ (14) **IM2**, **IM3** and **3n** : $R_1 = H$, $R_2 = C_6H_{11}S-$

Scheme 1 Reaction pathways, Reagents and Conditions: **a** Esterification; absolute Methanol, conc. H_2SO_4 , Reflux, 4–5 h; **b** Thioetherification; substituted aryl/cyclohexylthiols, CsF-Celite, CH_3CN , Reflux, 3–18 h; **c** Ammonolysis; NH_2NH_2 (90%), Reflux, 45 min.; **d** Condensation; 4-Formylbenzoic acid, absolute ethanol, Reflux, 40 min.

167.12–163.53 ppm for $C=N$ peak, aromatic carbons around δ 145.77–122.70 ppm and aliphatic carbon around δ 78.67–25.18 ppm. Two carbons of the aromatic ring (**3e** and **3l**) displayed chemical shifts at δ 157.34 and 157.46 due to carbon attached with methoxy group. Mass spectra of all the newly synthesized compounds exhibited a prominent molecular ion peak and isotopic peaks with different intensities. All the newly synthesized compounds were also characterized by elemental chemical analysis and gave satisfactory experimental values and acceptable error range ($\pm 0.4\%$) compared to calculated values.

PPAR γ in vitro activity and structure–activity relationships

The synthesized compounds were screened on full length PPAR receptor transfected in HepG2 cells (Table 1) following the procedure described in our earlier

publication [32]. Two compounds **3 k** (80.21%) and **3 m** (94.60%) showed significant PPAR γ transactivation activity as fold activation and rest of the compounds were exhibited moderate to weak activity in the range of 67.26–17.26% (Table 1). The effect of substituents at R_1 and R_2 position of the compound on hPPAR γ transactivation activity was determined. Dimethyl substitution (**3m**) provides more hPPAR γ transactivation activity as compare to monomethyl substitution (**3k**) at para position of the phenyl ring (Hydrophobic tail part). Potency of the compounds also indicates that para phenylsufanyl substituents are more effective than ortho phenylsufanyl substituents. The potency for PPAR γ agonistic activity was significantly increased by the introduction of electron donating groups at the phenyl ring of the tail part of the compounds. The compounds (**3g**, **3n**) having unsubstituted cyclohexyl moiety in place of substituted phenyl ring were least active. These findings may be due to, the bulky moieties containing tail part comprise at least one substituted phenyl group capable of vander waals interaction to the receptor surface and one substituted phenylsulfanyl moiety for hydrophobic bonding interactions. Moreover, it has been hypothesized that two phenyl groups as bulky moieties exhibited more potency than one phenyl plus a cyclohexyl ring. This would imply that two flat- surfaced benzene rings are better than one and their combined vander walls forces and hydrophobic interactions important for increased biological potency.

Table 1 In vitro PPAR γ agonistic activity as hPPAR γ transactivation activities#

Compound	In vitro activation(Mean \pm SEM)*
3a	0.81 \pm 0.51 (29.13%)
3b	0.99 \pm 0.22 (35.61%)
3c	1.45 \pm 0.21 (52.15%)
3d	1.54 \pm 0.40 (55.39%)
3e	1.00 \pm 0.42 (35.95%)
3f	1.87 \pm 0.42 (67.26%)
3g	0.48 \pm 0.41 (17.26%)
3h	0.90 \pm 0.51 (32.37%)
3i	0.76 \pm 0.35 (27.33%)
3j	1.23 \pm 0.18 (44.24%)
3k	2.23 \pm 0.38 (80.21%)
3l	1.13 \pm 0.18 (40.64%)
3m	2.63 \pm 0.50 (94.60%)
3n	0.62 \pm 0.41 (22.30%)
Rosiglitazone	2.78 \pm 0.20 (100.00%)

*A mean from three determinations at concentration 0.02 μ M.
#Activities are presented as fold induction of hPPAR γ activation. EC₅₀ of the compounds were not determined. Fold activation relative to maximum activation obtained with rosiglitazone (100%)

In vivo activity

In vivo studies were carried in wistar strain of albino rats. Streptozotocin (STZ) was used for induction of hyperglycemia in rats. STZ is well known for its selective pancreatic β -cell cytotoxicity and has been extensively used to induce diabetes mellitus in animals and allows a consistent production of hyperglycemia as well as hyperlipidemia as diabetic like symptoms within a short period of time [33–35].

The intraday fasting blood glucose level at 6th hour for group I, II, III and IV were found 92.66, 303.50, 79.83 and 110.00 mg/dl respectively. While the synthesized benzoic acid derivatives (**3a–3n**) has exhibited intraday fasting blood glucose level at 6th hour in the range of 94.65 mg/dl to 137.50 mg/dl (Table 2). Thus, all the synthesized compounds showed significant reduction in fasting blood glucose level in comparison to diabetic control (group II).

The interday fasting blood glucose level at 21st day of group I, II, III and IV were found 86.66, 337.65, 78.16 and 104.16 mg/dl respectively. The interday fasting blood glucose level at 21st day of **3k** and **3m** were found 84.33 and 106.33 mg/dl respectively. The fasting blood glucose levels of interday study showed consistent blood glucose reduction at 1st, 7th, 14th, 21st day (Fig. 3). Treatment with benzoic acid derivatives in normal rats for 21 days did not produce hypoglycemic conditions. In the diabetic untreated rats (group II) the glucose levels remained higher without much change in the whole experimental period.

After 21 days treatment with compound **3k** and **3m** biochemical parameters such as serum total cholesterol (TC), triglycerides (TG), high density lipoprotein (HDL), low density lipoprotein (LDL) and alkaline phosphatase (AP) were also determined. It was found that the levels of HDL were significantly increased and TC, TG and LDL levels were significantly decreased compared to diabetic untreated rats (Fig. 4). It is interesting to observe in the present study that treatment with benzoic acid derivatives have not only lowered the TG, TC and LDL levels but also enhanced the cardio protective lipid HDL after 21st day treatment. AP which is a hepatic toxicity marker was found higher in diabetic rats treated with standard drug and untreated diabetic control group compared to diabetic rats treated with compound **3k** and **3m**. Thus, benzoic acid derivatives might have protective effect against liver toxicity caused by STZ.

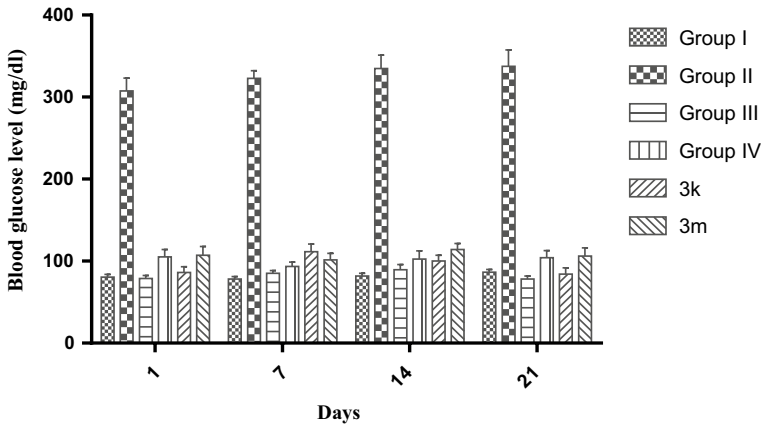
Further, at the end of 21st day treatment, the body weights of the overnight fasted experimental rats were also determined. It was found that, compound treated rats showed less weight gain compare to rosiglitazone treated rats, whereas the body weights of untreated rats (control diabetic) decreased significantly. Untreated rats have shown marked reduction in their body weights compared to normal rats, which could be due to their uncontrolled diabetes (Fig. 5).

At the end of study (21st day), compound **3k** and **3m** treated rat were sacrificed and the stomachs and intestines were removed. A longitudinal incision along the lesser curvature is made. The stomach and intestine of animals was rinsed in running water and the presence and absence of ulcers were determined in control group, test group and standard group and data reported in Table 3.

Table 2 Effects of test compounds on intraday fasting blood glucose levels (mg/dl) of normal and STZ induce rats

Groups/compounds	0 h	1 h	3 h	6 h
Group I	89.50 ± 3.76	89.16 ± 3.49	90.66 ± 3.43	92.66 ± 3.15
Group II	309.30 ± 16.65	307.00 ± 15.10	305.50 ± 16.84	303.50 ± 17.75
Group III	81.66 ± 2.41	76.66 ± 2.96	80.40 ± 3.76	79.83 ± 3.68
Group IV	307.16 ± 16.52	252.16 ± 4.82	130.66 ± 6.19	110.00 ± 1.82
3a	293.17 ± 13.28 ^b	189.00 ± 17.76 ^a	121.83 ± 0.83 ^a	119.86 ± 1.02 ^a
3b	311.52 ± 12.60 ^c	164.50 ± 20.31 ^a	114.33 ± 4.07 ^a	112.66 ± 2.37 ^a
3c	287.66 ± 12.43 ^b	205.65 ± 14.56 ^a	120.83 ± 0.30 ^a	120.33 ± 0.33 ^a
3d	311.66 ± 18.15 ^c	199.83 ± 16.40 ^a	118.50 ± 0.93 ^a	116.16 ± 0.47 ^a
3e	303.34 ± 14.05 ^c	163.00 ± 6.44 ^a	132.34 ± 2.06 ^a	119.46 ± 2.65 ^a
3f	295.56 ± 20.55 ^b	193.16 ± 7.82 ^a	117.16 ± 0.98 ^a	115.83 ± 1.06 ^a
3g	296.00 ± 15.28 ^b	175.85 ± 18.23 ^a	130.16 ± 3.62 ^a	118.16 ± 2.27 ^a
3h	312.00 ± 12.80 ^c	248.50 ± 13.05 ^a	133.60 ± 3.7 ^a	117.03 ± 6.30 ^a
3i	286.66 ± 11.60 ^b	205.67 ± 22.82 ^a	149.66 ± 5.81 ^a	137.50 ± 4.93 ^a
3j	296.83 ± 9.33 ^b	194.43 ± 7.71 ^a	102.66 ± 3.79 ^a	94.65 ± 5.46 ^a
3k	307.06 ± 9.96 ^c	206.16 ± 7.03 ^a	102.00 ± 5.93 ^a	96.83 ± 4.62 ^a
3l	309.83 ± 8.03 ^c	220.03 ± 25.15 ^a	149.66 ± 5.81 ^a	127.50 ± 4.23 ^a
3m	298.83 ± 12.63 ^b	182.66 ± 7.00 ^a	112.33 ± 3.20 ^a	109.33 ± 3.01 ^a
3n	288.83 ± 19.96 ^b	180.66 ± 10.96 ^a	150.50 ± 15.96 ^a	132.13 ± 2.16 ^a

^a $P < 0.001$ indicates statistically more significant when compared with Group II. ^b $P < 0.05$ indicates statistically significant when compared with Group II. ^c $P > 0.05$ not significant compared with Group II. Each value in table is represented as (mean ± SD)

**Fig. 3** Effect of the most active compounds on interday fasting blood glucose levels (mg/dl) of normal and STZ induce rats

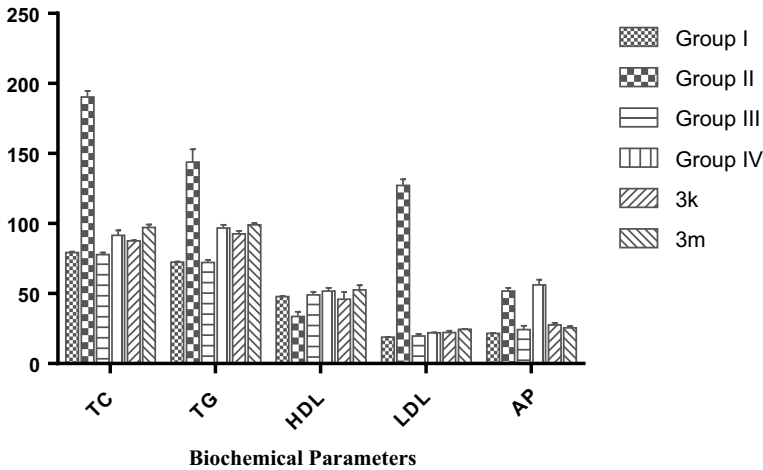


Fig. 4 Effect of the most active compounds on biochemical parameters of normal and STZ induce rats after 21 days of treatment Change in body weight of normal and STZ induce rats at day 1 and day 21

Conclusion

Here, we described the design, syntheses and evaluation of novel benzoic acid derivatives as PPAR γ agonists. In this investigation, the phenyl variants were utilized aiming to enhance the hydrophobicity and the effects of substituents on the phenyl ring at tail group examined successfully. Among these compounds, compound **3k** and **3m** have displayed marked in vitro PPAR γ agonist and in vivo hypoglycemic activity in comparison to rosiglitazone. Further the values of change in body weight by compound **3k** and **3m** in comparison to rosiglitazone

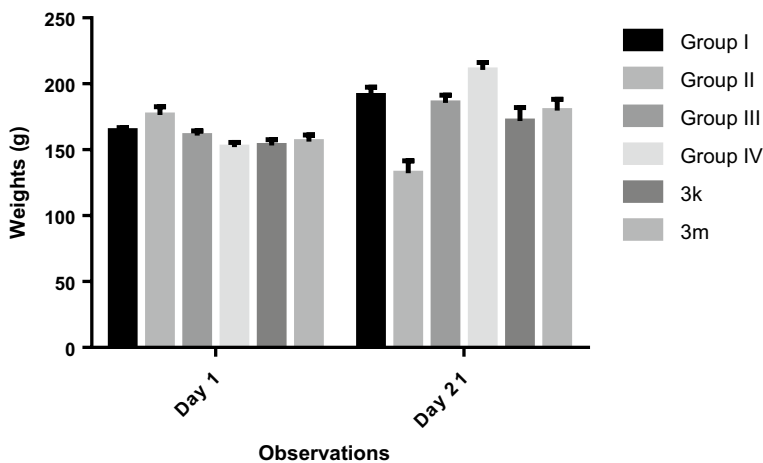


Fig. 5 Change in body weight of normal and STZ induce rats at day 1 and day 21

Table 3 Gastro-ulcerogenic toxicity of the most active compounds in rats

Compounds	Ulcer score	Ulceration (%)
Vehicle	0/6	0.0
3k	0/6	0.0
3m	0/6	0.0
Indomethacin	6/6	100

Bold values provides us information whether synthesized compounds are causing gastric ulcer or not

exhibited that the compounds might be devoid of weight gain, the common adverse effect of TZDs.

Supplementary Information The online version contains supplementary material available at <https://doi.org/10.1007/s11164-021-04555-y>.

Acknowledgements The authors are grateful to management of Zydus Research Centre for skilled and needful support and Mr. Manoj Rathore, School of Pharmacy for animal handling and Dept of Life sciences, Devi Ahilya Vishwavidyalaya for necessary support.

Declarations

Conflicts of interest Authors declares no conflict of interest.

References

1. R. Mukherjee, *Drug News Perspect.* **15**, 261 (2002)
2. R. Walczak, P. Tontonoz, *J. Lipid Res.* **43**, 2 (2002)
3. D.P. Guh, W. Zhang, N. Bansback, Z. Amarsi, C.L. Birmingham, A.H. Anis, *BMC Public Health* **9**, 88 (2009)
4. D. Withrow, D.A. Alter, *Obes. Rev.* **12**, 2 (2011)
5. J.L. Collins, S.G. Blanchard, G.E. Boswell, P.S. Charifson, J.E. Cobb, B.R. Henke, E.A. Hull-Ryde, W.M. Kazmierski, D.H. Lake, L.M. Leesnitzer, J. Lehmann, J.M. Lenhard, L.A. Orband-Miller, Y. Gray-Nunez, D.J. Parks, K.D. Plunkett, W.Q. Tong, *J. Med. Chem.* **41**, 25 (1998)
6. J.E. Cobb, S.G. Blanchard, E.G. Boswell, K.K. Brown, P.S. Charifson, J.P. Cooper, J.L. Collins, M. Dezube, B.R. Henke, E.A. Hull-Ryde, D.H. Lake, J.M. Lenhard, W. Jr. Olive, J. Oplinger, M. Pentti, D.J. Parks, K.D. Plunkett, W.Q. Tong, *J. Med. Chem.* **41**, 25 (1998)
7. B.R. Henke, S.G. Blanchard, M.F. Brackeen, K.K. Brown, J.E. Cobb, J.L. Collins, W.W. Jr. Harrington, M.A. Hashim, E.A. Hull-Ryde, I. Kaldor, S.A. Kliewer, D.H. Lake, L.M. Leesnitzer, J.M. Lehmann, J.M. Lenhard, L.A. Orband-Miller, J.F. Miller, R.A. Jr. Mook, S.A. Noble, W. Jr. Olive, D.J. Parks, K.D. Plunkett, J.R. Szewczyk, T.M. Willson, *J. Med. Chem.* **41**, 25 (1998)
8. T.M. Willson, P.J. Brown, D.D. Sternbach, B.R. Henke, *J. Med. Chem.* **43**, 4 (2000)
9. M.K. Mahapatra, R. Saini, M. Kumar, *Res. Chem. Intermed.* **42**, 8239 (2016)
10. F. Ohsawa, K. Morishita, S. Makoto, M. Makishima, H. Kakuta, *A.C.S. Med. Chem. Lett.* **1**, 9 (2010)
11. M. Nomura, K. Yumoto, T. Shinozaki, S. Isogai, Y. Takano, K. Murakami, *Bioorg. Med. Chem. Lett.* **22**, 334 (2012)
12. X. Tang, W. Hu, L. Fan, H. Wang, M. Tang, D. Yang, *Future Med. Chem.* **12**, 11 (2020)
13. P. Cronet, J.F. Petersen, R. Folmer, N. Blomberg, K. Sjoblom, U. Karlsson, E.L. Lindstedt, K. Bamberg, *Structure.* **9**, 8 (2001)

14. S. Khanna, M.E. Sobhia, P.V. Bharatam, *J. Med. Chem.* **48**, 8 (2005)
15. C. Pirat, A. Farce, N. Lebègue, N. Renault, C. Furman, R. Millet, S. Yous, S. Specca, P. Berthelot, P. Desreumaux, P. Chavatte, *J. Med. Chem.* **55**, 9 (2012)
16. G. Zapata-Sudo, L.M. Lima, S.L. Pereira, M.M. Trachez, F.P. da Costa, B.J. Souza, C.E. Monteiro, N.C. Romero, É.D. D'Andrea, R.T. Sudo, E.J. Barreiro, *Curr. Top. Med. Chem.* **12**, 19 (2012)
17. G. Zapata-Sudo, I.K. da Costa Nunes, J.S. Araujo, J.S. da Silva, M.M. Trachez, T.F. da Silva, F.P. da Costa, R.T. Sudo, E.J. Barreiro, L.M. Lima, (2016) *Drug. Des. Devel. Ther.* **10**, 2869
18. R. Thomsen, M.H. Christensen, *J. Med. Chem.* **49**, 11 (2006)
19. R.T. Nolte, G.B. Wisely, S. Westin, J.E. Cobb, M.H. Lambert, R. Kurokawa, M.G. Rosenfeld, T.M. Willson, C.K. Glass, M.V. Milburn, *Nature* **395**, 137 (1998)
20. J.C. Lee, Y. Choi, *Synth. Commun.* **28**, 812 (1998)
21. M. Perfumi, R. Tacconi, *Indian J. Pharmacol.* **34**, 41 (1996)
22. Recommendations of the Deutsche Gesellschaft für Klinische Chemie (Rec. GSCC DGKC), *J. Clin. Chem. Clin. Biochem.* **10** (1972)
23. N.Rifai, P.S. Bachorik, J.J. Albers, *Textbook of Clinical Chemistry* (Philadelphia, 1999), pp. 809.
24. M. Burstein, H.R. Scholnick, R. Morfin, *J. Lipid Res.* **11**, 6 (1970)
25. W. Heerspink, J.C. Haikenachaid, H. Siepel, J. van der Ven-Jongekrýg, *Enzyme* **25**, 333 (1980)
26. H. Gerhard Vogel, In: *Drug Discovery and Evaluation Pharmacological Assays*, 2nd Edn, (Springer, 2002) pp. 545, 561, 694,696,716, 725, 751,759, 760,769,770.
27. M.V. Liberato, A.S. Nascimento, S.D. Ayers, J.Z. Lin, A. Cvaro, R.L. Silveira, L. Martinez, P.C. Souza, D. Saidemberg, T. Deng, A.A. Amato, M. Togashi, W.A. Hsueh, K. Phillips, M.S. Palma, F.A. Neves, M.S. Skaf, P. Webb, I. Polikarpov, *PLoS ONE* **7**, e36297 (2012)
28. L.C. Tavares, T.C.V. Penna, A.T. Amaral, *Boll. Quim. Farm.* **136**, 3 (1997)
29. L.C Tavares, J.J. Chiste, M.G.B Santos, T.C.V. Penna, *Boll. Chim. Farm.* **138** (1999)
30. A. Masunari, P. Rezende, L.C. Tavares, Abstracts of papers, CADD &D society in Turkey, (2004)
31. S.T.A. Shah, K.M. Khan, A.M. Heinrich, W. Voelter, *Tetrahedron Lett.* **43**, 8281 (2002)
32. H. Pingali, M. Jain, S. Shah, P. Makadia, P. Zaware, A. Goel, M. Patel, S. Giri, H. Patel, P. Patel, *Bioorg. Med. Chem.* **16**, 15 (2008)
33. B. Murtaza, A. Abbas, A. Aslam, M.S. Akhtar, S. Bashir, M. Khalid, M.M. Naseer, *Res. Chem. Intermed.* **42**, 4161 (2016)
34. K. Raju, R. Balaraman, *Phcog. Mag.* **4**, 197 (2008)
35. T. Szudelski, *Physiol. Res.* **50**, 6 (2001)

Publisher's Note Springer Nature remains neutral with regard to jurisdictional claims in published maps and institutional affiliations.

[View PDF](#)

Access through Devi Ahilya University


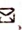
[Purchase PDF](#)

Journal of Drug Delivery Science and Technology

Volume 64, August 2021, 102580

Research paper

Enhancement of cytotoxicity of diallyl disulfide toward colon cancer by Eudragit S100/PLGA nanoparticles

Apeksha Saraf^a  , Nidhi Dubey^a, Nitin Dubey^b, Mayank Sharma^c[Show more](#) [Outline](#) | [Share](#) [Cite](#)<https://doi.org/10.1016/j.jddst.2021.102580>[Get rights and content](#)

Abstract

According to WHO cancer is the second leading cause of death globally, amounting to about 1 in 6 deaths. Among these, colon cancer is the third leading cause of mortalities worldwide. Current measures for cancer treatment: chemotherapy, radiation, and surgery are accompanied by myriad side effects. In light of a mediocre success of synthetic drugs against cancer exploring the treasure of naturally occurring compounds with anti-cancer activity can be an effective strategy. Diallyl disulfide (DADS), a dietary phytochemical derived from garlic possesses a substantial anti-cancer activity against colon cancer. Nevertheless, its poor water solubility and restricted selectivity towards tumor tissues have limited its clinical applications. Moreover, to deliver intact drugs is another major concern in the treatment of ailments associated with the colon. To address these aforementioned clinically significant issues, we report dual functioning DADS loaded polymeric nanoparticles composed of a combination of Eudragit S100 (ES100) as a pH

FEEDBACK 

Home (<http://ipindia.nic.in/index.htm>) About Us (<http://ipindia.nic.in/about-us.htm>) Who's Who (<http://ipindia.nic.in/whos-who-page.htm>)
 Policy & Programs (<http://ipindia.nic.in/policy-pages.htm>) Achievements (<http://ipindia.nic.in/achievements-page.htm>)
 RTI (<http://ipindia.nic.in/right-to-information.htm>) Feedback (<https://ipindiaonline.gov.in/feedback>) Sitemap (<http://ipindia.nic.in/itemap.htm>)
 Contact Us (<http://ipindia.nic.in/contact-us.htm>) Help Line (<http://ipindia.nic.in/helpline-page.htm>)

[Skip to Main Content](#) [Screen Reader Access \(screen-reader-access.htm\)](#)



(<http://ipindia.nic.in/index.htm>)



(<http://ipindia.nic.in/>)

Patent Search

Invention Title	ANTACID HERBAL NANOEMULSION FORMULATION AND PREPARATION METHOD THEREOF
Publication Number	11/2022
Publication Date	18/03/2022
Publication Type	INA
Application Number	202221010454
Application Filing Date	27/02/2022
Priority Number	
Priority Country	
Priority Date	
Field Of Invention	CHEMICAL
Classification (IPC)	A61K0009107000, A61K0036670000, A61K0036230000, B82Y0005000000, A61K0047260000

Inventor

Name	Address	Country	Nat
Ms. Anamika Singh	Research Scholar, School of Pharmacy, Devi Ahilya Vishwavidyalaya, Takshashila Campus, Indore, Madhya Pradesh, India-453771	India	Indi
Dr. Gajanan Narayanrao Darwhekar	Principal, Acropolis Institute of Pharmaceutical Education and Research, Manglia Square, Indore, Madhya Pradesh, India-453771	India	Indi
Dr. Tamanna Narsinghani	Reader, School of Pharmacy, Devi Ahilya Vishwavidyalaya, Takshashila Campus, Indore, Madhya Pradesh, India-453771	India	Indi
Ms. Supriya Shidhaye	Assistant Professor, University Institute of Pharmacy, Oriental University, Sanwer Road, Opposite Revati Range, Jakhya, Indore, Madhya Pradesh, India-453555	India	Indi
Dr. Sweta Srivastava Koka	Associate Professor, Acropolis Institute of Pharmaceutical Education and Research, Manglia Square, Indore, Madhya Pradesh, India-453771	India	Indi
Dr. Dileep Kumar	Assistant Professor, Department of Pharmaceutical Chemistry, Poona college of Pharmacy, Bharti Vidyapeeth University, Erandwane, Pune, Maharashtra, India-411038	India	Indi

Applicant

Name	Address	Country	Nati
Ms. Anamika Singh	Research Scholar, School of Pharmacy, Devi Ahilya Vishwavidyalaya, Takshashila Campus, Indore, Madhya Pradesh, India-453771	India	Indi

Abstract:

ANTACID HERBAL NANOEMULSION FORMULATION AND PREPARATION METHOD THEREOF The present invention provides a herbal nanoemulsion formulation. The herbal nanoemulsion formulation of present invention comprises of Trachyspermum ammi essential oil, Trachyspermum ammi extract, Piper betel extract and pharmaceutically acceptable additives such as Tween 20 (surfactant) 10 ml, ethanol (co-surfactant) 3.3 ml and distilled water q. s. The ratio of surfactant and co-surfactant in herbal nanoemulsion formulation is 3:1. The ratio of oil phase and mixture of surfactant and co-surfactant in herbal nanoemulsion formulation is 2:4. In 50 ml herbal nanoemulsion formulation quantity of ingredients is Trachyspermum ammi essential oil 2.5 g, Trachyspermum ammi extract 0.1 g and Piper betel extract 0.1 g. The present invention also provides p for preparing herbal nanoemulsion formulation. The herbal nanoemulsion formulation of present invention are useful as antacid.

Complete Specification

Claims: I Claim:

1. A herbal nanoemulsion, comprising:

a) Trachyspermum ammi essential oil;

b) Trachyspermum ammi extract;

c) Piper betel extract; and

d) pharmaceutically acceptable excipients,

wherein the 50 ml herbal nanoemulsion comprises Trachyspermum ammi essential oil 2.5 g, Trachyspermum ammi extract 0.1 g and Piper betel extract 0.1 g.

2. The herbal formulation as claimed in claim 1, wherein the ratio of surfactant and co-surfactant is 3:1.

3. The herbal formulation as claimed in claim 1, wherein the ratio of oil phase and mixture of surfactant and co-surfactant is 2:4.

4. The herbal formulation as claimed in claim 1, wherein the herbal composition is useful as antacid.

5. The herbal formulation as claimed in claim 1, wherein the pharmaceutically acceptable additives are Tween 20, ethanol and distilled water.

6. The herbal formulation as claimed in claim 1, wherein pharmaceutically acceptable additives in 50 ml herbal formulation is Tween 20 10 ml, Ethanol 3.3 ml and distilled water q. s.

7. A process for preparing herbal nanoemulsion, comprising:

a) extracting volatile oil of Trachyspermum ammi:

[View Application Status](#)



**Department of Industrial
Policy and Promotion**
Government of India

Terms & conditions (<http://ipindia.gov.in/terms-conditions.htm>) Privacy Policy (<http://ipindia.gov.in/privacy-policy.htm>)

Copyright (<http://ipindia.gov.in/copyright.htm>) Hyperlinking Policy (<http://ipindia.gov.in/hyperlinking-policy.htm>)

Accessibility (<http://ipindia.gov.in/accessibility.htm>) Archive (<http://ipindia.gov.in/archive.htm>) Contact Us (<http://ipindia.gov.in/contact-us.htm>)

Help (<http://ipindia.gov.in/help.htm>)

Content Owned, updated and maintained by Intellectual Property India, All Rights Reserved.

Page last updated on: 26/06/2019



Get Access



Biopharmaceutics and Pharmacokinetics Considerations



Volume 1 in Advances in Pharmaceutical Product Development and Research

2021, Pages 17-27

Chapter 2 - Pharmacokinetics and biopharmaceutics: “a leader or attendant”

Kuldeep Rajpoot¹, Rakesh Kumar Tekade¹, Mukesh Chandra Sharma², Muktika Tekade²

¹ National Institute of Pharmaceutical Education and Research-Ahmedabad (NIPER-A), An Institute of National Importance, Government of India, Department of Pharmaceuticals, Ministry of Chemicals and Fertilizers, Gandhinagar, Gujarat, India

² School of Pharmacy, Devi Ahilya Vishwavidyalaya, Takshila Campus, Indore, India

Available online 15 July 2021, Version of Record 15 July 2021.

Show less ^

+ Add to Mendeley Share Cite

<https://doi.org/10.1016/B978-0-12-814425-1.00020-6>

[Get rights and content](#)



Chapter 5 - Biopharmaceutical considerations in the pediatric and geriatric formulation development

Kuldeep Rajpoot¹, Rakesh Kumar Tekade¹, Bappaditya Chatterjee^{2,3}, Mukesh Chandra Sharma⁴, Muktika Tekade⁴

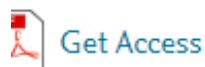
¹ National Institute of Pharmaceutical Education and Research-Ahmedabad (NIPER-A), An Institute of National Importance, Government of India, Department of Pharmaceuticals, Ministry of Chemicals and Fertilizers, Gandhinagar, Gujarat, India

² Shobhaben Pratapbhai Patel School of Pharmacy & Technology Management, SVKM's NMIMS, Mumbai, India

³ Kulliyah of Pharmacy, International Islamic University Malaysia, Kuantan, Malaysia

⁴ School of Pharmacy, Devi Ahilya Vishwavidyalaya, Takshila Campus, Indore, India

Available online 15 July 2021, Version of Record 15 July 2021.



Biopharmaceutics and Pharmacokinetics Considerations



Volume 1 in Advances in Pharmaceutical Product Development and Research

2021, Pages 279-334

Chapter 9 - Pharmacokinetics modeling in drug delivery

Kuldeep Rajpoot¹, Rakesh Kumar Tekade¹, Mukesh Chandra Sharma², Maliheh Safavi³, Muktika Tekade²

¹ National Institute of Pharmaceutical Education and Research-Ahmedabad (NIPER-A), An Institute of National Importance, Government of India, Department of Pharmaceuticals, Ministry of Chemicals and Fertilizers, Gandhinagar, Gujarat, India

² School of Pharmacy, Devi Ahilya Vishwavidyalaya, Takshila Campus, Indore, India

³ Department of Biotechnology, Iranian Research Organization for Science and Technology, Tehran, Iran

Available online 15 July 2021, Version of Record 15 July 2021.



Biopharmaceutics and Pharmacokinetics Considerations

Volume 1 in Advances in Pharmaceutical Product Development and Research

2021, Pages 451-463



Chapter 14 - Influence of fever on pharmacokinetics of drugs

Nimeet Desai¹, HariPriya Koppiseti¹, Kuldeep Rajpoot¹, Muktika Tekade², Mukesh Chandra Sharma², Rakesh Kumar Tekade¹

¹ National Institute of Pharmaceutical Education and Research-Ahmedabad (NIPER-A), An Institute of National Importance, Government of India, Department of Pharmaceuticals, Ministry of Chemicals and Fertilizers, Gandhinagar, Gujarat, India

² School of Pharmacy, Devi Ahilya Vishwavidyalaya, Takshila Campus, Indore, India

Available online 15 July 2021, Version of Record 15 July 2021.



Get Access



Pharmacokinetics and Toxicokinetic Considerations

Volume 2 in Advances in Pharmaceutical Product Development and Research

2022, Pages 1-26



Chapter 1 - Principles and concepts in toxicokinetic

Kuldeep Rajpoot¹, Muktika Tekade², Mukesh Chandra Sharma², Basel Arafat³, Rakesh Kumar Tekade¹

- ¹ National Institute of Pharmaceutical Education and Research-Ahmedabad (NIPER-A), An Institute of National Importance, Government of India, Department of Pharmaceuticals, Ministry of Chemicals and Fertilizers, Gandhinagar, India
- ² School of Pharmacy, Devi Ahilya Vishwavidyalaya, Indore, India
- ³ Faculty of Health, Education, Medicine, and Social Care, Anglia Ruskin University, Chelmsford, United Kingdom

Available online 11 February 2022, Version of Record 11 February 2022.



Get Access



Pharmacokinetics and Toxicokinetic Considerations

Volume 2 in *Advances in Pharmaceutical Product Development and Research*

2022, Pages 27-50



Chapter 2 - Factors influencing drug toxicity

Rachna Gupta¹, Kuldeep Rajpoot¹, Muktika Tekade², Mukesh Chandra Sharma², Maliheh Safavi³, Rakesh Kumar Tekade¹

- ¹ National Institute of Pharmaceutical Education and Research-Ahmedabad (NIPER-A), An Institute of National Importance, Government of India, Department of Pharmaceuticals, Ministry of Chemicals and Fertilizers, Gandhinagar, India
- ² School of Pharmacy, Devi Ahilya Vishwavidyalaya, Indore, India
- ³ Department of Biotechnology, Iranian Research Organization for Science and Technology, Tehran, Iran

Available online 11 February 2022, Version of Record 11 February 2022.



Chapter 3 - Molecular biology of apoptotic, necrotic, and necroptotic cell death

Suryanarayana Polaka¹, Hari Priya Koppiseti¹, Rutuja Satvase¹, Aparna Lakshmi Manchikalapudi¹, Muktika Tekade², Mukesh Chandra Sharma², Rakesh Kumar Tekade¹

¹ National Institute of Pharmaceutical Education and Research-Ahmedabad (NIPER-A), An Institute of National Importance, Government of India, Department of Pharmaceuticals, Ministry of Chemicals and Fertilizers, Gandhinagar, India

² School of Pharmacy, Devi Ahilya Vishwavidyalaya, Indore, India

Available online 11 February 2022, Version of Record 11 February 2022.



Get Access



Pharmacokinetics and Toxicokinetic Considerations



Volume 2 in Advances in Pharmaceutical Product Development and Research

2022, Pages 73-98

Chapter 4 - Toxicogenomics in drug safety assessment

Suryanarayana Polaka ¹, Nupur Vasdev ¹, Sivaroopa Raji ², Vaishali Makwana ¹, Amarjitsing Rajput ^{3, 4}, Madhur Kulkarni ⁵, Muktika Tekade ⁶, Prashant Pingale ⁷, Mukesh Chandra Sharma ⁶, Rakesh Kumar Tekade ¹

- ¹ National Institute of Pharmaceutical Education and Research-Ahmedabad (NIPER-A), An Institute of National Importance, Government of India, Department of Pharmaceuticals, Ministry of Chemicals and Fertilizers, Gandhinagar, India
- ² National Centre for Cell Science, NCCS Complex, S. P. Pune University, Ganeshkhind, India
- ³ Nanomedicine Laboratory, Department of Biosciences and Bioengineering, Indian Institute of Technology Bombay, Powai, India
- ⁴ Department of Pharmaceutics, Poona College of Pharmacy, Bharti Vidyapeeth Deemed University, Pune, India
- ⁵ SCES Indira College of Pharmacy, Pune, Tathwade, India
- ⁶ School of Pharmacy, Devi Ahilya Vishwavidyalaya, Indore, India
- ⁷ Department of Pharmaceutics, GES's Sir Dr. M. S. Gosavi College of Pharmaceutical Education and Research, Nashik, India

Available online 11 February 2022, Version of Record 11 February 2022.



Get Access



Pharmacokinetics and Toxicokinetic Considerations

Volume 2 in Advances in Pharmaceutical Product Development and Research

2022, Pages 99-116



Chapter 5 - Understanding the concept of signal toxicity and its implications on human health

Muktika Tekade ¹, HariPriya Koppiseti ², Mukesh Chandra Sharma ¹, Kuldeep Rajpoot ², Pinaki Sengupta ², Manoj Kumar ^{3, 4}, Rakesh Kumar Tekade ²

¹ School of Pharmacy, Devi Ahilya Vishwavidyalaya, Indore, India

² National Institute of Pharmaceutical Education and Research-Ahmedabad (NIPER-A), An Institute of National Importance, Government of India, Department of Pharmaceuticals, Ministry of Chemicals and Fertilizers, Gandhinagar, India

³ Department of Radiology, Stanford University, Stanford, CA, United States

⁴ Canary Center at Stanford for Cancer Early Detection, Stanford University, Palo Alto, CA, United States

Available online 11 February 2022, Version of Record 11 February 2022.



Get Access



Pharmacokinetics and Toxicokinetic Considerations

Volume 2 in Advances in Pharmaceutical Product Development and Research

2022, Pages 117-144



Chapter 6 - Importance of toxicity testing in drug discovery and research

Rachna Gupta¹, Suryanarayana Polaka¹, Kuldeep Rajpoot¹, Muktika Tekade², Mukesh Chandra Sharma², Rakesh Kumar Tekade¹

- ¹ National Institute of Pharmaceutical Education and Research-Ahmedabad (NIPER-A), An Institute of National Importance, Government of India, Department of Pharmaceuticals, Ministry of Chemicals and Fertilizers, Gandhinagar, India
- ² School of Pharmacy, Devi Ahilya Vishwavidyalaya, Indore, India

Available online 11 February 2022, Version of Record 11 February 2022.



Get Access



Pharmacokinetics and Toxicokinetic Considerations

Volume 2 in Advances in Pharmaceutical Product Development and Research

2022, Pages 145-174



Chapter 7 - Methods and models for in vitro toxicity

Rachna Gupta ¹, Kuldeep Rajpoot ¹, Muktika Tekade ², Mukesh Chandra Sharma ², Rakesh Kumar Tekade ¹

- ¹ National Institute of Pharmaceutical Education and Research-Ahmedabad (NIPER-A), An Institute of National Importance, Government of India, Department of Pharmaceuticals, Ministry of Chemicals and Fertilizers, Gandhinagar, India
- ² School of Pharmacy, Devi Ahilya Vishwavidyalaya, Indore, India

Available online 11 February 2022, Version of Record 11 February 2022.



Get Access



Pharmacokinetics and Toxicokinetic Considerations

Volume 2 in *Advances in Pharmaceutical Product Development and Research*

2022, Pages 175-219



Chapter 8 - New emerging technologies for genetic toxicity testing

Nupur Vasdev¹, Mrudul Deshpande¹, Pratik Katare¹, Vaishali Makwana¹, Suryanarayana Polaka¹, Muktika Tekade², Pinaki Sengupta¹, Mukesh Chandra Sharma², Dinesh Kumar Mishra³, Rakesh Kumar Tekade¹

- ¹ National Institute of Pharmaceutical Education and Research-Ahmedabad (NIPER-A), An Institute of National Importance, Government of India, Department of Pharmaceuticals, Ministry of Chemicals and Fertilizers, Gandhinagar, India
- ² School of Pharmacy, Devi Ahilya Vishwavidyalaya, Indore, India
- ³ Indore Institute of Pharmacy, IIST Campus, Rau, Indore, India

Available online 11 February 2022, Version of Record 11 February 2022.



Get Access



Pharmacokinetics and Toxicokinetic Considerations

Volume 2 in Advances in Pharmaceutical Product Development and Research

2022, Pages 221-240



Chapter 9 - Zebrafish models for toxicological screening

Suryanarayana Polaka ¹, HariPriya Koppiseti ¹, Shreya Pande ¹, Muktika Tekade ², Mukesh Chandra Sharma ², Rakesh Kumar Tekade ¹

- ¹ National Institute of Pharmaceutical Education and Research-Ahmedabad (NIPER-A), An Institute of National Importance, Government of India, Department of Pharmaceuticals, Ministry of Chemicals and Fertilizers, Gandhinagar, India
- ² School of Pharmacy, Devi Ahilya Vishwavidyalaya, Indore, India

Available online 11 February 2022, Version of Record 11 February 2022.




Chapter 10 - Impact of ageing on the pharmacokinetics and pharmacodynamics of the drugs

Suryanarayana Polaka ¹, Jai Divya Tella ², Muktika Tekade ³, Mukesh Chandra Sharma ³, Rakesh Kumar Tekade ¹

- ¹ National Institute of Pharmaceutical Education and Research-Ahmedabad (NIPER-A), An Institute of National Importance, Government of India, Department of Pharmaceuticals, Ministry of Chemicals and Fertilizers, Gandhinagar, India
- ² Department of Pharmacy Practice, Chalapathi Institute of Pharmaceutical Sciences (CLPT)-Chalapathi Nagar, Lam, Guntur, India
- ³ School of Pharmacy, Devi Ahilya Vishwavidyalaya, Indore, India

Available online 11 February 2022, Version of Record 11 February 2022.

 Get Access



Pharmacokinetics and Toxicokinetic Considerations

Volume 2 in Advances in Pharmaceutical Product Development and Research

2022, Pages 263-289



Chapter 11 - Food–drug interactions and their implications on oral drug bioavailability

Suryanarayana Polaka ¹, Kuldeep Rajpoot ¹, Muktika Tekade ², Mukesh Chandra Sharma ², Rakesh Kumar Tekade ¹

¹ National Institute of Pharmaceutical Education and Research-Ahmedabad (NIPER-A), An Institute of National Importance, Government of India, Department of Pharmaceuticals, Ministry of Chemicals and Fertilizers, Gandhinagar, India

² School of Pharmacy, Devi Ahilya Vishwavidyalaya, Indore, India

Available online 11 February 2022, Version of Record 11 February 2022.



Chapter 12 - Drug–drug interactions and their implications on the pharmacokinetics of the drugs

Suryanarayana Polaka¹, Hari Priya Koppiseti¹, Muktika Tekade², Mukesh Chandra Sharma², Pinaki Sengupta¹, Rakesh Kumar Tekade¹

¹ National Institute of Pharmaceutical Education and Research-Ahmedabad (NIPER-A), An Institute of National Importance, Government of India, Department of Pharmaceuticals, Ministry of Chemicals and Fertilizers, Gandhinagar, India

² School of Pharmacy, Devi Ahilya Vishwavidyalaya, Indore, India

Available online 11 February 2022, Version of Record 11 February 2022.



Get Access



Pharmacokinetics and Toxicokinetic Considerations

Volume 2 in Advances in Pharmaceutical Product Development and Research

2022, Pages 323-356



Chapter 13 - Clinical importance of herb–drug interaction

Suryanarayana Polaka ¹, Sayali Chaudhari ¹, Muktika Tekade ², Mukesh Chandra Sharma ², Neelesh Malviya ³, Sapna Malviya ⁴, Rakesh Kumar Tekade ¹

- ¹ National Institute of Pharmaceutical Education and Research-Ahmedabad (NIPER-A), An Institute of National Importance, Government of India, Department of Pharmaceuticals, Ministry of Chemicals and Fertilizers, Gandhinagar, India
- ² School of Pharmacy, Devi Ahilya Vishwavidyalaya, Indore, India
- ³ Smriti College of Pharmaceutical Education, Indore, India
- ⁴ Modern Institute of Pharmaceutical Sciences, Indore, India

Available online 11 February 2022, Version of Record 11 February 2022.



Get Access



Pharmacokinetics and Toxicokinetic Considerations

Volume 2 in Advances in Pharmaceutical Product Development and Research

2022, Pages 357-383



Chapter 14 - In silico methods for the prediction of drug toxicity

Kuldeep Rajpoot¹, Nimeet Desai¹, HariPriya Koppiseti¹, Muktika Tekade², Mukesh Chandra Sharma², Santosh Kumar Behera¹, Rakesh Kumar Tekade¹

- ¹ National Institute of Pharmaceutical Education and Research-Ahmedabad (NIPER-A), An Institute of National Importance, Government of India, Department of Pharmaceuticals, Ministry of Chemicals and Fertilizers, Gandhinagar, India
- ² School of Pharmacy, Devi Ahilya Vishwavidyalaya, Indore, India

Available online 11 February 2022, Version of Record 11 February 2022.



Get Access



Pharmacokinetics and Toxicokinetic Considerations

Volume 2 in Advances in Pharmaceutical Product Development and Research

2022, Pages 385-400



Chapter 15 - Organ-on-chip for assessing environmental toxicants

Suryanarayana Polaka ¹, Priyanka Pulugu ¹, Muktika Tekade ², Mukesh Chandra Sharma ², Rakesh Kumar Tekade ¹

¹ National Institute of Pharmaceutical Education and Research-Ahmedabad (NIPER-A), An Institute of National Importance, Department of Pharmaceuticals, Ministry of Chemicals and Fertilizers, Government of India, Gandhinagar, India

² School of Pharmacy, Devi Ahilya Vishwavidyalaya, Indore, India

Available online 11 February 2022, Version of Record 11 February 2022.



Get Access



Pharmacokinetics and Toxicokinetic Considerations

Volume 2 in Advances in Pharmaceutical Product Development and Research

2022, Pages 401-424



Chapter 16 - Toxicity and toxicokinetic considerations in product development and drug research

Saket Asati ¹, Vikas Pandey ^{1, 2}, Vishal Gour ¹, Rahul Tiwari ^{1, 3}, Vandana Soni ¹, Kuldeep Rajpoot ⁴, Muktika Tekade ⁵, Mukesh Chandra Sharma ⁵, Rakesh Kumar Tekade ⁴

¹ Department of Pharmaceutical Sciences, Dr. Harisingh Gour Vishwavidyalaya, Sagar, India

² Shri Rawatpura Sarkar Institute of Pharmacy, Jhansi, India

³ Faculty of Pharmacy, DIT University, Dehradun, Uttarakhand, India

⁴ National Institute of Pharmaceutical Education and Research-Ahmedabad (NIPER-A), An Institute of National Importance, Government of India, Department of Pharmaceuticals, Ministry of Chemicals and Fertilizers, Gandhinagar, India

⁵ School of Pharmacy, Devi Ahilya Vishwavidyalaya, Indore, India

Available online 11 February 2022, Version of Record 11 February 2022



Get Access



Pharmacokinetics and Toxicokinetic Considerations

Volume 2 in Advances in Pharmaceutical Product Development and Research

2022, Pages 487-511



Chapter 18 - Excipient toxicity and safety

Vikas Pandey¹, Suryanarayana Polaka², Lakshmi Vineela Nalla³, Muktika Tekade⁴, Mukesh Chandra Sharma⁴, Rakesh Kumar Tekade²

- ¹ Department of Pharmaceutics, Guru Ramdas Khalsa Institute of Science and Technology (Pharmacy), Jabalpur, India
- ² National Institute of Pharmaceutical Education and Research- Ahmedabad (NIPER—A), An Institute of National Importance, Government of India, Department of Pharmaceutics, Ministry of Chemicals and Fertilizers, Gandhinagar, India
- ³ National Institute of Pharmaceutical Education and Research-Ahmedabad (NIPER—A), An Institute of National Importance, Government of India, Department of Pharmacology and Toxicology, Ministry of Chemicals and Fertilizers, Gandhinagar, India
- ⁴ School of Pharmacy, Devi Ahilya Vishwavidyalaya, Takshila Campus, Indore, India

Available online 11 February 2022, Version of Record 11 February 2022.



Get Access



Pharmacokinetics and Toxicokinetic Considerations



Volume 2 in Advances in Pharmaceutical Product Development and Research

2022, Pages 513-542

Chapter 19 - Pharmaceutical excipients: special focus on adverse interactions

Suryanarayana Polaka¹, Shyam Sudhakar Gomte¹, Vikas Pandey², Jai Divya Tella³, Muktika Tekade⁴, Mukesh Chandra Sharma⁴, Nagashekhara Molugulu⁵, Rakesh Kumar Tekade¹

- ¹ National Institute of Pharmaceutical Education and Research-Ahmedabad (NIPER-A), An Institute of National Importance, Government of India, Department of Pharmaceuticals, Ministry of Chemicals and Fertilizers, Gandhinagar, India
- ² Department of Pharmaceutics, Guru Ramdas Khalsa Institute of Science and Technology (Pharmacy), Jabalpur, India
- ³ Department of Pharmacy Practice, Chalapathi Institute of Pharmaceutical Sciences (CLPT)-Chalapathi Nagar, Lam, Guntur, India
- ⁴ School of Pharmacy, Devi Ahilya Vishwavidyalaya, Indore, India
- ⁵ School of Pharmacy, Monash University, Bandar Sunway, Selangor, Malaysia

Available online 11 February 2022, Version of Record 11 February 2022.



Get Access



Pharmacokinetics and Toxicokinetic Considerations

Volume 2 in Advances in Pharmaceutical Product Development and Research

2022, Pages 543-567



Chapter 20 - Emerging role of novel excipients in drug product development and their safety concerns

Suryanarayana Polaka¹, Bhakti Pawar¹, Muktika Tekade², Rutuja Satvase¹, Aparna Lakshmi Manchikalapudi¹, Mukesh Chandra Sharma², Vikas Pandey³, Aditya Narayan Jhariya⁴, Rakesh Kumar Tekade¹

- ¹ National Institute of Pharmaceutical Education and Research-Ahmedabad (NIPER-A), An Institute of National Importance, Government of India, Department of Pharmaceuticals, Ministry of Chemicals and Fertilizers, Gandhinagar, India
- ² School of Pharmacy, Devi Ahilya Vishwavidyalaya, Indore, India
- ³ Department of Pharmaceutics, Guru Ramdas Khalsa Institute of Science and Technology (Pharmacy), Jabalpur, India
- ⁴ School of Pharmacy and Medical Sciences, University of Bradford, Bradford, United Kingdom

Available online 11 February 2022, Version of Record 11 February 2022.



Get Access



Pharmacokinetics and Toxicokinetic Considerations

Volume 2 in Advances in Pharmaceutical Product Development and Research

2022, Pages 751-776



Chapter 26 - Toxicokinetic and toxicodynamic considerations in drug research

Kuldeep Rajpoot¹, Pratik Katare¹, Muktika Tekade², Mukesh Chandra Sharma², Suryanarayana Polaka¹, Pinaki Sengupta¹, Rakesh Kumar Tekade¹

¹ National Institute of Pharmaceutical Education and Research-Ahmedabad (NIPER-A), An Institute of National Importance, Government of India, Department of Pharmaceuticals, Ministry of Chemicals and Fertilizers, Gandhinagar, India

² School of Pharmacy, Devi Ahilya Vishwavidyalaya, Indore, India

Available online 11 February 2022, Version of Record 11 February 2022.

National Institutional Ranking Framework

Ministry of Education

Government of India

Welcome to Data Capturing System: PHARMACY

Submitted Institute Data for NIRF'2023'

Institute Name: Devi Ahilya Vishwavidyalaya [IR-P-U-0270]

Sanctioned (Approved) Intake

Academic Year	2021-22	2020-21	2019-20	2018-19	2017-18	2016-17
UG [4 Years Program(s)]	60	60	60	60	-	-
PG [2 Year Program(s)]	15	15	-	-	-	-

Total Actual Student Strength (Program(s) Offered by Your Institution)

(All programs of all years)	No. of Male Students	No. of Female Students	Total Students	Within State (Including male & female)	Outside State (Including male & female)	Outside Country (Including male & female)	Economically Backward (Including male & female)	Socially Challenged (SC+ST+OBC Including male & female)	No. of students receiving full tuition fee reimbursement from the State and Central Government	No. of students receiving full tuition fee reimbursement from Institution Funds	No. of students receiving full tuition fee reimbursement from the Private Bodies	No. of students who are not receiving full tuition fee reimbursement
UG [4 Years Program(s)]	122	147	269	251	18	0	72	158	123	0	0	107
PG [2 Year Program(s)]	10	19	29	24	5	0	9	16	13	0	0	12

Placement & Higher Studies

UG [4 Years Program(s)]: Placement & higher studies for previous 3 years

Academic Year	No. of first year students intake in the year	No. of first year students admitted in the year	Academic Year	No. of students admitted through Lateral entry	Academic Year	No. of students graduating in minimum stipulated time	No. of students placed	Median salary of placed graduates(Amount in Rs.)	No. of students selected for Higher Studies
2016-17	60	60	2017-18	1	2019-20	50	19	250000(two lakh fifty thousand only)	14
2017-18	60	54	2018-19	0	2020-21	52	10	202500(two lakh two thousand five hundred only)	17
2018-19	60	60	2019-20	0	2021-22	60	12	194000(one lakh ninety four thousand only)	25

PG [2 Years Program(s)]: Placement & higher studies for previous 3 years

Academic Year	No. of first year students intake in the year	No. of first year students admitted in the year	Academic Year	No. of students graduating in minimum stipulated time	No. of students placed	Median salary of placed graduates(Amount in Rs.)	No. of students selected for Higher Studies
2018-19	15	14	2019-20	14	9	259200(to lakh fifty nine thousand two hundred only)	0

2019-20	15	15	2020-21	15	8	264600(two lakh sixty four thousand six hundred only)	1
2020-21	15	14	2021-22	14	8	260000(two lakh sixty thousand only)	0

Ph.D Student Details

Ph.D (Student pursuing doctoral program till 2021-22 Students admitted in the academic year 2022-23 should not be entered here.)							
				Total Students			
Full Time				43			
Part Time				0			
No. of Ph.D students graduated (including Integrated Ph.D)							
		2021-22		2020-21		2019-20	
Full Time				2		2	
Part Time				0		0	

Financial Resources: Utilised Amount for the Capital expenditure for previous 3 years

Academic Year	2021-22	2020-21	2019-20
	Utilised Amount	Utilised Amount	Utilised Amount
Annual Capital Expenditure on Academic Activities and Resources (excluding expenditure on buildings)			
Library	33000 (thirty three thousand only)	149311 (one lakh forty nine thousand three hundred eleven)	59500 (fifty nine thousand five hundred)
New Equipment for Laboratories	76650 (seventy six thousand six hundred fifty)	0 (zero)	0 (zero)
Other expenditure on creation of Capital Assets (excluding expenditure on Land and Building)	73525 (seventy three thousand five hundred twenty five)	565960 (five lakh sixty five thousand nine hundred sixty)	172185 (one lakh seventy two thousand one hundred eighty five)

Financial Resources: Utilised Amount for the Operational expenditure for previous 3 years

Academic Year	2021-22	2020-21	2019-20
	Utilised Amount	Utilised Amount	Utilised Amount
Annual Operational Expenditure			
Salaries (Teaching and Non Teaching staff)	34054679 (three crore forty lakh fifty four thousand six hundred seventy nine)	26719983 (two crore sixty seven lakh nineteen thousand nine hundred eighty three)	39847045 (three crore ninety eight lakh forty seven thousand forty five)
Maintenance of Academic Infrastructure or consumables and other running expenditures(excluding maintenance of hostels and allied services,rent of the building, depreciation cost, etc)	1411554 (fourteen lakh eleven thousand five hundred fifty four)	1775573 (seventeen lakh seventy five thousand five hundred seventy three)	2792557 (twenty seven lakh ninety two thousand five hundred fifty seven)
Seminars/Conferences/Workshops	0 (zero)	0 (zero)	0 (zero)

IPR

Calendar year	2021	2020	2019
No. of Patents Published	2	0	1

No. of Patents Granted	1	0	0
------------------------	---	---	---

Sponsored Research Details

Financial Year	2021-22	2020-21	2019-20
Total no. of Sponsored Projects	0	0	0
Total no. of Funding Agencies	0	0	0
Total Amount Received (Amount in Rupees)	0	0	0
Amount Received in Words	Zero	Zero	Zero

Consultancy Project Details

Financial Year	2021-22	2020-21	2019-20
Total no. of Consultancy Projects	0	0	0
Total no. of Client Organizations	0	0	0
Total Amount Received (Amount in Rupees)	0	0	0
Amount Received in Words	Zero	Zero	Zero

PCS Facilities: Facilities of physically challenged students

1. Do your institution buildings have Lifts/Ramps?	Yes, more than 60% of the buildings
2. Do your institution have provision for walking aids, including wheelchairs and transportation from one building to another for handicapped students?	Yes
3. Do your institution buildings have specially designed toilets for handicapped students?	Yes, more than 80% of the buildings

Faculty Details

Srno	Name	Age	Designation	Gender	Qualification	Experience (In Months)	Currently working with institution?	Joining Date	Leaving Date	Association type
1	Dr Rajesh Sharma	49	Professor	Male	Ph.D	290	Yes	15-10-2001	--	Regular
2	Dr Gajendra Pratap Choudhary	46	Associate Professor	Male	Ph.D	256	Yes	18-08-2003	--	Regular
3	Dr Tamanna Narsinghani	42	Associate Professor	Female	Ph.D	228	Yes	10-11-2006	--	Regular
4	Dr E Manivannan	44	Assistant Professor	Male	Ph.D	237	Yes	12-10-2006	--	Regular
5	Dr Mukesh Chandra Sharma	44	Assistant Professor	Male	Ph.D	256	Yes	07-07-2009	--	Regular
6	Dr Jitendra Sainy	43	Assistant Professor	Male	Ph.D	179	Yes	07-07-2009	--	Regular
7	Dr Apeksha Saraf	37	Assistant Professor	Female	Ph.D	174	Yes	11-07-2009	--	Regular
8	Dr Gajanand Engla	46	Assistant Professor	Male	Ph.D	249	Yes	16-07-2009	--	Regular
9	Dr Devashish Rathore	36	Lecturer	Male	Ph.D	106	Yes	07-10-2015	--	Visiting
10	Dr Nidhi Dubey	41	Associate Professor	Female	Ph.D	228	Yes	16-12-2006	--	Regular

11	Dr Love Kumar Soni	45	Associate Professor	Male	Ph.D	227	Yes	01-08-2009	--	Regular
12	Dr Rashmi Dahima	46	Assistant Professor	Female	Ph.D	228	Yes	06-08-2003	--	Regular
13	Dr Masheer Ahmed Khan	52	Assistant Professor	Male	Ph.D	356	Yes	12-10-2006	--	Regular
14	Dr Vivek Vyas	40	Lecturer	Male	Ph.D	158	No	08-11-2021	11-02-2022	Visiting

National Institutional Ranking Framework

Ministry of Education

Government of India

Welcome to Data Capturing System: PHARMACY

Submitted Institute Data for NIRF'2022'

Institute Name: Devi Ahilya Vishwavidyalaya [IR-P-U-0270]

Sanctioned (Approved) Intake

Academic Year	2020-21	2019-20	2018-19	2017-18	2016-17	2015-16
UG [4 Years Program(s)]	60	60	60	60	-	-
PG [2 Year Program(s)]	15	15	-	-	-	-

Total Actual Student Strength (Program(s) Offered by Your Institution)

(All programs of all years)	No. of Male Students	No. of Female Students	Total Students	Within State (Including male & female)	Outside State (Including male & female)	Outside Country (Including male & female)	Economically Backward (Including male & female)	Socially Challenged (SC+ST+OBC Including male & female)	No. of students receiving full tuition fee reimbursement from the State and Central Government	No. of students receiving full tuition fee reimbursement from Institution Funds	No. of students receiving full tuition fee reimbursement from the Private Bodies	No. of students who are not receiving full tuition fee reimbursement
UG [4 Years Program(s)]	115	137	252	240	12	0	73	140	130	0	0	83
PG [2 Year Program(s)]	11	18	29	22	7	0	9	14	12	0	0	11

Placement & Higher Studies

UG [4 Years Program(s)]: Placement & higher studies for previous 3 years

Academic Year	No. of first year students intake in the year	No. of first year students admitted in the year	Academic Year	No. of students admitted through Lateral entry	Academic Year	No. of students graduating in minimum stipulated time	No. of students placed	Median salary of placed graduates(Amount in Rs.)	No. of students selected for Higher Studies
2015-16	60	54	2016-17	1	2018-19	39	7	220000(two lakh twenty thousand)	22
2016-17	60	60	2017-18	1	2019-20	50	19	250000(two lakh twenty thousand)	14
2017-18	60	54	2018-19	0	2020-21	52	10	202500(two lakh two thousand five hundred)	17

PG [2 Years Program(s)]: Placement & higher studies for previous 3 years

Academic Year	No. of first year students intake in the year	No. of first year students admitted in the year	Academic Year	No. of students graduating in minimum stipulated time	No. of students placed	Median salary of placed graduates(Amount in Rs.)	No. of students selected for Higher Studies
2017-18	18	14	2018-19	14	7	240000(two lakh forty thousand)	0
2018-19	15	14	2019-20	14	8	223200(two lakh twenty three thousand two hundred)	0

2019-20	15	15	2020-21	15	8	264600(two lakh sixty four thousand six hundred)	0
---------	----	----	---------	----	---	--	---

Ph.D Student Details

Ph.D (Student pursuing doctoral program till 2020-21 Students admitted in the academic year 2020-21 should not be entered here.)			
		Total Students	
Full Time		49	
Part Time		0	
No. of Ph.D students graduated (including Integrated Ph.D)			
	2020-21	2019-20	2018-19
Full Time	2	2	0
Part Time	0	0	0

Financial Resources: Utilised Amount for the Capital expenditure for previous 3 years

Academic Year	2020-21	2019-20	2018-19
	Utilised Amount	Utilised Amount	Utilised Amount
Annual Capital Expenditure on Academic Activities and Resources (excluding expenditure on buildings)			
Library	149311 (one lakh forty nine thousand three hundred eleven)	59500 (fifty nine thousand five hundred)	17000 (seventeen thousand)
New Equipment for Laboratories	0 (zero)	510987 (five lakh ten thousand nine hundred eighty seven)	1664775 (sixteen lakh sixty four thousand seven hundred seventy five)
Other expenditure on creation of Capital Assets (excluding expenditure on Land and Building)	565960 (five lakh sixty five thousand nine hundred sixty)	172185 (one lakh seventy two thousand one hundred eighty five)	630163 (six lakh thirty thousand one hundred sixty three)

Financial Resources: Utilised Amount for the Operational expenditure for previous 3 years

Academic Year	2020-21	2019-20	2018-19
	Utilised Amount	Utilised Amount	Utilised Amount
Annual Operational Expenditure			
Salaries (Teaching and Non Teaching staff)	26719983 (two crore sixty seven lakh nineteen thousand nine hundred eighty three)	39847045 (three crore ninety eight lakh forty seven thousand forty five)	17572465 (one crore seventy five lakh seventy two thousand four hundred sixty five)
Maintenance of Academic Infrastructure or consumables and other running expenditures(excluding maintenance of hostels and allied services,rent of the building, depreciation cost, etc)	1775573 (seventeen lakh seventy five thousand five hundred seventy three)	2792557 (twenty seven lakh ninety two thousand five hundred fifty seven)	1313434 (thirteen lakh thirteen thousand four hundred thirty four)
Seminars/Conferences/Workshops	0 (zero)	0 (zero)	0 (zero)

IPR

Calendar year	2020	2019	2018
No. of Patents Published	0	1	0
No. of Patents Granted	0	0	0

Sponsored Research Details

Financial Year	2020-21	2019-20	2018-19
Total no. of Sponsored Projects	1	1	1
Total no. of Funding Agencies	1	1	1
Total Amount Received (Amount in Rupees)	100000	250000	300000
Amount Received in Words	one lakh	two lakh fifty thousand	three lakh

Consultancy Project Details

Financial Year	2020-21	2019-20	2018-19
Total no. of Consultancy Projects	0	0	0
Total no. of Client Organizations	0	0	0
Total Amount Received (Amount in Rupees)	0	0	0
Amount Received in Words	Zero	Zero	Zero

PCS Facilities: Facilities of physically challenged students

1. Do your institution buildings have Lifts/Ramps?	Yes, more than 60% of the buildings
2. Do your institution have provision for walking aids, including wheelchairs and transportation from one building to another for handicapped students?	Yes
3. Do your institution buildings have specially designed toilets for handicapped students?	Yes, more than 80% of the buildings

Faculty Details

Srno	Name	Age	Designation	Gender	Qualification	Experience (In Months)	Currently working with institution?	Joining Date	Leaving Date	Association type
1	Dr Rajesh Sharma	48	Professor	Male	Ph.D	278	Yes	15-10-2001	--	Regular
2	Dr Gajendra Pratap Choudhary	45	Associate Professor	Male	Ph.D	244	Yes	18-08-2003	--	Regular
3	Dr Tamanna Narsinghani	41	Associate Professor	Female	Ph.D	216	Yes	10-11-2006	--	Regular
4	Dr E Manivannan	43	Assistant Professor	Male	Ph.D	225	Yes	12-10-2006	--	Regular
5	Dr Mukesh Chandra Sharma	43	Assistant Professor	Male	Ph.D	244	Yes	07-07-2009	--	Regular
6	Dr Jitendra Sainy	42	Assistant Professor	Male	Ph.D	167	Yes	07-07-2009	--	Regular
7	Dr Apeksha Saraf	36	Assistant Professor	Female	Ph.D	162	Yes	11-07-2009	--	Regular
8	Dr Gajanand Engla	45	Assistant Professor	Male	Ph.D	237	Yes	16-07-2009	--	Regular
9	Dr Devashish Rathore	35	Lecturer	Male	Ph.D	94	Yes	07-10-2015	--	Visiting
10	Dr Nidhi Dubey	40	Associate Professor	Female	Ph.D	216	Yes	16-12-2006	--	Regular
11	Dr Love Kumar Soni	44	Associate Professor	Male	Ph.D	215	Yes	01-08-2009	--	Regular

12	Dr Rashmi Dahima	45	Assistant Professor	Female	Ph.D	216	Yes	06-08-2003	--	Regular
13	Dr Masheer Ahmed Khan	51	Assistant Professor	Male	Ph.D	344	Yes	12-10-2006	--	Regular
14	Dr Vivek Vyas	39	Lecturer	Male	Ph.D	146	No	05-11-2020	06-03-2021	Visiting